Thesis

on

MULTI RESPONSE OPTIMIZATION OF WIRE ELECTRIC DISCHARGE MACHINING WITH ANALYTIC HIERARCHY PROCESS

Submitted in partial fulfillment of the requirement for the award of the degree of

Master of Engineering

in

PRODUCTION & INDUSTRIAL ENGINEERING

By

DHIMAN JOHNS

Roll No. 800982004

Under the guidance of

Dr. Ajay Batish

Professor & Head

Mechanical Engg. Deptt.,

Thapar University, Patiala

Mechanical Engineering Department

THAPAR UNIVERSITY

Patiala, Punjab

DECLARATION

This is to certify that the thesis entitled **"Multi Response Optimization of Wire Electric Discharge Machining with Analytic Hierarchy Process"** is an authentic record of my study carried out as requirements for the award of the degree of **Master of Engineering in Production and Industrial Engineering** from **Thapar University, Patiala,** under the guidance of **Dr. Ajay Batish**, Professor & Head, Mechanical Engineering Department, Thapar University, Patiala during **July 2010 to July 2011.** This matter embodied in this thesis has not been submitted in part or full to any other university or institute for the award of any degree.

Date: 13/07/2011

Dhiman Johns

Dhiman Johns

(Roll No: 800982004)

This is to certify that above declaration made by the student concerned is correct to the best of my knowledge & belief.

Dr. Ajay Batish
Professor & Head
Mechanical Engg. Deptt.,
Thapar University,
Patiala-147004

Countersigned by:

Dr. S.K. Mohapatra
Dean of Academic Affairs,
Thapar University,
Patiala-147004

ACKNOWLEDGEMENTS

With deep sense of gratitude I express my sincere thanks to my guide, Dr. Ajay Batish, Professor & Head, Mechanical Engineering Department, Thapar University, Patiala**,** for his valuable guidance, proper advise and constant encouragement during my thesis work from the initial level to final level.

I would also like to thank Mr. Anirban Bhattacharya, Assistant Professor, Mechanical Engineering Department, Thapar University, Patiala for his kind cooperation and guidance, which helped me in the completion of this work.

I express my sincere gratitude to Sardar Jagjit Singh Chandan of M/s J. S. Engineering Works, Patiala, for providing me the Wire Electric Discharge Machine to carry out my thesis work.

The generous and intellectual support of all the staff members of Mechanical Engineering Department is greatly appreciated. Finally, I would like to express my heartfelt thanks to my parents and friends for their help and wishes for the successful completion of this work.

Above all, I express my indebtedness to the "**ALMIGHTY**" for all His blessing and kindness.

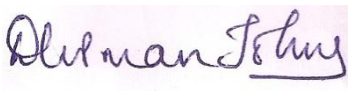

Dhiman Johns

Roll No. 800982004

ABSTRACT

Modernization of mechanical industry has lead to the increase in demand for hard and tough materials and thus various non traditional methods have been developed in order to machine such hard and tough materials. Wire Electric discharge machine is one of the most commonly used machine which is employed in machining of conductive metals of any hardness or that are difficult or impossible to cut with traditional methods. WEDM is one of the most popular machining methods in present industry which specializes in cutting complex shapes or geometries. The literature survey has revealed that very less work has been done in order to achieve optimal levels of process parameters for AISI 304, AISI 410, EN 31 and H21 using molybdenum wire electrode. Also machine operators perform machining operations on these materials using their operational skills and experience. These materials have been selected keeping in view their application and hence machined using Concord United WEDM, Model-DK7740CH. The objective of the present study is to study the effect of different process parameters viz. peak current, pulse on time, pulse off time and work piece on the response variables such as material removal rate, surface finish, kerf width and gap current using molybdenum wire electrode (0.18 mm diameter). Taguchi design methodology has been chosen for design of experiment and L16 orthogonal array has been selected for present study. Two different sets of experiments based on L16 OA have been designed using two different workpiece materials (AISI 304 and AISI 410 for first set of experiment and EN 31 and H21 for second set of experiment). Analysis of variance and main effect plot have been used to find the significant process parameters and their effect on the response variables. The process parameters for each workpiece materials have been optimized using analytic hierarchy process.

CONTENTS

LIST OF FIGURES

LIST OF TABLES

ABBREVATIONS

ANOVA	Analysis of Variance
CNC	Computer Numerical Control
DC	Direct Current
DOF	Degree of Freedom
EDM	Electric Discharge Machine
HB	Higher the better
I_p	Peak Current
KW	Kerf Width
LB	Lower the Better
MRR	Material Removal Rate
MS	Mean Square
MSD	Mean Square Deviation
NB	Nominal the Better
OA	Orthogonal Array
SS	Sum of Square
SN	Signal to Noise Ratio
SR	Surface Roughness
T_{on}	Pulse on time
T_{off}	Pulse off time
WEDM	Wire Electric Discharge Machine

CHAPTER 1
INTRODUCTION

1.1 INTRODUCTION TO NON TRADITIONAL MACHINING

Machining removes certain parts of the work pieces to change them to final parts. Machining nowadays has been classified in two types: (1) Traditional Machining; (2) Non-traditional Machining. Traditional Machining, also known conventional machining requires the presence of a tool that is harder than the work piece to be machined. This tool should be penetrated in the work piece to a certain depth. Moreover, a relative motion between the tool and work piece is responsible for forming or generating the required shape. The absence of any of these elements in any machining process such as the absence of tool-work piece contact or relative motion, makes the process a non-traditional or non-conventional one [1].

Non-conventional machining processes are well established in modern manufacturing industries as they are capable of machining hard materials. Non-conventional machining processes are classified according to the machining action which helps in material removal from the work piece. The material removal mechanism, machining system components, process variables, technological characteristics, and industrial applications are different for all these processes [1].

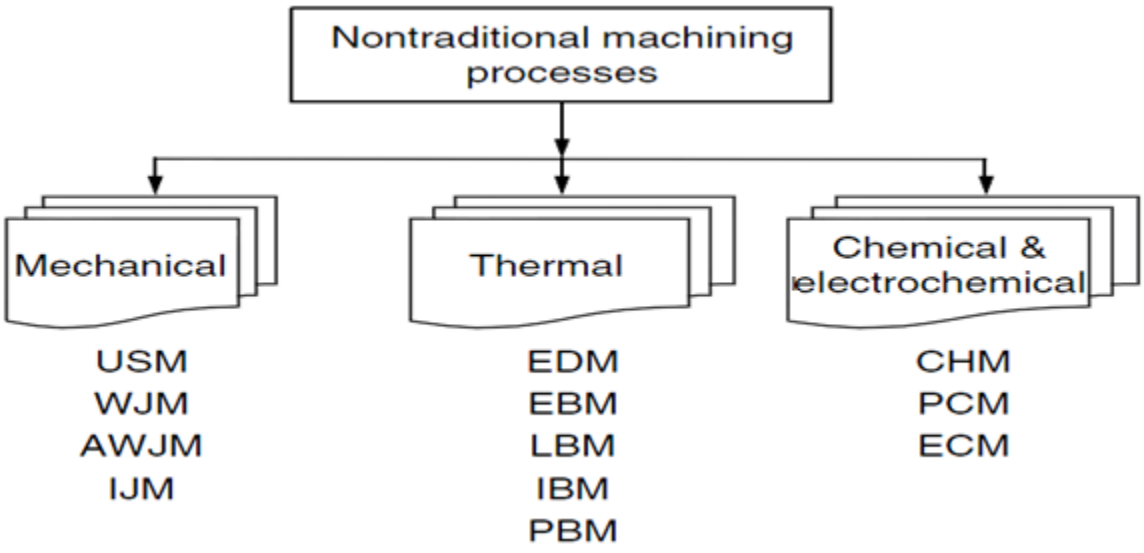

Figure 1.1 Classification of Non-Traditional processes [1]

1.2 ELECTRICAL DISCHARGE MACHINING (EDM)

The phenomenon of erosion of metals by electric spark was first noticed by Joseph Priestily in 1878 but this was not used for machining of metals until 1930s. Controlled machining of metals by electric sparks was first done by Lazarenko in Russia in 1944 [2].

One of the most widely used Non-Conventional Machining process in industry is Electrical Discharge Machining (EDM). Electric Discharge Machining is a non-traditional concept which is based on the principle of removing material by means of repeated electrical discharges between the tool termed as electrode and the work piece in the presence of a dielectric fluid [3]. Electrical Discharge Machining (EDM) uses thermal energy to achieve a high-precision metal removal process from a fine, accurately controlled electrical discharge. The electrode is moved towards the work piece until the gap is small enough so that the impressed voltage is great enough to ionize the dielectric [1]. Short duration discharges are generated in a liquid dielectric gap, which separates tool and work piece. The material is removed with the erosive effect of the electrical discharges from tool and work piece. EDM does not make direct contact between the electrode and the work piece thus it can eliminate mechanical stresses, chatter and vibration problems during machining [3, 4].

EDM is commonly used for machining very hard and tough materials such as tool steels and carbides and for finishing parts for aerospace, automotive industry and surgical components. It is also used to produce complex shapes and small diameter holes, which are difficult or impossible to machine using conventional methods. Since EDM uses an electric discharge to cut the material, its use is limited to conductive materials [1, 3-5].

Table 1.1 Some materials that can be EDMed [6]

Inconel	Aluminium	Vasconal 300
Tool Steels: 01, A2, D2, S7	Aluminium Bronze	PCD Diamond
Carbide	Copper	Nitronic
Ferro-Tic	Brass	Beryllium Copper
CPM 10V	Cold Roll Steel	Hastalloy
4130	Hot Rolled Steel	Stellite
Graphite	Stainless Steels	Titanium

1.3 CLASSIFICATION OF EDM

There are several EDM processes such as Wire Electrical Discharge Machining, Electrical Discharge Milling, Electrical Discharge Grinding (EDG), Electrical Discharge Dressing (EDD), Ultrasonic Aided EDM (UEDM), Abrasive Electrical Discharge Grinding (AEDG), Micro Electrical Discharge Machining (MEDM), Micro Wire EDM (MWEDM), Mole EDM, and Double Rotating Electrodes EDM [3]. Pandey and Shan [7] classified EDM processes into three main categories as shown in figure 1.2.

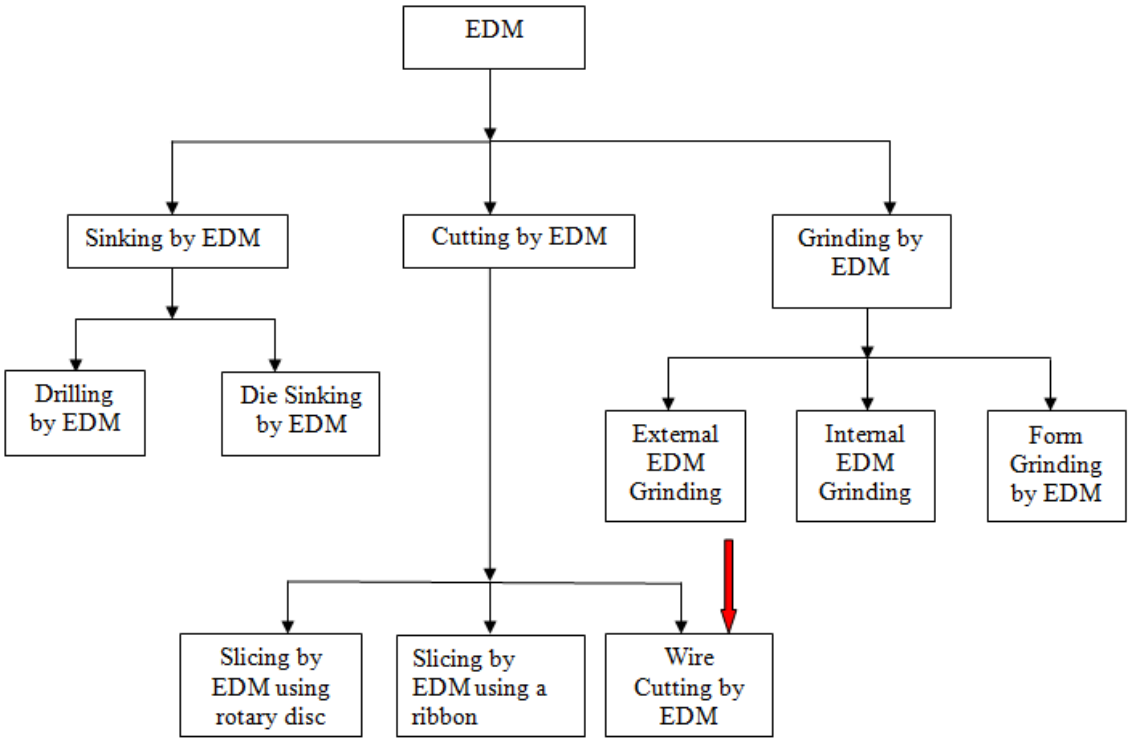

Figure 1.2 Classification of EDM

1.4 WIRE ELECTRIC DISCHARGE MACHINING (WEDM)

WEDM is considered as a unique adoption of the conventional EDM process which comprises of a main worktable, wire drive mechanism, a CNC controller, working fluid tank and attachments. The work piece is placed on the fixture table and fixed securely by clamps and bolts. The table moves along X and Y-axis and it is driven by the DC servo motors. Wire electrode usually made of thin copper, brass, molybdenum or tungsten of diameter 0.05-0.30 mm, which transforms electrical energy to thermal energy, is used for cutting materials. The wire is stored and wound on a wire drum which can rotate at 1500rpm. The wire is continuously fed from wire drum which moves though the work piece and is supported under tension between a pair of wire guides located at the opposite

sides of the work piece. During the WEDM process, the material is eroded ahead of the wire and there is no direct contact between the work piece and the wire, eliminating the mechanical stresses during machining. Also the workpiece and the wire electrode (tool) are separated by a thin film of dielectric fluid that is continuously fed to the machining zone to flush away the eroded particles. The movement of table is controlled numerically to achieve the desired three-dimensional shape and accuracy of the workpiece [8].

1.4.1 History

In 1969, the SWISS FIRM 'AGIE' produced the world's first WEDM, the process was fairly simple, not complicated and wire choices were limited to copper and brass only. Early WEDM produced were extremely slow but as more and more research was done on WEDM, cutting speed and overall capabilities of WEDM have been modified. In the early 70s, a typical machine cut 2 square inches per hour (i.e. 21 mm^2/min), in the early 80s, 6 square inches per hour (i.e. 64 mm^2/min), however WEDM which are under operation today can cut 20 times faster than these earlier machines.

In recent years, the technology of WEDM has been improved significantly to meet the requirements in various manufacturing needs, especially in the precision mold and die industry. WEDM has greatly improved in terms of accuracy, quality, productivity and precision, thus immensely helped the tooling and manufacturing industry. WEDM operated in industry today are equipped with Computer Numerical Control (CNC) which helps in improving efficiency and accuracy [6].

1.4.2 Importance of WEDM in Industry

The degree of accuracy of workpiece dimensions obtainable and the fine surface finishes make WEDM particularly valuable for applications involving manufacture of stamping dies, extrusion dies and prototype parts [9]. Its broad capabilities have allowed it to encompass the production, aerospace and automotive industries and virtually all areas of conductive material machining. This is because WEDM provides the best alternative or sometimes the only alternative for machining conductive, exotic, high strength and temperature resistive materials, conductive engineering ceramics with the scope of generating intricate shapes and profiles [9, 10]. WEDM is being used to machine a wide

variety of miniature and micro-parts from metals, alloys, sintered materials, cemented carbides, ceramics and silicon.

Without WEDM, the fabrication of precision work piece would require many hours of manual grinding and polishing [11]. With this process, alloy steel, conductive ceramics and aerospace materials can be machined irrespective to their hardness and toughness. Furthermore, WEDM is capable of producing a fine, precise, corrosion and wear resistant surface.

WEDM has tremendous potential in its applicability in the present day metal cutting industry for achieving a considerable dimensional accuracy, surface finish and contour generation features of products or parts. Moreover, the cost of wire contributes only 10% of operating cost of WEDM process. The difficulties encountered in the die sinking EDM are avoided by WEDM, because complex design tool is replaced by moving conductive wire and relative movement of wire guides.

1.4.3 WEDM Process

WEDM is a process which erodes and removes material by using the channel of plasma generated by electric sparks between two conductive materials (i.e. electrode and the work piece), this channel of plasma converted into thermal energy at a temperature range of 8000 to 12000º C at a pulsating direct current supply of 20000 to 30000 Hz. The electrode and work piece are separated by a small gap being immersed in dielectric fluid, an electric spark is produced in between this small gap and the work piece material is eroded, as the pulsating current is turned off, the plasma breaks down which leads to sudden reduction in the temperature and the eroded material is flushed away with the help of dielectric fluid in the form of microscopic debris. With each electric spark discharge a small crater is formed on both the work piece and the electrode which is a prime decider in the final surface quality [3, 12]. The taper can ranging from 15º for a 100 mm thick to 30º for a 400 mm thick workpiece can be obtained on the cut surface material [13]. A WEDM schematic is shown in figure 1.3.

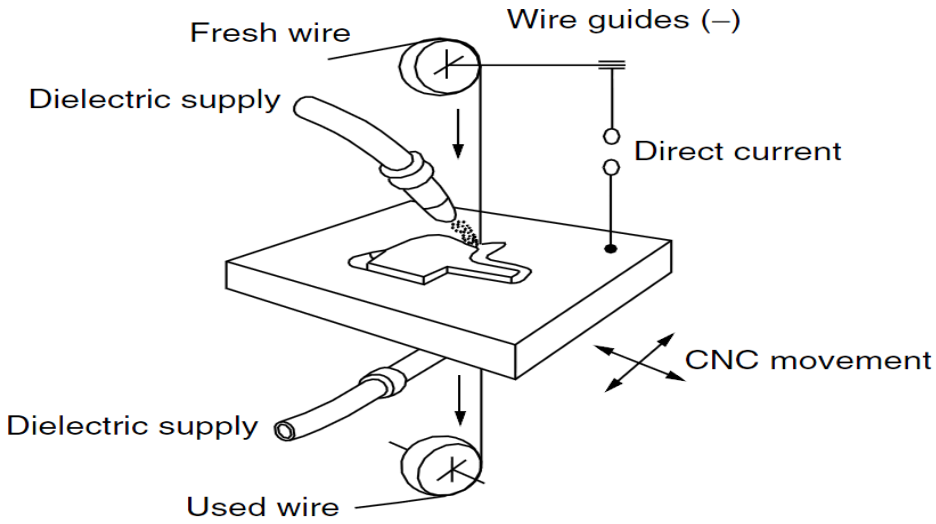

Figure 1.3 WEDM schematic [1]

Deionized water is used as the dielectric as it is the purest form of water and it acts as an insulator. Normal tap water contains minerals which may be too conductive for Wire EDM, in order to control the water conductivity; water is deionized by passing it through a resin tank which eliminates the conductive elements of water. This deionized water is circulated with the help of a pump. As the machining operation is performed, conductivity of water rises and it is again re-circulated through the resin tank [6]. The purpose of deionised water is to stabilise the spark erosion path and to act as the dielectric medium which is forced into the cutting gap to flush out the eroded metal. There is virtually no cutting force on the part of the machine because the wire electrode and work piece never make contact [3].

WEDM process is usually used in conjunction with CNC and will only work when a part is to be cut completely through. The melting temperature of the parts to be machined is an important parameter for this process rather than strength or hardness. The surface quality and material removal rate (MRR) of the machined surface by wire EDM will depend on different machining parameters such as applied peak current, and wire materials. WEDM process is commonly conducted on submerged condition in a tank fully filled with dielectric fluid; nevertheless it also can be conducted in dry condition. This method is used due to temperature stabilization and efficient flushing in cases where the work piece has varying thickness [14].

1.4.4 Step by Step procedure of WEDM Process

Step: 1

Generation of Volts and Amps as wire is surrounded by deionized water as shown in figure 1.4 [6].

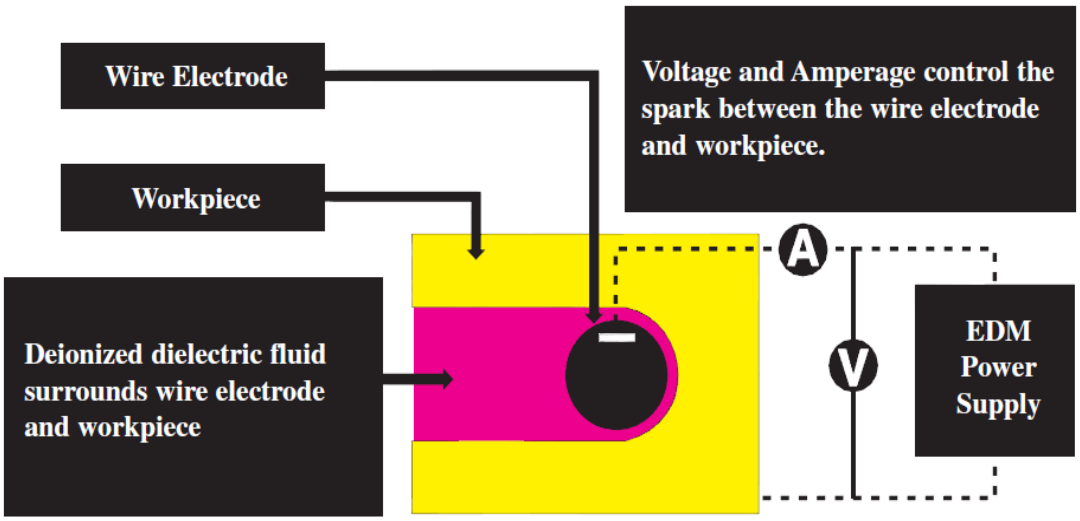

Figure 1.4 Volts and Amps produced by power supply [6]

Step: 2

During pulse on time controlled sparks are produced between work piece and electrode which helps in erosion and hence precisely melts and vaporize the material as shown in figure 1.5.

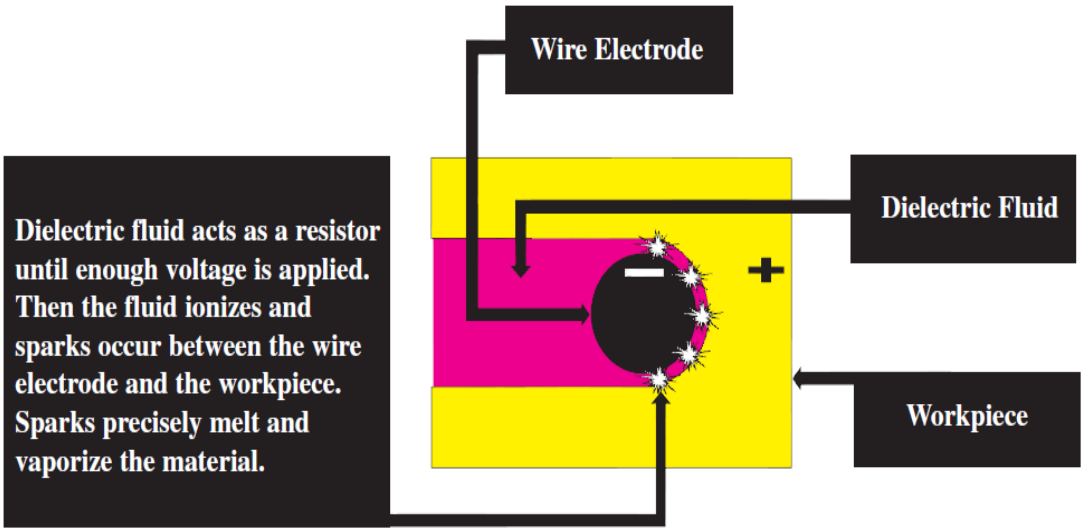

Figure 1.5 Spark generation and erosion of material [6]

Step: 3

During pulse off time pressurized dielectric fluid cools the material and flushes away the eroded particles as shown in figure 1.6.

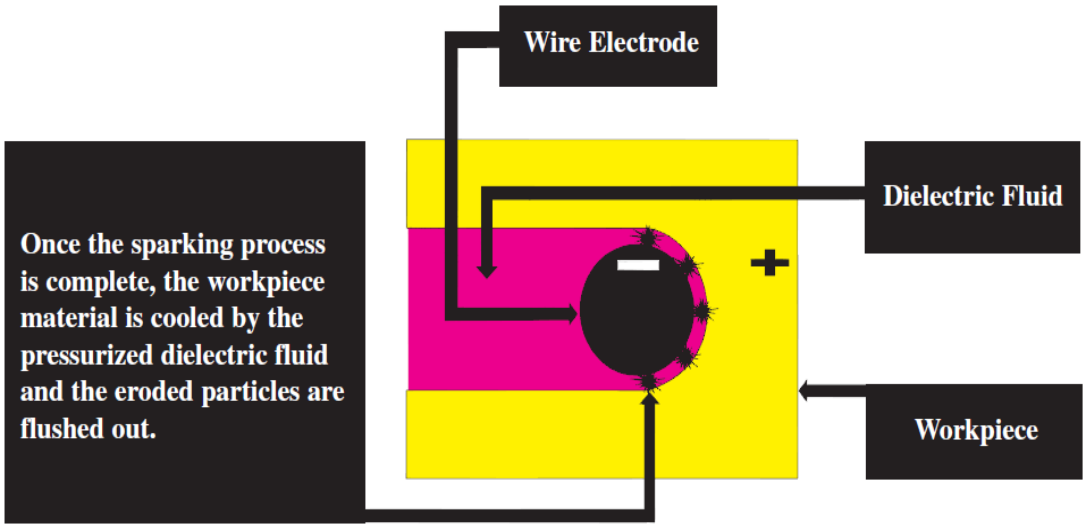

Figure 1.6 Flushing of corroded particles [6]

Step: 4

A filter system is used to filter the eroded particles from the dielectric fluid and the fluid is thus reused as shown in figure 1.7.

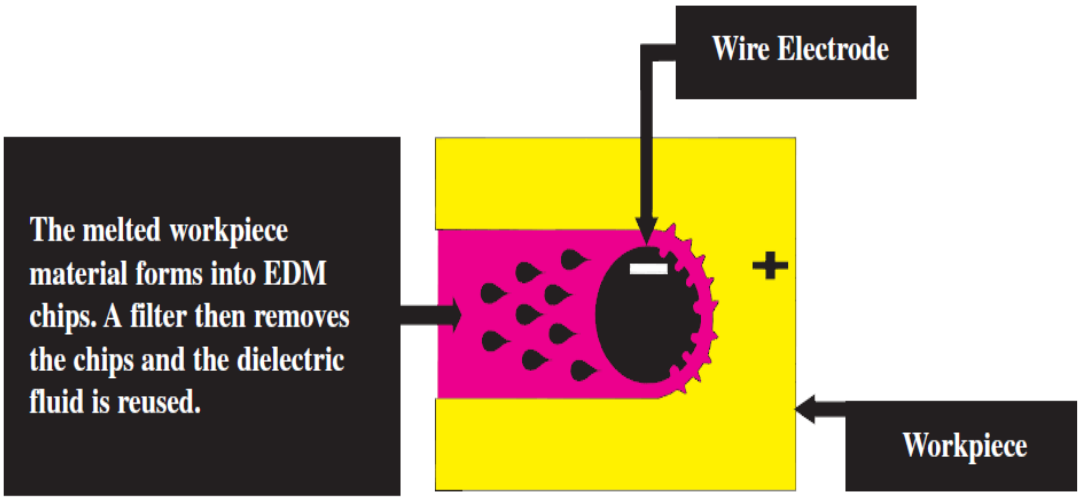

Figure 1.7 Filtration and reuse of dielectric [6]

1.4.5 Features of WEDM process

Features of Wire EDM process are [5]:

- Forming electrode adapted to product shape is not required.
- Electrode wear is negligible.

- Machined surfaces are smooth.
- Geometrical & dimensional tolerances are tight.
- Relative tolerance between punch & die is extremely high & die life is extended.
- Straight holes can be produced to close tolerances.
- EDM machine can be operated unattended for long time at high operating rate.
- Machining is done without requiring any skills.
- Any electrically conductive material can be machined irrespective of its hardness & strength.
- EDM allows the shaping of complex structures with high machining accuracy in the order of several micrometres.

1.4.6 Advantages of WEDM Process

Advantages of WEDM process are [15]:

- As continuously travelling wire is used as the negative electrode, so electrode fabrication is not required as in EDM.
- There is no direct contact between the work piece and the wire, eliminating the mechanical stresses during machining.
- WEDM process can be applied to all electrically conducting metals and alloys irrespective of their melting points, hardness, toughness or brittleness.
- Users can run their work pieces over night or over the weekend unattended.

1.4.7 Disadvantages of WEDM Process

Disadvantages of WEDM process are [15]:

- High capital cost is required for WEDM process
- There is a problem regarding the formation of recast layer
- WEDM process exhibits very slow cutting rate
- It is not applicable to very large work piece

1.5 MAJOR COMPONENTS OF WEDM

1.5.1 Work Table

In older WEDM machines, servo systems were used to move the work table but now linear motors have replaced servo systems in majority of the machines. Linear motors are superior to rotating motors in travelling speed and positional accuracy. These motors can

move with accuracy in increments of 1 micrometer. The linear motors and/or servo systems are the muscles of the work table enabling it to move along the programmed path [16]. The CNC system controls the motions of the work table and follows the inputs given to it through a program. The motion controllers works in partnership with the CNC system and the linear motors. They control the high-speed and high-precision motions of linear motors based on commands from the CNC units. The motion controllers tell the work table where it is in comparison to the electrode. The entire system works on the principal of the Cartesian coordinate system. Every point within the work table of the machine can be defined and located thus enabling it to follow a given path allowing it to cut the programmed part. These CNC systems make WEDM machines highly reliable and productive [17].

1.5.2 EDM Wire: The Electrode

EDM wire is the tool of the Wire EDM and it never makes contact with the material being machined. The work piece and the wire represents positive and negative terminals respectively in a DC electrical circuit and are always separated by a controlled gap. This gap is being filled with deionized water which acts as an insulator and cooling agent and also flushes away the eroded particles from the work material [16]. The wire is continually being fed vertically through the work piece while the work piece is moved along a horizontal plane. The resultant motion along this horizontal plane cuts a slot through the work piece that is slightly larger than the diameter of the wire [17].

Wire is typically perpendicular to the surface of the work piece, except when tapers are being machined, in which case the wire can pass through the material at an angle of up to 30 degrees [16].

Wire selection basically depends on the properties of work piece material, however an ideal wire electrode should possess following characteristics, i.e. high electrical conductivity; sufficient mechanical strength (tensile strength, elongation etc.) and optimum spark and flushing characteristics [17, 18].

Impact of these characteristics has been explained below: [17, 18]

- A high conductivity rating is important because, at least theoretically, it means the wire can carry more current, which equates to a “hotter” spark and increased cutting speed.

- Mechanical strength, typically stated as tensile strength, needs to be sufficient to maintain wire straightness, with minimal vibration, under the tension applied by the machine’s wire feed mechanism. There are some practical limitations, since the high hardness sometimes associated with cold-drawn, high tensile strength wires can result in a “kinky” or “springy” wire which is not suitable for high taper angles or automatic wire threading.

- The ability of the wire material to enhance spark formation and the flushing process has become increasingly important with the growing need for both higher productivity and accuracy. It is highly desirable for the wire to erode, or wear, because the vaporized wire material aids in the formation of subsequent spark ionization channels. In addition, a higher degree of vaporization into microscopic particles, rather than melting, greatly improves the efficiency of the flushing process and, by suppressing arcing, the stability of the cut.

Types of wires:

- Copper: The first material used in the production of EDM wire was copper. Copper possesses excellent conductivity rating, low tensile strength, high melting point and low vapour pressure rating which severely limited its potential [17]. As the power supplies and controllers for the wire-EDM became more sophisticated, they exceeded the capabilities of the pure copper wire [16].

- Brass: As new materials and demands came, developers subsequently experimented with the use of brass in order to meet the new demands. Brass is an alloy of copper and zinc. Generally, the higher the zinc percentage, the better the wire is for EDM. However, if the zinc concentration is too great, the wire may become difficult to fabricate consistently. The optimum balance between copper and zinc is an alloy in the range of 35–37% zinc and 63–65% copper [3]. Brass quickly became the most widely used electrode material for general purpose wire

EDM. It is now commercially available in a wide range of tensile strengths and hardness [17].

- Coated Wires: These wires are also called as plated or “stratified” wire or speed wires as they offer higher Metal removal rate [17]. Brass wires cannot efficiently be produced with higher percentages of zinc than those that have been listed above, therefore a brass or copper wire core is coated with zinc in order to obtain the desired properties that are provided by zinc while maintaining sufficient levels of tensile strength and conductivity along with enhanced the properties of spark formation and flushing [16].

- Fine Wires (Molybdenum & Tungsten): These wires are being used for high precision work on wire EDM machines, requiring small inside radii and thus wire diameters in the range of 0.001 - 0.004. Since brass and coated wires are not practical, due to their low load carrying capacity in these sizes, molybdenum and tungsten wires are used. These wires possess low conductivity, high melting points and low vapour pressure ratings, therefore these are not suitable for very thick work and have low metal removing rates if used [17].

1.5.3 Electric Discharge Power Unit: The Spark Generator

The electrical discharge power unit is the system that controls the electricity so that it is delivered to the electrode in the appropriate amounts and at the correct time. A series of voltage pulses (as shown in figure 1.8) of magnitude about 20 to 120 V and frequency on the order of 5 kHz is applied between the two electrodes, which are separated by a small gap, typically 0.01 to 0.5 mm [1].

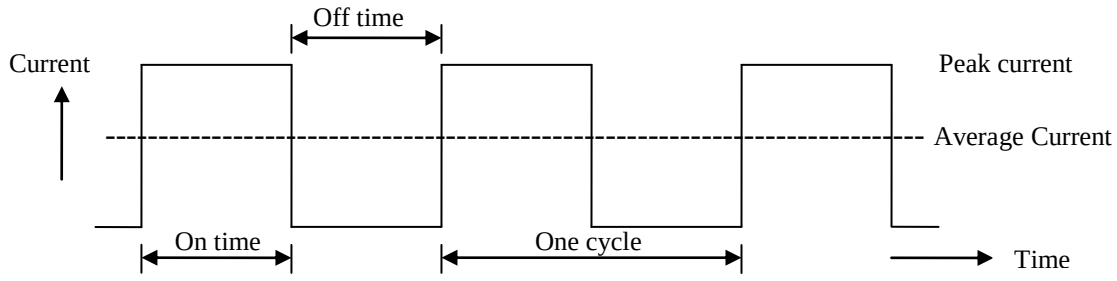

Figure 1.8 Typical EDM pulse current train for controlled pulse generator

The system executes this function by controlling the on-time, the off-time, and the amperage that is run through the electrode. A single cycle of the EDM process is the combination of the on-time and the off-time (shown in figure 1.8). This time is measured in microseconds (μ sec) [16]. A basic representation of the electrical circuit is shown in Figure 1.9.

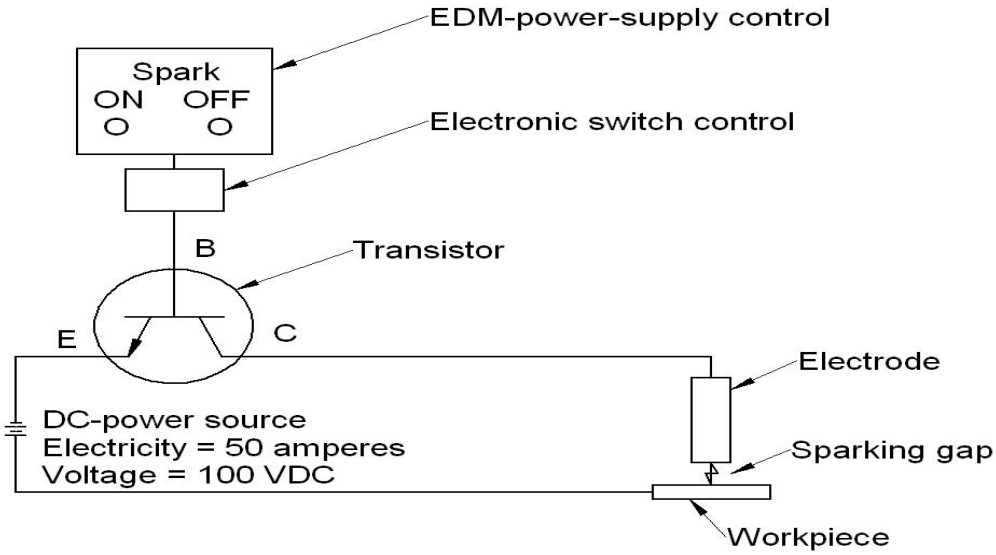

Figure 1.9 Basic electrical circuit [16]

The on-time is defined as the time when the current is turned on. During this time several things are happening. The voltage increases until it has a sufficient amount of energy to align the few ions and microscopic particles in the dielectric fluid and jump the spark gap between the electrode and the work piece. Once the spark connects the two pieces the voltage decreases and the amperage increases [16]. The material that is in direct contact with the spark is vaporized, and a gas bubble is created around the spark. At some point, enough of the spark energy is used so that vaporization ceases and melting begins. At this point, power is turned off thus beginning the off-time. The bubble that formed around the spark now implodes, pulling most of the molten metal out of the crater created by the spark. The size of the crater depends on the energy turned out by the spark generator. The range of the sparks varies from a few microns to 1 mm [17]. It is extremely important for the gap between the electrode and the work piece to be kept constant. In order to achieve the required surface finish values, the gap should be kept as small as possible. Currently, the computer-aided spark generators are used to control the spark. Dielectric fluid rushes

in and cools the affected areas. The compromised dielectric fluid and the debris are flushed out of the kerf allowing the process to begin again [1, 16].

1.5.4 Dielectric Fluid and its Filtration

The vast majority of wire-EDM machines use deionized water for the dielectric fluid as Oil, which is normally used as a dielectric fluid in vertical or plunge EDM, does not cool down the part surface as quickly as water does and thus microscopic cracks occurs on the surface of work piece [16]. The electrolysis effect is proportional to the conductivity of the water (i.e., its ion content). The ions may be invisible, but they make their presence felt by increasing the solution's electrical conductivity. That's why water must be deionized to ensure it contains as few ions as possible [3].

The main functions of the dielectric fluid are [1]:

1. It acts as an insulator between the electrode and work piece.
2. It acts as cooling agent for the electrode and work piece.
3. It offers cooling to the vaporized material that becomes the EDM chip upon solidification.
4. Flush the eroded particles from the machining gap.

As the dielectric fluid gets contaminated because of creation of ions which results from the EDM process fresh dielectric fluid needs to be introduced into the cutting environment. Flushing is the process of introducing clean dielectric fluid into and through the spark gap. This serves several purposes like:

- introduces fresh dielectric to the cut for reionization
- flushes away the chips and debris from the spark gap
- cools the electrode (or wire) and work piece

Flushing of the dielectric plays a major role in the maintenance of stable machining and the achievement of close tolerance and high surface quality. Inadequate flushing can result in arcing, decreased electrode life and increased production time [1].

- *Filtration*

In order to maintain the quality of the dielectric fluid, wire-EDM utilizes two different filtration processes [16]:

1. Mechanical filtration, which filters out the particles that have contaminated the dielectric fluid. Common mechanical filtration systems are disposable paper filters, permanent paper media, plastic cartridge filters, diatomaceous earth filters, electrostatic filtration, and centrifuge.
2. Chemical filtration, which removes the ions from the dielectric fluid which were created through the EDM process.

1.6 WEDM PROCESS PARAMETERS AND RESPONSE VARIABLES

The main goals of WEDM are to achieve a better stability and higher productivity. As newer and more exotic materials are developed, and more complex shapes are required, conventional machining operation will continue to reach their limitations and the increased use of WEDM in manufacturing will continue to grow at an accelerated rated [19]. However, due to a large number of variables in WEDM, it is difficult to achieve the optimal performance of WEDM processes and the effective way of solving this problem is to establish the relationship between the response variables of the process and its controllable input parameters [20].

1.6.1 Process Parameters

The process parameters for WEDM process are discussed below.

I. *Pulse duration (on time)*

During WEDM all the work is done during pulse duration (On time). The erosion rates are affected mainly by pulse parameter. The spark gap is bridged, current is generated and the work is accomplished [20]. The longer the spark is sustained, the higher is the material removal. Consequently the resulting craters will be broader and deeper; therefore the surface finish will be rougher. Obviously with shorter duration of sparks the surface finish will be better [19].

II. *Pulse interval (off time)*

While most of the machining takes place during on time of the pulse, the off time during which the pulse rests and the re-ionization of the die-electric takes place, can affect the

speed of the operation in a large way [21]. Longer is the off time greater will be the machining time. But this is an integral part of the EDM process and must exist. The off time also governs the stability of the process. An insufficient off time can lead to erratic cycling and retraction of the advancing servo, slowing down the operation cycle. In addition, the interval time also provides the time to clear the disintegrated particles from the gap between the electrode and work piece for efficient cut removal. Too short pulse interval will increase the relative wear ratio and will increase the surface roughness of the machine surface [19].

III. *Peak current*

Peak current is also another important primary input of WEDM process. The stronger the discharge current, MRR, overcut and surface roughness will increase. In other hand, decrease the rate of electrode wear [21]. To minimize the electrode wear and keep the current density between the tolerance limit it is necessary to select an appropriate value of current.

IV. *Servo voltage*

The preset voltage determines the width of the spark gap between the leading edge of the electrode and the work piece. High voltage settings increase the gap and hence the flushing and machining. Some material may be necessary for high open-open voltage due to high electrical resistance and high discharge voltage [22].

V. *Wire feed*

The rate at which the wire electrode travels and continuously fed along the wire guide path for continuous sparking is called wire feed. The wire feed range available on the present WEDM machine is available in two levels, i.e. low (4 m/sec) and high speed (11 m/sec). Maximum wire feed is required in order to avoid wire breakage, to have better machining and better material removal rates.

VI. *Wire tension*

The amount of stretch in the wire between the upper and lower wire guides is called the wire tension and it is measured as gram equivalent load. In order to keep wire straight between two guides wire is kept continuously kept under tension. Wire tension is directly proportional to the thickness of the workpiece, i.e. more the thickness of workpiece more

is the tension required. Improper setting of tension may result in the inaccuracies as well as wire breakage.

1.6.2 Response Variables

WEDM performance is mainly measured by the material removal rate (MRR), gap current, kerf width and surface roughness of the work piece that has been machined. These four machining characteristics have been identified by the previous researchers as the most significant machining criteria that can influence the WEDM performance [23-25]. The process parameters should be chosen properly so as to have maximum MRR, minimum roughness value and minimum width of cut [19-21].

The response variables for WEDM process are discussed below.

I. *Material removal rate (MRR)*

The material removal rate (MRR) of the workpiece is the amount of the material removed per minute. MRR and Cutting speed capabilities of WEDM have increased enormously over the years. They are influenced by the age and type of machine along with the properties and characteristics of the workpiece being cut [16]. The machine settings set by the operator and programmer also affect the MRR and cutting speed.

II. *Surface roughness(SR) or surface finish*

The smoothness of the part surface machined by a given process is referred to as surface finish. No standard has been universally adopted for measuring the surface finish of parts. Different methods for calculating the numerical representation of the surface finish and the typical units used to define the measurements is shown in table 1.2.

Table 1.2 Commonly Used Surface Finish Measurements

Scale	**Definition**	**Unit***
RMS	Root Mean Square	µin.
AA	Arithmetic Mean (average)	µin. or µm
R_a	Roughness Average	µin. or µm
H_{max}	Maximum Roughness Depth	µin. or µm
R_{max}	Maximum Roughness Depth	µin. or µm

*1 µin. = 1/1,000,000 inches or 0.025 µm

1 µm = 1/1,000,000 meter or 40 µin.

The standard which is utilized in the United States is the Roughness Average (R_a). This is defined as the arithmetic average of all departures of the roughness profile from the centerline of the evaluation length. It is also known as the arithmetic average (AA) and the centerline average (CLA). The finest surface finishes will be of the order of R_a 0.10 (µm), and the visual effect is almost like a mirror finish [16].

III. *Kerf width(KW)*

Kerf width is one of the important performance measures in WEDM. It is the measure of the amount of the material that is wasted during machining and determines the dimensional accuracy of the finishing part. The internal corner radius to be produced in WEDM operations are also limited by the Kerf width. In setting the machining parameters, the main goal is the maximum MRR with the minimum Kerf width [26]. The detailed section of the Kerf width is shown in figure 1.10.

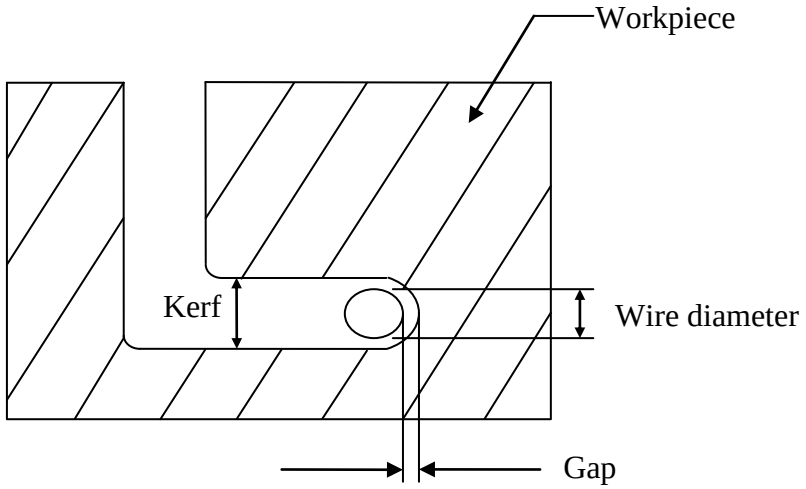

Figure 1.10 Details of kerf width

During WEDM processes, sparking occurs between the side and machine surface of the workpiece. The sparking area consists only the front of the electrode diameter (180^o) as it progress into the cut while the clearance is equal to the spark length of the wire electrode [28]. Each spark forms an ionization channel under extremely high heat and pressure resulting in vaporization of localized sections. The vaporized metallic debris created by this process, from both the workpiece and wire material, is subsequently quenched and

flushed away by the flow of dielectric fluid through the gap [17]. Correlation between the machining parameters and kerf width has been established for determining the WEDM performance [29].

IV. *Gap current*

In WEDM machining a small amount of gap as shown in figure 1.10 is maintained between the job and the electrode wire. A pulse of current is generated by the pulse generator in order to start the cutting process and the current that passes through the material is measured which is called the gap current.

1.7 ORGANIZATION OF THESIS

- Chapter 1 covers brief introduction to non-conventional machining, principle of Wire electric discharge machining (WEDM), mechanism of material removal, WEDM components and process parameters of WEDM.

- Chapter 2 presents an available literature of WEDM process. The available literature has been categorized in two broad classifications i.e. literature based on experimental work and optimization. Summary of the literature and gap in literature also discussed.

- Chapter 3 presents the area of research work to be undertaken has been identified. Objective and work plan also discussed. Methodology to be adopted also described in brief.

- Chapter 4 presents the analysis and results of the response variables. Results after the Analysis of Variance (ANOVA) and Taguchi Signal-to-Noise ratio are outlined in this chapter. Main effect plots for different response variables are discussed in this chapter. Optimal design conditions have been discussed.

- Chapter 5 presents the conclusions and recommendations from the experimental work.

CHAPTER 2

LITERATURE REVIEW

2.1 LITERATURE REVIEW: BASED ON EXPERIMENTAL WORK

Huang et al. [19] performed WEDM operation on SKD11 alloy steel with Brass wire as electrode (0.25 mm diameter). Influence of various machining parameter such as pulse-on time, pulse-off time, table feed-rate, flushing pressure, distance between wire periphery and work piece surface, and machining history has been observed on the machining performance of WEDM in finish cutting operations. The parameters measured during experiment are gap width, the surface roughness and the white layer depth and the same have been evaluated using Taguchi quality design and numerical analysis technique. It has been thus found out that pulse-on time and the distance between the wire periphery and the work piece surface are two factors which affect the machining performance significantly. Algorithmic methodology has been proposed to chalk out a strategy for obtaining optimal multi-cut and machining parameters. The proposed approach as compared with that of a well-skilled operator offers a better surface quality and less machining time with greater accuracy.

Mohammadi et al. [30] investigated the effect of various process parameters for Turning WEDM such as power, time-off, voltage, servo, wire tension, wire speed along with rotational speed on surface roughness and roundness. 1.731 cemented steel was chosen as work piece material. Taguchi standard orthogonal array was chosen for the design of experiments and ANOVA was used for determining level of importance of machining parameters on surface roughness and roundness. Experimentation result shows that power has significant effect on surface roughness and other factors do not impact the surface roughness and other factor do not have significant effect on roundness. Factors affecting the surface roughness are power, wire speed, voltage, wire tension, time-off, servo, and rotational speed affect the surface roughness. If comparison is done then it has been shown by experiments that wire speed, power, and servo effects roundness more significantly than time-off, voltage, wire tension, and rotational speed. Thus a multiple linear regression equation had been derived for surface roughness.

Liao and Yu [20] proposed Specific Discharge Energy (SDE), which is defined as the real energy required removing a unit volume of material. Experiments were conducted on number alloys using brass wire for different control parameters of discharge on time, off time, arc on time, arc off time, servo voltage, thickness, wire speed and flushing pressure. A relative relationship has been established for SDE between different materials and it has been observed that SDE for different material is fixed as long as these materials are machined under the same machining conditions. Materials having very close value of SDE show similar machining characteristics. Discharge gap and discharge shows an inverse relationship. As the material removal is increased, efficiency of material decreases with an increase in discharge on time. For higher value of SDE, surface roughness becomes better. Thus it has been identified that SDE characteristics helps in determining parameter settings for different materials.

Kim [24] presented a relationship between electrical conductivity of a dielectric fluid, metal removal rate and surface quality in a WEDM process. One Low Carbon Steel specimen and three specimens of Carbide grades G10, G20 & G30 were chosen as work piece material for experimental analysis and electrode used was brass wire. Dielectric used during the experiments was of different electric conductivity. Experimental results show that carbide with low cobalt shows higher metal removal rate. Water having high electrical conductivity gives high MRR but poor surface finish, thus it has been verified by experiments that ideal conductivity varies from 5 to 10 μS/cm to avoid corrosion and to have fine surface finish. Finally it has been concluded that some wire electrode material gets deposited onto the work piece and some of the work piece material also gets deposited on wire electrode.

Singh and Garg [21] investigated MRR of hot die steel (H11) by varying various process parameters such as pulse on time (TON), pulse off time (TOFF), gap voltage (SV), peak current (IP), wire feed (WF) and wire tension (WT) and also predicted optimal values for these process parameters to maximize MRR. Wire electrode used for experimental analysis was Brass wire (0.25 mm diameter). It has been found out by experiments that Wire feed and wire tension have no effect on MRR and are taken as neutral parameters where as pulse on time and peak current are directly proportional to MRR. Pulse off time and servo voltage has an inverse relation with the MRR.

Kim and Hur [31] investigated MRR and Surface roughness characteristics of a PCD blank (work piece material) machined by WEDM. Influence of discharge frequency and pulse width were related to the above said response parameters. The Experimental results were studied by comparing Scanning Electron Microscope (SEM) photographs with Energy Dispersive Spectrometers (EDS). Experimental analysis concluded that WEDM is a reliable process for machining PCD and with optimized parameters better MRR and Surface Roughness can be achieved. From EDS analysis, it has been shown that some amount of electrode material gets deposited on work piece material during WEDM and some elements of work piece can also be seen on wire electrode.

Juhr et al. [32] developed a new needle-pulse energy source for WEDM process for cemented carbide work piece. Performance parameters chosen for WEDM process were Pulse duration, current magnitude and pulse energy. Experiments were conducted and it has been observed that correct parameters should be used for main cut and post cuts. Materials deteriorating by high pulse energy can be corrected and pulse durations <500 ns can be used without any problem. Material properties of cemented carbide improve after WEDM process and it is proved by an increase in the bending fraction stress. It has also been proposed that post cuts increasing the total productivity of the machining and significantly lowering the costs.

Peng and Liao [33] proposed a strategy to slice a semiconductor material by using WEDM process. Semiconductor material chosen for experimentation was Silicon Ingot and complete feasibility study for the process was done before conducting experiments. Experiments were performed for different machine settings of current on time, current off time, water pressure and wire tension and response parameters observed were kerf ratio, average cutting speed and surface roughness. It has been observed that if wafer thickness if 1mm and wire used is of 0.25 mm diameter the material losses due to kerf and polish are under 26%. It has also been proved experimentally that WEDM method can used for silicon slicing as long as the wafer required is small in size and surface roughness delivered by the process is reasonable along with satisfactory geometric errors.

Kapoor et al. [18] presented a study on different Wire electrodes which are being used in the industry and some high performance electrodes have been observed. It has been investigated that wire electrode contribute directly to cutting speed and dimensional

accuracy. Some of the electrodes studied are copper, brass and coated wire electrodes. It has been observed that for different materials different metal wire electrodes are preferred as they offer better response parameters such as better surface finish, higher MRR etc. Composite wires have replaced zinc coated wires. Wires having higher tensile strength offer breakage resistance and can be obtained at the expense of fracture toughness. Copper clad wires are used for tall workpieces. High performance wires offer better productivity but with certain limitations such as cost, flaking etc., also they cannot be used all WEDM machines.

Islam et al. [34] investigated the WEDM process for its dimensional accuracy. Mild steel 1040 is used as work piece material for the investigations and the wire material used is brass of 0.25 mm diameter. Process parameters for WEDM were varied to have obtained different results. Experimental results were analyzed by three different techniques namely traditional analysis, the Taguchi method, and Pareto ANOVA analysis. The effect of the process parameters was related to three different accuracy characteristics which are dimensional errors, flatness errors, and perpendicularity errors of corner surfaces. By using the results the input parameters were optimized for better dimensional accuracy. It has been proposed that dimensional accuracy in WEDM is not as much high as it has been anticipated. It has also been observed that wire tension is the only significant factor that leads to better dimensional accuracy and the input parameters are needed to be varied at different levels so as to maintain better dimensional accuracy.

Rakwal and Bamberg [35] performed experiments for machining of Germanium wafers using WEDM process. Molybdenum wire of two different diameters was used as electrode used during the process. The process parameters that have been varied were wire speed, voltage and capacitance, the response parameters that have been observed during the experiments were kerf and etch rates. Surface profiler and Scanning Electron microscopy is used to propose surface material characteristics for the wafers. Material wastage has been investigated for combination of different thin wire diameters. Two different chemical etchants were used to measure thickness of recast layer and quality of cleaning of wafers was analyzed with the help of Raman spectroscopy. It has been observed by performing experiments that use of thin wires offer advantage in terms of less material wastage. WEDM can slice germanium wafers at a much quicker rate than Wire Saws and WEDM do not create any damage in the form of micro cracks.

Hsue et al. [36] proposed a concept of discharge angle and also determined a mathematical expression for the same. Mathematical model for measuring MRR has been presented. The computed MRR is compared with measured sparking frequency of the process and a very good relation has been obtained. It has been observed that discharge-angle and MRR drop drastically to a minimum value and recover to same level of straight-path cutting slowly. Also variation of load has been calculated with relative to MRR. With an abrupt change of MRR, drastic variation of sparking frequency in corner cutting has been observed. It has been concluded that with a proper control of sparking frequency better geometrical accuracy can be achieved.

Patil and Brahmankar [22] investigated electrical and non electrical process parameters for machining metal matrix composite. The metal matrix composite chosen for this experiment is reinforced aluminium matrix composite and wire used is a brass wire of 0.25 mm diameter. Process parameters that have been chosen were reinforcement percentage current, pulse on-time, off time, servo reference voltage, maximum feed speed, wire speed, flushing pressure and wire tension whereas the response parameters were cutting speed surface finish, and kerf width. Taguchi design methodology has been used to study the effect of performance parameters on the response parameters. It has been observed that WEDM is a good process to machine metal matrix composites and reinforcement percentage current and pulse on time have significant effect on cutting rate, surface finish, and kerf width. Wire breakages have been observed for higher cutting speeds and also wire shifting leads to deterioration of the machined surface.

Plaza et al. [37] proposed two original models for the prediction of angular error in WEDM taper-cutting application. WEDM process variables for taper cutting have been identified as part thickness and angle. Work piece specimen used was AISI D2 tool steel and a copper wire of 0.25 mm diameter was used during the experiment. A quadratic regression equation has been determined to predict the angular accuracy. Angle obtained from the equation comes out to be 4′33″. And it has been proposed that equation can also be used to determine the angle that can be programmed in the NC machine. Mechanical behavior of the wire is investigated by performing finite element modeling of the wire and acute angle observed during the analysis was 4′52″. It has been shown by the above two models that angular error can be reduced below 3′45″ in 75% of cases and thus the

proposed models are much better than the trial and error models that are being used in the industry.

Rakwal et al. [38] investigated µ-WEDM process parameters for machining p-type silicon wafers with the help different wire electrodes. The different wire electrodes that have been chosen are Molybdenum, brass, tungsten & zinc coated steel wires of different diameters which vary from 0.05 to 0.25 mm diameter. The process parameters that have been selected for investigation are voltage and capacitance to measure slicing rate, kerf and surface roughness as performance parameters. Also two step etching process has been implied to remove the recast layer that has formed on the silicon electrode. SEM imaging was also done for the silicon electrodes and no micro cracks have been found. Also finite element analysis has been done to observe that electrode geometries should have less lateral rigidity so as to have minimum breakage. It has been observed that tapered electrodes have minimum bending stiffness and thus this shape of electrodes is preferred. Also it has been proposed that different coatings decrease the contact resistance of silicon and thus increased slicing rates can be achieved.

Murphy and Lin [39] developed a combined structural-thermal model using energy balance approach to describe the vibration and stability characteristics of an EDM wire. High-temperature effects were also included resulting from the energy discharges. The thermal field was used to determine the induced thermal stresses in the wire. An equilibrium and eigen value analysis (for small vibrations about the computed equilibrium) showed that the transport speed influenced the stability of the straight equilibrium configuration. The wire had an extended residency time in the kerf and the wire thermally buckled.

Dodun et al. [40] investigated the machining errors for WEDM which are obtained while machining sharp corners for small thickness work pieces. Work piece material used for experimentation was steel and aluminum alloy and a copper wire electrode of 0.25 mm diameter has been used for machining. The process parameters that have been varied are pulse on time, pulse off time, open voltage, wire axial tension and machining errors were studied which have been by machining with different set of values for process parameters. It has been observed that outside corners bend towards the direction of wire electrode. It

has also been proposed that machining error depends on the corner angle, α and the work piece thickness, h and for WEDM production process these errors should be corrected.

Han et al. [41] investigated various methods that are in practice to measure wire temperature of WEDM process but all these methods are just mathematical analysis. A relationship between the wire temperature and resistance has been established and thus a measuring system has been proposed so as to measure average temperature increment of wire electrode. It has been thus observed that average temperature increment of wire can be 130° C. During the measurement of temperature different discharge energies has been used and FEM analysis have been performed for the same. It has been observed that for very low discharge energy the system proposed is quite sensitive. Finally it has been proposed that temperature variation is effected by a combination of factors, such as energy density, kerf conditions, and flushing pressure, also the convective heat-transfer coefficient is also an important parameter for heat-transfer analysis of WEDM.

Spedding and Wang [42] attempted to optimize the process parametric combinations by modeling the process using artificial neural networks (ANN) and characterizing the WEDM machined surface through time series techniques. A feed-forward back-propagation neural network based on a central composite rotatable experimental design is developed to model the machining process. Optimal parametric combinations are selected for the process. The periodic component of the surface texture is identified and an autoregressive AR (3) model is used to describe its stochastic component.

Miller et al. [43] investigated the effect of spark on-time duration and spark on-time ratio on the material removal rate (MRR) and surface integrity of four types of advanced material; porous metal foams, metal bond diamond grinding wheels, sintered Nd-Fe-B magnets and carbon–carbon bipolar plates. Regression analysis was applied to model the wire EDM MRR. Scanning electron microscopy (SEM) analysis was used to investigate effect of important EDM process parameters on surface finish. Machining the metal foams without damaging the ligaments and the diamond grinding wheel to precise shape was very difficult. Sintered Nd-Fe-B magnet material was found very brittle and easily chipped by using traditional machining methods. Carbon–carbon bipolar plate was delicate but could be machined easily by the EDM.

Saha et al. [44] developed a second order multi-variable regression model and back-propagation neural network (BPNN) model for WEDM process. The process parameters chosen for the experimentation were pulse on-time, pulse off time, peak current, and capacitance with the performance measures namely cutting speed and surface roughness. Work piece material chosen was tungsten carbide-cobalt (WC-Co) composite material which has been machined with the help of uncoated brass wire of 0.25mm diameter. The effect of input parameters have been studied and correlated with that of results obtained from the above said models. Also SEM analysis has been performed for the same. Multi variable regression model yields an error of 6.02% while BPNN yields an overall error of 3.29% thus it has been observed that these models also exhibit the parametric effect on the cutting speed and surface roughness. It has been observed that increase in both peak current and capacitance lead to the increment of cutting speed and surface roughness. From the SEM imaging, micro cracks have been observed as loosely bound WC grains are present on the machined surface and with increase in energy levels these cracks also increase.

2.2 LITERATURE REVIEW: BASED ON OPTIMIZATION TECHNIQUES

Ramakrishnan and Karunamoorthy [45] performed experiments on heat-treated tool steel work piece using zinc coated brass wire for different cutting conditions of pulse on time, wire tension, delay time, wire feed speed, and ignition current intensity and these parameters have been optimized with the multi response characteristics of the material removal rate, surface roughness, and wire wear ratio. Taguchi methodology has been used for the measuring performance characteristics and ANOVA is used to identify the level of importance of the machining parameters on the multiple performance characteristics considered. Experimental studies conclude that the pulse on time and ignition current intensity have influenced more than the other parameters and material removal rate, surface roughness, and wire wear ratio for the WEDM process can be improved concurrently.

Mahapatra and Patnaik [23] identified discharge current, pulse duration, pulse frequency, wire speed, wire tension, and dielectric flow as the significant control parameters which affect the performance of Wire EDM during rough cutting operation, by using Taguchi's parameter design method. Work piece material taken for conducting experiment was D2 Tool Steel and wire taken is zinc coated copper wire. A non linear regression model has

been used for establishing a relationship between the control factors and response parameters such as MRR, SF and kerfs. Further Genetic Algorithm approach has been applied in order to optimize for maximization of MRR, SF as well as minimization of kerfs, separate models were developed and errors associated with MRR, SF and Kerf were found out to be 3.14, 1.95 and 3.72% respectively. It has been found out that genetic algorithm is a better method to optimize for global parameters instead of using traditional optimization techniques which are basically used for local optimal parameters. It has been thus concluded that different combinations of parameters lead to optimization of performance measure and thus the parameters can be adjusted for better MRR, Surface finish and cutting width simultaneously.

Kuriakose and Shunmugam [46] carried out experiments with titanium alloy (Ti-6Al-4V) and used a data-mining technique to study the effect of various input parameters of WEDM process on the cutting speed and SR. They reformulated the WEDM domain as a classification problem to identify the important decision parameters. In their approach, however, the optimal process parameters for the multiple responses need to be decided by the engineers based on judgment.

Datta and Mahapatra [25] proposed a quadratic mathematical model and conducted experiments by taking six WEDM process parameters: discharge current, pulse duration, pulse frequency, wire speed, wire tension and dielectric flow rate. Experiments were carried out on D2 Tool Steel using a Zinc coated Copper wire electrode. The response parameters noticed for each experiment were MRR, Surface Roughness and Kerf. A statistical analysis has been carried for each result and responses have been utilized to fit the quadratic model which represents the above said six parameters. Grey based Taguchi technique has been utilized to evaluate optimal parameter combination to achieve maximum MRR, minimum roughness value and minimum width of cut. It has been found out that for continuous quality improvement Grey based Taguchi method is a very reliable method to predict optimal parameter values and all the parameters involved in the experimentation are independent of each other.

Tzeng and Chiu [47] conducted experiments on castek-03 for medium carbon steel material having excellent wear resistance. The most important factors affecting the EDM process robustness were pulse on time, applied electric current in low voltage and

sparking current in high voltage. The most important factors affecting the machining speed were pulse on time and applied electric current in low voltage. The gain of 13.17 dB was able to decrease the variation range to 21.84%, which improved process robustness by 4.6 times.

Guven et al. [48] determined a model for WEDM process by using back-propagation (BPN) and General Regression Neural Networks (GRNN). Experiments were performed on a Steel Plate by using Brass wire of 0.25mm diameter. The variable process parameter chosen were Pulse duration, open circuit voltage, wire speed and dielectric flushing pressure and relation these parameters were compared for surface roughness and thus different relationships were observed for different set of data. Results for both BPN and GRNN were compared and it has been proposed that BPN modelling is better than GRNN as it has a better generalization ability and learning ability (with average error of 4.99 % and multiple coefficient of R2 of 99 %) than the GRNN (with average error of 6.04 % and multiple coefficient of R2 of 0.96).

Lin and Lin [49] reported the use of an orthogonal array, grey relational generating, grey relational coefficient, grey-fuzzy reasoning grade and analysis of variance to study the performance characteristics of the WEDM machining process. The machining parameters (pulse on time, duty factor and discharge current) with considerations of multiple responses (electrode wear ratio, material removal rate and surface roughness) were effective. The grey-fuzzy logic approach helped to optimize the electrical discharge machining process with multiple process responses. The process responses such as the electrode wear ratio, material removal rate and surface roughness in the electrical discharge machining process could be greatly improved.

Kumar et al. [50] proposed a combined model of Taguchi method and Grey Relational Analysis to optimize process parameters of WEDM for machining of Incoloy800 super alloy (Work Piece material) by using a Brass Wire electrode of 0.25 mm diameter. The process parameters chosen for the experimental analysis were Gap Voltage, Pulse On-time, Pulse Off-time and Wire Feed and response parameters measured were Material Removal Rate (MRR), surface roughness and Kerf. Experimental results show that optimal values for machining Incoloy 800 are 50 V Gap Voltage, 10 μs pulse on-time, 6 μs pulse off-time and 8 mm/minute Wire Feed rate. It has also been observed that Grey-

Taguchi Method is most ideal and suitable for parametric optimization of multiple performance characteristics such as MRR (Material Removal Rate), Surface Roughness and kerf width. It has also been proposed that mathematical models can be used in estimating the material removal rate, surface roughness and kerf width without conducting experiments.

Parashar et al. [51] proposed suitable machining parameters for Stainless Steel 304L by using WEDM process. Optimization was done on the basis of Taguchi's dynamic design and the parameters which have been varied are gap voltage, pulse ON time, pulse OFF time, wire feed and dielectric flushing pressure. Experiments were conducted for different combination of these parameters to observe Surface Roughness. From this experimental data signal to noise ratio was applied to measure the performance characteristics deviating from the actual value. It has been observed that Pulse On Time is the most significant parameter for surface roughness and wire feed has least impact on value of surface roughness. Optimal values for smooth cutting and better surface finish have been proposed. It has also been observed that Taguchi's parameter design is a simple, systematic, reliable and efficient tool for optimizing the performance characteristics of WEDM process parameters.

Mahmood et al. [52] applied regression modeling analysis to develop a relationship between various input and response parameters of WEDM process. Experiments were conducted on different work piece materials i.e. Steel, Brass, Copper and Tungsten and the wire electrodes used were cobra cut A, cobra cut D, Molybdenum and Tungsten. Mathematical models were developed for investigating cutting speed. SSE (sum of square error), MSE (mean square error), coefficient of determination and PRESS statistics act as the selection criteria for the models. Error ratio has been proposed which can be used in case MSE, PRESS and other traditional plots fail to observe suitability of the model. Finally it has been concluded that there exists a complex relationship between input and output parameters of WEDM process and generalized linear modeling can easily represent this relationship.

Kanlayasiri and Boonmung [26] investigated influences of wire-EDM machining variables on surface roughness of newly developed DC 53 die steel of width, length, and thickness 27, 65 and 13 mm, respectively. The machining variables included pulse-on

time, pulse-off time, pulse-peak current, and wire tension. The variables affecting the surface roughness were identified using ANOVA technique. Results showed that pulse-on time and pulse-peak current were significant variables to the surface roughness of wire-EDMed DC53 die steel. The maximum prediction error of the model was less than 7% and the average percentage error of prediction was less than 3%.

Pasam et al. [53] developed a mathematical model by using linear regression analysis in order to present a relationship between control parameters and response parameters. Titanium alloy is chosen as work piece material. Control parameters which have been varied are Ignition pulse current, Short pulse duration, Time between two pulses, Servo speed, Servo reference voltage, Injection pressure, Wire speed and Wire tension and the response parameter studied for the above parameters is surface roughness. Genetic algorithm modeling has been used to optimize the process parameters for surface roughness. Regression coefficient of 0.943 is obtained for surface roughness model by regression analysis and surface roughness of 1.85 μm is obtained with selected optimum control parameters in the WEDM of Ti6Al4V alloy.

Gauri and Chakraborty [54] investigated results of various multiresponse optimisation methods for WEDM process. Experimental data was taken from various research papers and various multi response approaches such as Grey Relational Analysis (GRA), Multi response Signal to Noise (MRSN) ratio, Weighted Signal to Noise (WSN) ratio, and VIKOR methods have been applied in order to establish relationship between process parameters and the response parameters so as to obtain optimal values for the same. It has been thus observed that out of all these approaches i.e. GRA, MRSN ratio, WSN ratio, and VIKOR; results of WSN ratio approach leads better overall quality and thus better optimal values.

Saha et al. [55] considered four input parameters such as pulse on-time, pulse off-time, wire feedrate, and average gap voltage for WEDM process whereas the performance parameters that have been measured are cutting speed and kerf width. Work piece material chosen is 5% volume TiC/Fe in situ metal matrix composite (MMC). It has been observed that TiC particles and formation of Fe_2O_3 makes the machining process unstable, thus modelling of the process was done by Normalized Radial Basis Function Network (NRBFN) with enhanced k-means technique and NRBFN with traditional k-

means technique. From the experiments and its parametric study results it has been observed that pulse on time has less effect on cutting speed and kerf width compared to average gap voltage.. As the gap voltage increases cutting speed decreases and kerf width increases. It has been concluded from the parametric study that NRBFN with enhanced k-means technique yields better results that NRBFN with traditional k-means technique.

2.3 IDENTIFIED GAPS IN THE LITERATURE

- After a comprehensive study of the existing literature, a number of gaps have been observed in machining of WEDM.
- Literature review reveals that the researchers have carried out most of the work on WEDM developments, monitoring and control but very limited work has been reported on optimization of process variables.

- The effect of machining parameters on Stainless Steel grades AISI 304, AISI 410, hot working tool steel H21 and EN31 has not been fully explored using WEDM.

- Most of the research work on Wire EDM has been performed by using Brass Wire alone and very less work has been done by using other wire electrodes such as Molybdenum.

- Multi-response optimization of WEDM process is another thrust area which has been given less attention in past studies.

So in the thesis work it is proposed to study the effect of different input parameters, namely, current, workpiece material, pulse on time and pulse off time on the MRR, surface roughness, kerf width and gap current. The effect of various input parameters on output responses have been analyzed using Analysis of Variance (ANOVA) in order to establish optimal levels process variables parameters for WEDM.

2.4 OBJECTIVE OF THE PRESENT STUDY

- Investigation of the process parameters of WEDM process and their levels.

- Selection of different materials to be used for experimentation.

- To determine the effect of process parameters that influences the machining responses during (WEDM) of different materials by using Molybdenum wire electrode.

- To evaluate the performance of Wire Electro-Discharge Machining (WEDM) on different materials with respect to various response variables such as gap current, material removal rate, surface finish and kerf width and to determine significant process parameters using Taguchi's technique.

- Multi-objective optimization of the process parameters of WEDM process using Analytic Hierarchy Process and to establish optimal design model for Material removal rate (MRR), surface roughness (SR) and kerf width (KW) during WEDM of different materials.

CHAPTER 3

DESIGN OF STUDY & PILOT EXPERIMENTATION

3.1 INTRODUCTION

A large number of input process parameters can be varied in the WEDM process, each having its own impact on output parameters such as Material Removal Rate (MRR), surface roughness, kerf width etc. Various input parameters are:

a. Pulse on-time
b. Pulse off-time
c. Peak current
d. Servo voltage
e. Wire tension
f. Wire feed
g. Dielectric flushing pressure

The effect of each of these parameters on WEDM process is discussed in the literature review in detail. It is also known from the previous research works that out of the above listed parameters, four parameters directly affect the MRR, surface roughness, kerf width and gap current in WEDM. These four parameters are peak current, pulse on-time, pulse off-time and servo voltage. Out of these parameters, three parameters have been investigated thoroughly in this research work. Servo voltage along with other parameters has been kept constant for the whole experiment. The levels of three parameters (i.e. pulse on, pulse off & peak current) for the experimentation have been decided from the machine software.

3.2 EXPERIMENTAL DESIGN METHODOLOGY

The full factorial design is referred as the technique of defining and investigating all possible conditions in an experiment involving multiple factors while the fractional factorial design investigates only a fraction of all the combinations. Although these approaches are widely used, they have certain limitations: they are inefficient in time and cost when the number of the variables is large; they require strict mathematical treatment in the design of the experiment and in the analysis of results; the same experiment may have different designs thus produce different results; further, determination of contribution of each factors is normally not permitted in this kind of design. The Taguchi

method has been proposed to overcome these limitations by simplifying and standardizing the fractional factorial design. The methodology involves identification of controllable and uncontrollable parameters and the establishment of a series of experiments to find out the optimum combination of the parameters which has greatest influence on the performance and the least variation from the target of the design. The effect of various parameters (work piece material, electrode, pulse on time, pulse off time, current and powder) and some of the effects of interactions between the main factors were also be studied using parameterization approach developed by Taguchi.

3.3 PROCEDURE OF EXPERIMENTAL DESIGN

The whole procedure of Taguchi method is as under.

1. Establishment of objective functions.
2. Selection of factors and/or interactions to be evaluated.
3. Identifications of uncontrollable factors and test conditions.
4. Selection of number of levels for the controllable and uncontrollable factors.
5. Calculation total degree of freedom needed
6. Select the appropriate Orthogonal Array (OA).
7. Assignment of factors and/or interactions to columns.
8. Execution of experiments according to trial conditions in the array.
9. Analyze results.
10. Confirmation experiments

3.4 ESTABLISHMENT OF OBJECTIVE FUNCTION

As the objective of this research work is Multi Response Optimization of WEDM which is carried out by varying machining parameters such as pulse on time, pulse off time, peak current and work piece materials in order to find out their impact on the response variables which are the MRR, surface roughness, kerf width and gap current while other parameters kept constant during the whole experimentation.

3.5 DEGREE OF FREEDOM (DOF)

The number of factors and level for factors determine the total degree of freedom required for the entire experiment. The degree of freedom for each factor is given by the number of levels minus one.

dof for each factor : k-1

where k is the number of level for each factor

3.6 SELECTION OF FACTORS AND THEIR LEVELS

The determination of which factors to investigate depends on the responses of interest. The factors which affect the responses were identified using cause and effect analysis, brainstorming and pilot experimentation. The factors selected can be summarized as follows:

a. Four levels of peak current
b. Four levels of pulse on-time
c. Two levels of pulse off-time

Selected levels of the process parameters for the present work are shown in table 3.1.

Table 3.1 Selected levels of the process parameters

Process parameters	Symbols	Units	Levels Selected			
			Level 1	Level 2	Level 3	Level 4
Peak Current	I_P	A	1	2	3	4
Pulse On time	T_{on}	µs	30	35	40	45
Pulse Off time	T_{off}	µs	150	180	-	-

Apart from these parameters, two different work pieces have been used each set of experiment, thus making it a fourth variable for the experimentation. Workpieces used for experiment 1 and 2 are given in table 3.2.

Table 3.2 Details of work pieces

Set No.	Work Piece, W1	Work Piece, W2
1	AISI 304	AISI 410
2	EN 31	H21

Thus the orthogonal array was to be selected for four variables (namely peak current, pulse on-time, pulse off-time and material) which would constitute the orthogonal array.

In this experiment, there are two parameters at four levels each and two parameters of two levels each. The degree of freedom (DOF) of a four level parameter is 3 (number of levels - 1) and DOF for two level experiment is 1 (number of levels – 1), hence total DOF for the experiment is 8 (3+3+1+1). The most suitable Orthogonal Array (OA) that can be used is L16 (table 3.1) having 15 dof. The additional seven dof were used to measure the random error.

The total dof for the experiment is given in table 3.3.

Table 3.3 Degree of freedom

Factor	Peak Current, A	Pulse on time, B	Material, C	Pulse off time, D	Total
DOF	3	3	1	1	8

3.7 ORTHOGONAL ARRAY

OA plays a critical part in achieving the high efficiency of the Taguchi method. OA is derived from factorial design of experiment by a series of very sophisticated mathematical algorithms including combinatorics, finite fields, geometry and error-correcting codes. The algorithms ensure that the OA to be constructed in a statistically independent manner that each level has an equal number of occurrences within each column; and for each level within one column, each level within any other column will occur an equal number of times as well. Then, the columns are called orthogonal to each other. OA's are available with a variety of factors and levels in the Taguchi method. Since each column is orthogonal to the others, if the results associated with one level of a specific factor are much different at another level, it is because changing that factor from one level to the next has strong impact on the quality characteristic being measured. Since the levels of the other factors are occurring an equal number of times for each level of the strong factor, any effect by these other factors will be ruled out. The Taguchi method apparently has the following strengths:

1. Consistency in experimental design and analysis.
2. Reduction of time and cost of experiments.
3. Robustness of performance without removing the noise factors.

The selection of orthogonal array depends on:

- The number of factors
- The number of levels for the factors of interest

Taguchi's orthogonal arrays are experimental designs that usually require only a fraction of the full factorial combinations. The arrays are designed to handle as many factors as possible in a certain number of runs compared to those dictated by full factorial design. The columns of the arrays are balanced and orthogonal. This means that in each pair of columns, all factor combinations occur same number of times. Orthogonal designs allow estimating the effect of each factor on the response independently of all other factors. Once the degrees of freedom are known, the next step, selecting the orthogonal array (OA) is easy. The number of treatment conditions is equal to the number of rows in the orthogonal array and it must be equal to or greater than the degrees of freedom. The interactions to be evaluated will require an even larger orthogonal array. Once the appropriate orthogonal array has been selected, the factors can be assigned to the various columns.

3.8 DESCRIPTION OF WEDM, ELECRODE, DIELECTRIC AND MATERIALS

3.8.1 Machine

The machine used for experiments is Concord United Wire EDM, Model-DK7740CH, incorporated with reusable molybdenum wire technology which is installed at M/s J. S. Engineering Works, Patiala, Punjab as shown in figure 3.1.

Figure 3.1 Wire Electric Discharge Machine

The machine consists of a coordinate worktable, wire running system (figure 3.2), wire frame (figure 3.3), Micro computer based control cabinet and dielectric supply system (figure 3.4). In this machine reusable molybdenum wire is used to perform cutting operation and wire is wound and stored a wire drum which can rotate at a speed of 1500 rpm. Guide pulleys are mounted on wire frame and wire can run through these guide pulleys at a speed of 11 m/sec in reversible directions alternatively. Work piece is mounted on the worktable with the help of clamps and bolts and the micro controller delivers the pulse signals to the servo motors which rotates accordingly and through the variable gears, lead screws and nuts, these motions will be transmitted to the worktable for performing the cutting operation.

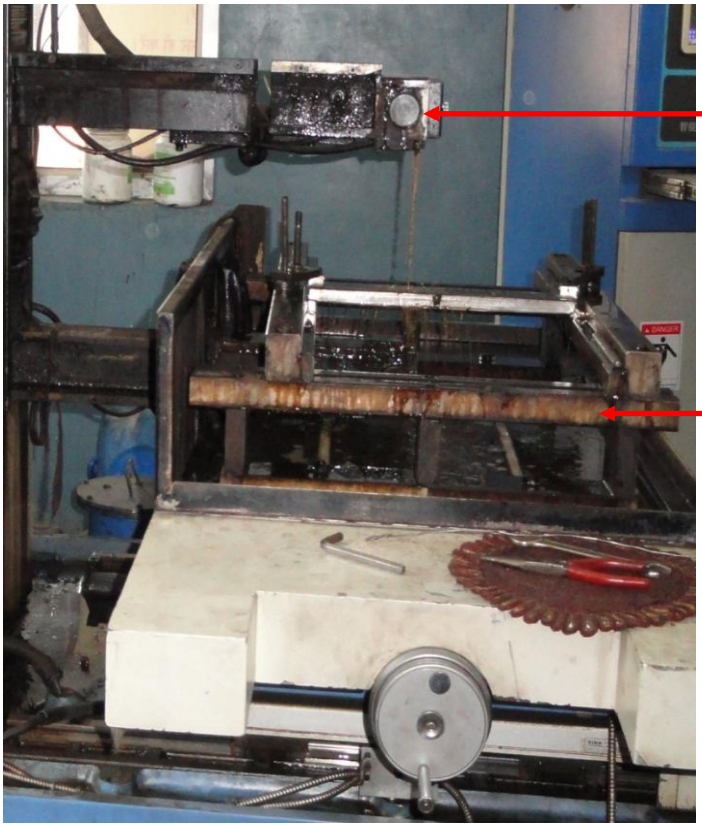

Figure 3.2 Coordinate work table and wire frame

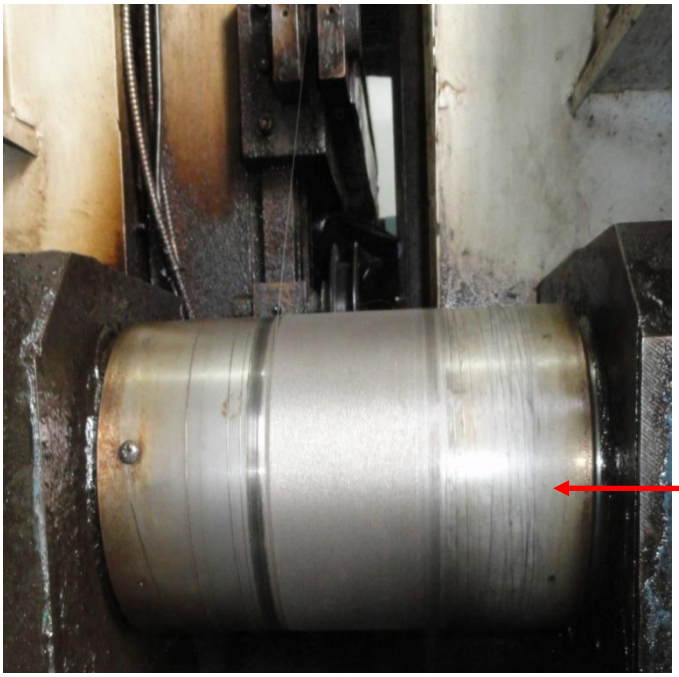

Figure 3.3 Wire running system

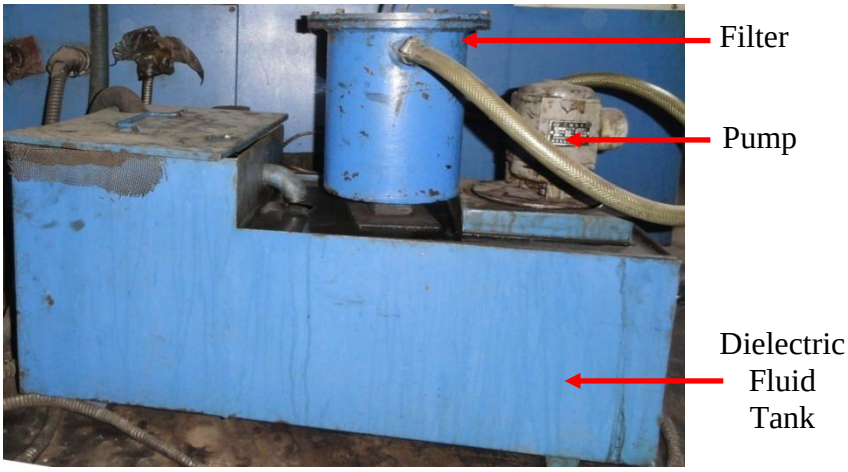

Figure 3.4 Dielectric supply system

Programming, controlling, pulse power supply and electric part of machine are integrated in one single unit i.e. Micro computer based control cabinet as shown in figure 3.5. This system uses industrial controlling computer as mainframe, equipped with controlling units like specialized circuit board for programming & controlling system and intelligent cutting.

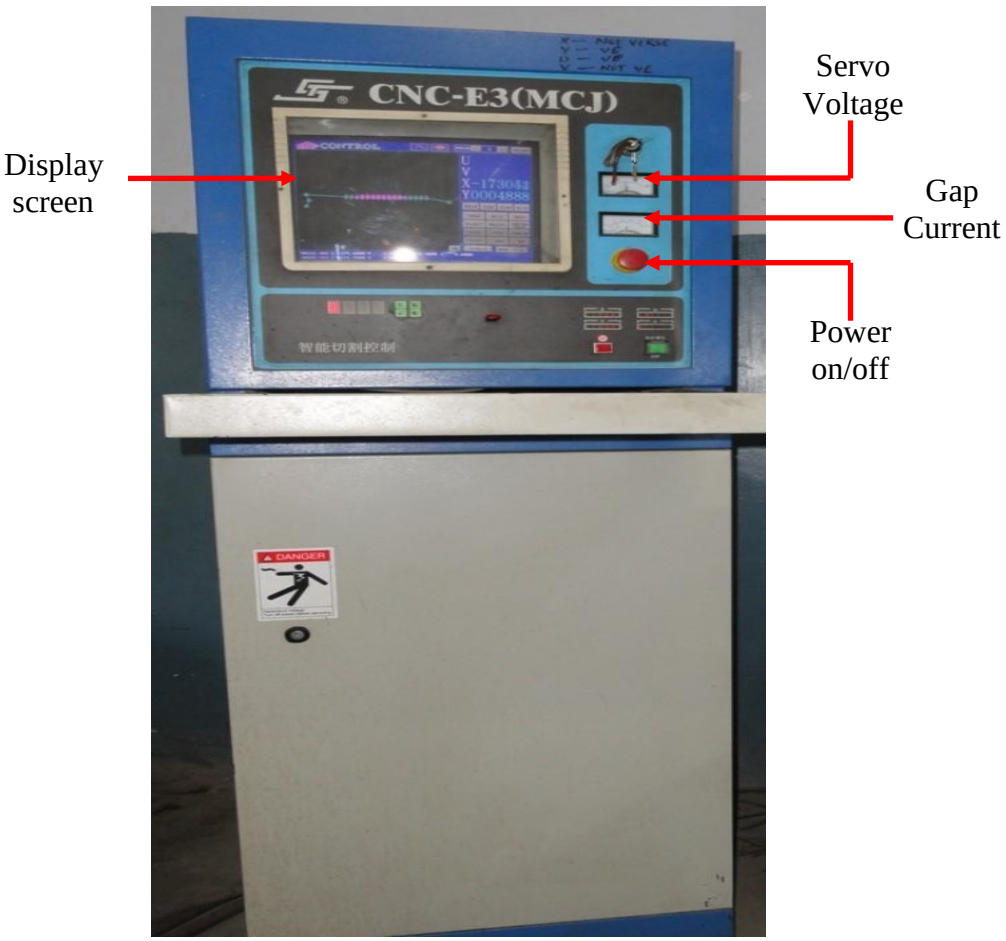

Figure 3.5 Control Cabinet

The specification of the WEDM used for the experiment is given in table 3.4.

Table 3.4 Specifications of WEDM tool

Design	Fixed column, moving table
Overall Dimensions of Machine	
Length	1440mm
Width	1150mm
Height	1450mm
Table size	
Width of table	480 mm
Length of table	700 mm
Maximum dimensions of work piece	
Length	500 mm (X)
Width	400 mm (Y)
Depth	400 mm
Maximum Work piece weight	500 kg
Wire electrode diameter	0.18 mm
Maximum Length of wire stored	230 m
Speed of Wire electrode	11 m/sec
Micro Computer controller	CNC-E3 (MCJ)
Controlled axes	X Y, U, V simultaneous / independent
Interpolation	Linear & Circular
Maximum programmable dimensions	± 999.999
Dielectric Fluid	Distilled water + gel
Dielectric Capacity	55 litres
Dielectric flow rate	25 l/min

Input Voltage	3 phase AC, 380V
Total Machine Load	1.5 KVA
Max Short circuit current	8 A
Pulse Power Supply Output Voltage	75 V

3.8.2 Electrode

It has been found out from the literature survey and preliminary investigations that most of the Optimization study on WEDM had been carried out by using Brass wire electrode of 0.25mm wire which is not reusable. However the current experiments have been performed by using Molybdenum wire of 0.18 mm which can be reused. Size of the wire was measured before and after every trial experiment by using a digital micrometer of least count 0.001 mm as shown in figure 3.6 below.

Molybdenum is used to make small, whole EDM electrodes and EDM wire for specialized applications. Molybdenum is a refractory metal with good strength and arc erosion resistance due to the metal's high melting point (2610^{o} C). Molybdenum Wire is used in limited applications which require very high tensile strength to provide a reasonable load carrying capacity in small diameter wires. Molybdenum wire is very abrasive to power feeds and wire guides, and is often difficult to auto thread.

Figure 3.6 Measurement of Wire by Using Digital Micrometer

3.8.3 Dielectric Fluid

A mixture of distilled water and **JR-3A WEDM super concentrated gel is used as dielectric fluid during the experimentation. 1 kg of dielectric gel is mixed in 40-50 ltrs of water.** WEDM gel used is shown in figure 3.7.

Figure 3.7 WEDM Gel

The Gel is based on solid soap. It inherits the advantage of solid soap like high oil: water ratio and dissolves as quickly as oil. Some of the features as given by product supplier are given below:

1. Uniform and white finish surface almost without stripe.
2. Improve machining efficiency 30% more.
3. Improve machining process indexes especially when cutting work piece thicker than 300 mm.
4. Work piece is easy to take off and clean.
5. Especially suitable for multiple-cut of WEDM-HS.

Streams of dielectric fluid is supplied over the work piece with help of four nozzles, two above and two below the work piece as shown in figure 3.8.

Figure 3.8 Nozzle for dielectric

3.8.4 Materials

In the present experimentation work, four different grades of steels AISI 304 & AISI 410 (stainless steel grades), H-21(hot die steel) & EN 31(tool steel) have been used as work materials. These materials have been chosen through literature survey and preliminary investigations.

Two different experiments have been performed, by taking two different work piece materials for one experiment. Details of materials used for experiments are given below.

Materials used for experiment 1 are AISI 304 and AISI 410. Size of work piece material is given in table 3.5.

Table 3.5 Size of work piece material for experiment set 1

Length	130 mm
Breadth	24 mm
Thickness	24 mm

AISI 304 is an austenitic stainless steel sometimes referred to as 18-8 stainless as it has a nominal composition of 18% chromium and 8% nickel. It is widely used almost in all industrial applications is accounted for approximately 50% of the world's stainless steel production and consumption. Because of its aesthetic view in architectures, superior mechanical and physical properties, weldability, resistance against corrosion and chemicals, it became as the most preferred material. AISI 304 stainless steel material for the present investigation is having a wide range of applications in the industrial field: Chemical, Pharmaceutical, Cryogenic, Food, Dairy, Paper industries etc.

AISI 410 is a martensitic stainless steel and has the lowest alloy content of all general purpose stainless steel. It is selected for highly stressed parts needing the combination of strength and corrosion resistance, such as fasteners, machinery parts and press plates. AISI 410 martensitic steel is used extensively in pump and valve shafts, steam generators, expansion joints, super-heaters and re-heaters, plastic moulds, etc. due to its high strength, toughness and resistance to creep and oxidation damages at elevated temperatures. One of the special applications of this steel in the form of bimetallic sheet with other materials such as Cu and Ag is in aerospace for manufacturing the housing of bearings in jet engines.

The chemical composition of AISI 304 and 410 as obtained by EDAX (Electro Dispersive X-ray Spectroscopy) test is given in table 3.6.

Table 3.6 Chemical composition of AISI 304 and AISI 410 in percentage

Material/Element	C	Cr	Mn	Ni	P	S	Si
AISI 304	0.047	18.07	1.37	8.11	0.028	0.0006	0.46
AISI 410	0.13	11.5	0.60	0.20	0.034	0.021	0.36

Materials used for experiment 2 are EN 31 and H 21. Size of work piece material is given in table 3.7.

Table 3.7 Size of work piece material for experiment set 2

Length	130 mm
Breadth	24 mm
Thickness	24 mm

EN-31 steel is a high carbon alloy steel with high degree of hardness, compressive strength and abrasion resistance. EN-31 finds its typical applications in the manufacturing of machine tool parts like spindles, shafts, bearings and automobile products. Properties of EN-31 steel alloy, like low specific heat, tendency to high strain harden and diffuse between tool and work material, give rise to certain problems in its machining such as high chip-tool interface temperature, large cutting forces, poor quality of surface finish and built-up-edge formation. This material is thus difficult to machine with high speed tool steels as large forces are required during machining which may result in tool factor and high cutting temperatures.

Hot work tool steels are special type of tool steel, made to withstand a combination of heat, pressure and abrasion and are denoted by letter 'H' according to AISI. All hot-work tool steels are used in a quenched and tempered condition. The most essential properties for these types of steels are high levels of hot strength, ductility, toughness, thermal conductivity, creep strength, temper resistance and also low thermal expansion. H 21 hot work steel also known as Tungsten hot work steel is generally used to make mandrels and extrusion dies for high temperature applications, such as the extrusion of brass, nickel alloys and steel. It is also suitable for use in hot-forging dies of rugged design.

The chemical composition of EN 31 and H 21 as obtained by EDAX (Electro Dispersive X-ray Spectroscopy) test is given in table 3.8.

Table 3.8 Chemical composition of EN 31 and H 21 in percentage

Material/Element	C	Cr	Mn	P	S	Si	W	V
EN 31	1.07	1.12	0.58	0.04	0.03	0.32	-	-
H 21	0.29	2.43	0.47	-	-	-	9.39	0.38

3.9 EXPERIMENTATION

3.9.1 Preparation of Specimens

The work piece in the form of square rod of 130 mm x 24 mm x 24 mm size is mounted on the WEDM machine tool and cuts of 15mm depth at a distance of 7mm have been obtained for each experiment. The close up view of rod being mounted on the machine work table is shown figure 3.9. A set of cut specimens after experimentation is shown in figure 3.10.

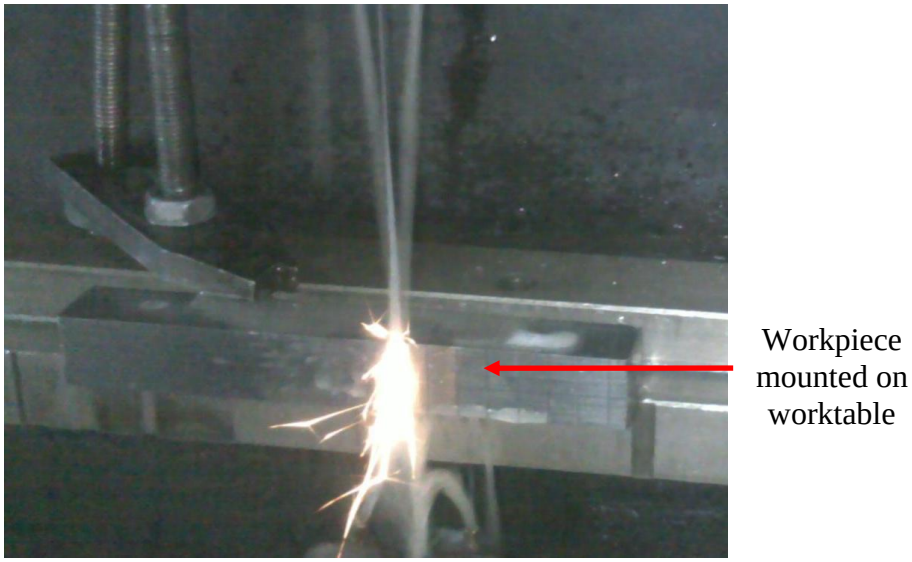

Figure 3.9 Work piece mounted on Work Table

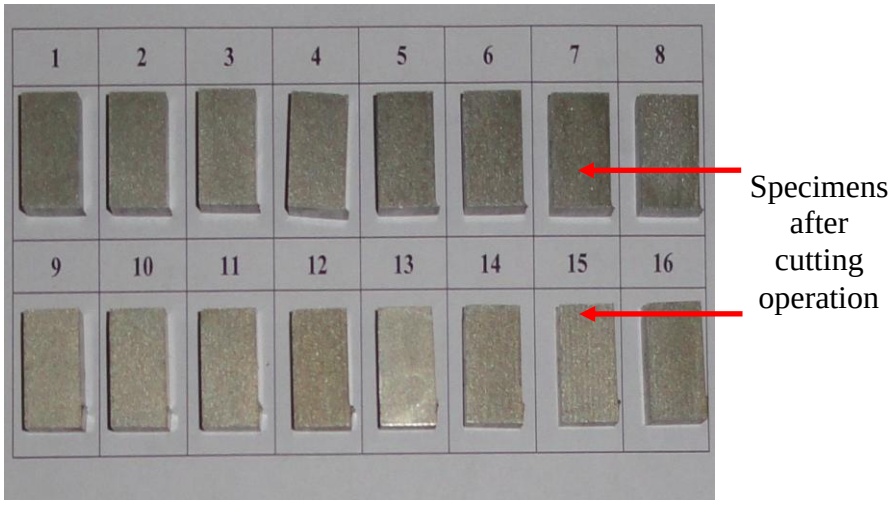

Figure 3.10 Specimen after experimentation

3.9.2 Procedure

The experiments were accomplished on a Concord United WEDM machine. Following steps were followed in the cutting operation:

1. The wire was made vertical with the help of verticality block.
2. The work piece was mounted and clamped on the work table.
3. A reference point on the work piece was set for setting work co-ordinate system (WCS). The programming was done with the reference to the WCS. The reference point was defined by the ground edges of the work piece.
4. The program was made for cutting operation of the work piece and a cut of 15 mm depth was obtained.

While performing various experiments, the following precautionary measures were taken:

1. Each set of experiments was performed at room temperature in a narrow temperature range (32±2° C).
2. Before taking measurements of surface roughness, the work piece was cleaned with acetone.

3.9.3 Pilot Experimentation

The purpose of the pilot experiments is to study the variations of the WEDM process parameters on performance measures such as material removal rate, surface roughness, kerf width and gap current.

Two set of pilot experiments were performed on Concord United WEDM machine. Various input parameters varied during the experimentation are pulse on time (T_{on}), pulse off time (T_{off}) and peak current (I_P). The effects of these input parameters are studied on material removal rate, surface roughness, kerf width and gap current using one factor at a time approach.

Selected levels of the process parameters for the present work are shown in table 3.1. Apart from these parameters, two different work pieces have been used each set of experiment, thus making it a fourth variable for the experimentation. Workpieces used for experiment 1 and 2 are given in table 3.2.

Parameters which have been kept constant during the experiments are given in table 3.9.

Table 3.9 Fixed input process parameters

S. No.	Machining Parameter	Fixed Value
1	Open Circuit Voltage	75 V
2	Type of dielectric	Water + gel
3	Wire speed	11 m/sec
4	Dielectric flow	25 l/min
5	Wire electrode	Molybdenum Wire
6	Size of wire (diameter in mm)	0.18 mm

The set of trials performed according to the L16 Orthogonal Array for the experiment set 1 and experiment set 2 are shown in table 3.10 and 3.11 respectively.

Table 3.10 L16 Orthogonal Array for Experiment 1

Exp. No.	Peak Current (A)	Pulse On (μs)	Work piece	Pulse Off (μs)
1	1	30	AISI 304	150
2	1	35	AISI 304	150
3	1	40	AISI 410	180
4	1	45	AISI 410	180
5	2	30	AISI 410	180
6	2	35	AISI 410	180
7	2	40	AISI 304	150
8	2	45	AISI 304	150
9	3	30	AISI 304	180
10	3	35	AISI 304	180
11	3	40	AISI 410	150
12	3	45	AISI 410	150
13	4	30	AISI 410	150
14	4	35	AISI 410	150
15	4	40	AISI 304	180
16	4	45	AISI 304	180

Table 3.11 L16 Orthogonal Array for Experiment 2

Exp. No.	Peak Current (A)	Pulse On (μs)	Work piece	Pulse Off (μs)
1	1	30	EN 31	150
2	1	35	EN 31	150
3	1	40	H21	180
4	1	45	H21	180
5	2	30	H21	180
6	2	35	H21	180
7	2	40	EN 31	150
8	2	45	EN 31	150
9	3	30	EN 31	180
10	3	35	EN 31	180
11	3	40	H21	150
12	3	45	H21	150
13	4	30	H21	150
14	4	35	H21	150
15	4	40	EN 31	180
16	4	45	EN 31	180

3.10 METHODOLOGY FOR ANALYSIS OF RESPONSE VARIABLES

3.10.1 Material Removal Rate or MRR

It is measured in g/min (grams per minute). Weight of the work piece has been measured before and after each machining operation and time for each machining operation has been noted from the digital display of the machine. Material removal rate is denoted by MRR in this report.

Mathematical formula used for measuring MRR for all experiments is given below:

$$MRR = \frac{(Wi - Wf)}{t}$$

Where W_i = Initial weight of workpiece material (grams)

W_f = Final weight of workpiece material (grams)

t = Time period of each trials in minutes

3.10.2 Surface Roughness (Ra)

Roughness is a measure of the texture of a surface. It is quantified by the vertical deviations of a real surface from its ideal form. If these deviations are large, the surface is rough; if small, the surface is smooth. Surface roughness is denoted by SR in this report.

In this work the surface roughness was measured by Mitutoyo surftest as shown in figure 3.11. The surftest is a shop–floor type surface-roughness measuring instrument, which traces the surface of various machined parts and calculates the surface roughness based on roughness standards, and displays the results in μm.

Figure 3.11 Mitutoyo Surftest Machine

3.10.3 Kerf Width

It is measured in millimeters (mm). It is the measure of the amount of the material that is wasted during machining and determines the dimensional accuracy of the finishing part.

For present experiments kerf width has been measured using Nikon profile projector as shown in figure 3.12 below available in metrology lab of Mechanical Department of the Thapar University. Three different values have been taken at three different points of the

cut and average of these three values has been taken as the kerf width of the cut. Kerf width is denoted by KW in this report.

Figure 3.12 Nikon Profile Projector

3.10.4 Gap Current

In WEDM machining the specimen is mounted on the machine and during the process of cutting a small amount of gap is maintained between the job and the electrode wire. To initiate the cutting a pulse of current is given by the pulse generator and the current passes through the material being cut which is measured and named as gap current. The gap current is read on an ammeter, which is an integral part of the machine, in amperes and is shown in figure 3.13.

Figure 3.13 Ammeter for Gap Current

3.11 ANALYSIS OF RESULTS

3.11.1 Signal to Noise (SN) Ratio

The parameters that influence the output can be categorized into two classes, namely controllable (or design) factors and uncontrollable (or noise) factors. Controllable factors are those factors whose values can be set and easily adjusted by the designer. Uncontrollable factors are the sources of variation often associated with operational environment. The best settings of control factors as they influence the output parameters are determined through experiments. From the analysis point of view, there are three possible categories of the response characteristics explained below.

r is the number of tests in a trial (noise of repetitions regardless of noise levels)

$\sum_{i=1}^{r} y^2{}_i$ = summation of all response values under each trial

MSD = Mean square deviation

y_j = Observed value of the response characteristic

y_o = nominal or target value of the results

The three different response characteristics are given by the following.

1) Higher is Better. The SN for higher the better is given by:

$(SN)_{HB} = -10 \log (MSD_{HB})$ (Equation....3.1)

Where $MSD_{HB} = \frac{1}{r}\sum_{j=1}^{r}\left(\frac{1}{y_j^{\,2}}\right)$ (Equation....3.2)

MSD_{HB} = Mean Square Deviation for higher-the-better response.

2) Nominal is Better. The SN for nominal is better is:

$(SN)_{NB} = -10 \log (MSD_{NB})$ (Equation....3.3)

Where $MSD_{NB} = \frac{1}{r}\sum_{j=1}^{r}\left(y_j - y_0\right)^2$ (Equation....3.4)

3) Lower is Better. In this design situation, response is the type of ‘‘lower is better’’, which is a logarithmic function based on the mean square deviation (MSD), given by

$$(SN)_{LB} = -10\log(MSD) = -10\log[(\frac{1}{r}\sum_{i=1}^{r} y^2{}_i)$$ (Equation....3.5)

Where $MSD_{LB} = \frac{1}{r}\sum_{j=1}^{r}\left(y_j^{\,2}\right)$ (Equation....3.6)

- ***SN Ratio for Response Characteristics***

The parameters that influence the output can be categorized in two categories, controllable factors and uncontrollable factors. The control factors that may contribute to reduced variation can be quickly identified by looking at the amount of variation present in response. The uncontrollable factors are the sources of variation often associated with operational environment. For this experimental work, response characteristics are given in the table 3.12.

Table 3.12 Response Characteristics

Response Name	Response Type	Units
Material Removal Rate (MRR)	Higher the better	g/min
Surface Roughness	Lower the better	µm
Kerf width	Lower the Better	mm
Gap Current	Higher the Better	A

- ***Measurement of F-Value Of Fisher's F Ratio***

The principle of the F test is that the larger the F value for a particular parameter, the greater the effect on the performance characteristic due to the change in that process parameter. F value is defined as:

$$\mathrm{F} = \frac{\text{MS for a term}}{\text{MS for the error term}} \qquad \text{(Equation....3.7)}$$

Computation of average performance:

Average performance of a factor at certain level is the influence of the factor at this level on the mean response of the experiments.

3.12 ANALYSIS OF VARIANCE

The knowledge of the contribution of individual factors is critically important for the control of the final response. The analysis of variance (ANOVA) is a common statistical technique to determine the percent contribution of each factor for results of the experiment. It calculates parameters known as sum of squares (SS), pure SS, degree of freedom (DOF), variance, F-ratio and percentage of each factor. Since the procedure of ANOVA is a very complicated and employs a considerable of statistical formulae, only a brief description of is given as following.

The Sum of Squares (SS) is a measure of the deviation of the experimental data from the mean value of the data.

Let 'A' be a factor under investigation

$$SS_T = \sum_{i=1}^{N} (y_i - \overline{T})^2 \qquad \text{(Equation....3.8)}$$

Where N = Number of response observations, $\overline{T}$ is the mean of all observations y_i is the i th response

Factor Sum of Squares (SS_A) - Squared deviations of factor (A) averages from overall average

$$SS_A = \left[\sum_{i=1}^{k_A} \left(\frac{A_i^2}{n_{Ai}} \right) \right] - \frac{T^2}{N} \qquad \text{(Equation....3.9)}$$

Where

A_i =Average of all obseravtions under A_i level = A_i / n_{Ai}

T = sum of all observations

$\bar{T}$ = Average of all observations = T / N

n_{Ai} = Number of observations under A_i level

Error Sum of Squares (SS_e) - Squared deviations of observations from factor (A) averages

$$SS_e = \sum_{j=1}^{k_A} \sum_{i=1}^{n_{Ai}} \left(y_i - \bar{A}_j \right)^2 \qquad \text{(Equation....3.10)}$$

Sum of Squares ($SS_{A\times B}$) for interactions

$$SS_{A\times B} = \left[\sum_{i=1}^{c} \left(\frac{(A\times B)_i^2}{n_{(A\times B)i}} \right) \right] - \frac{T^2}{N} - SS_A - SS_B \qquad \text{(Equation....3.11)}$$

Sum of Squares of factors for dummy treatment level

The level symbols for A_1 & $A_{1^{**}}$, both indicate the same test condition w.r.t. factor A. Therefore

$$SS_A = \frac{(A_1 + A^{**}_1)^2}{n_{A1} + n_{A1^{**}}} + \frac{A_2^2}{n_{A2}} - \frac{T^2}{N} \qquad \text{(Equation....3.12)}$$

$$SS_e = \frac{(A_1 - A_1^{**})^2}{n_{A1} + n_{A1^{**}}} \qquad \text{(Equation....3.13)}$$

$$SS_{A\times B} = \left[\sum_{i=1}^{c} \left(\frac{(A\times B)_i^2}{n_{(A\times B)i}} \right) \right] - \frac{T^2}{N} - SS_A - SS_B - SS_e \qquad \text{(Equation....3.14)}$$

CHAPTER 4
RESULTS AND ANALYSIS

4.1 INTRODUCTION

This chapter includes the details of the experimental work performed on WEDM along with the results and analysis of the experimental work. The objective of the experimentation is to study the effect process parameters on the output parameters e.g. material removal rate, surface roughness, gap current and kerf width by using different work piece materials for two set of experiments.

For the design of experiments, Taguchi method has been used. Using Taguchi design, L16 Orthogonal Array has been selected (selection procedure has been described in the previous chapter) and experiments were performed according to the set of combinations of factors as given in L16 OA. Various factors for this study were peak current, pulse on-time and pulse off-time. Set of workpieces for experiment 1 were AISI 304 & AISI 410 and for experiment 2 were EN 31 and H21 and the electrode selected was of Molybdenum wire. Material testing of all the workpieces has been done details of which has been discussed previously. Once all the parameters have been decided and level values were set, experimentation was performed. After the experimental results have been obtained, analysis of the results was carried out using MINITAB software. For graphical analysis of the experimental results plots, showing effects of all the factors upon responses, are generated in MINITAB. Then ANOVA of the experimental data has been done to calculate the contribution of each factor in each response. Various responses to be considered are MRR, Surface roughness, Kerf Width and gap current. After studying the effect of all the factors on all the responses individually, Signal to noise ratio has been calculated for each response. For MRR and gap current, higher the best, for surface roughness and kerf width, lower the better approach was used. Then after optimal condition have been calculated for MRR, surface roughness, kerf width and gap current.

4.2 RESULTS AND ANALYSIS FOR MRR (EXPERIMENT SET 1)

The results for MRR for each of the 16 treatment conditions for experiment 1 are given in table 4.1. MRR of each sample is calculated from weight difference of workpiece before and after the performance trial, which is given by:

$$MRR = \frac{(Wi - Wf)}{t}$$

Where W_i ,= Initial weight of workpiece material (grams)

W_f = Final weight of workpiece material (grams)

t = Time period of each trials in minutes

Table 4.1 Results for MRR

Exp. No.	Peak Current (A)	Pulse on time (μs)	Work piece	Pulse off time (μs)	MRR (g/min)
1	1	30	AISI 304	150	0.029
2	1	35	AISI 304	150	0.029
3	1	40	AISI 410	180	0.022
4	1	45	AISI 410	180	0.022
5	2	30	AISI 410	180	0.046
6	2	35	AISI 410	180	0.045
7	2	40	AISI 304	150	0.059
8	2	45	AISI 304	150	0.056
9	3	30	AISI 304	180	0.07
10	3	35	AISI 304	180	0.071
11	3	40	AISI 410	150	0.084
12	3	45	AISI 410	150	0.082
13	4	30	AISI 410	150	0.102
14	4	35	AISI 410	150	0.105
15	4	40	AISI 304	180	0.099
16	4	45	AISI 304	180	0.097

4.2.1 Analysis of Variance for MRR

The results for MRR were analyzed using ANOVA for identifying the significant factors affecting the performance measures. The Analysis of Variance (ANOVA) for the mean MRR at 99% confidence interval is given in table 4.2. F-test was performed on the variance data for each factor to find significance of each. The principle of the F test is that the larger the F value for a particular parameter, the greater the effect on the performance characteristic due to the change in that process parameter. ANOVA table 4.2 for means of

MRR shows that current (F value 3794.83), pulse off time (F value 309.30) and pulse on time (F value 13.02) are the factors which significantly affect the MRR, and however workpiece (F value 0.23) is insignificant to affect the MRR. Table 4.3 shows the ranks of various factors in terms their relative significance. Current has the highest rank signifying highest contribution to MRR and workpiece has the lowest and was observed to be insignificant in affecting MRR.

Main effects plot for the MRR are shown in figure 4.1 which shows the variation of MRR with the input parameters. As the peak current is increased alongwith increase in pulse on time, MRR increases and decreases with increase in pulse off time. This is due the fact that discharge energy increases with peak current and pulse on time resulting in faster material removal rate. Also as the pulse off time decreases, the amount of current discharges within a given period becomes more which results in higher material rate.

Table 4.2 ANOVA for Means of MRR

Source	DF	Seq SS	Adj MS	F	P
Peak Current	3	0.012604	0.004201	3794.83	0.00
Pulse On	3	0.000043	0.000014	13.02	0.00
Work Piece	1	0.000000	0.000000	0.23	0.65
Pulse Off	1	0.000342	0.000342	309.13	0.00
Residual Error	7	0.000008	0.000001		
Total	15	0.012998			

Table 4.3 Response Table for Means of MRR

Level	Peak Current	Pulse On	Work Piece	Pulse Off
1	0.02550	0.06175	0.06375	0.06825
2	0.05150	0.06250	0.06350	0.05900
3	0.07675	0.06600		
4	0.10075	0.06425		
Delta	0.07525	0.00425	0.00025	0.00925
Rank	1	3	4	2

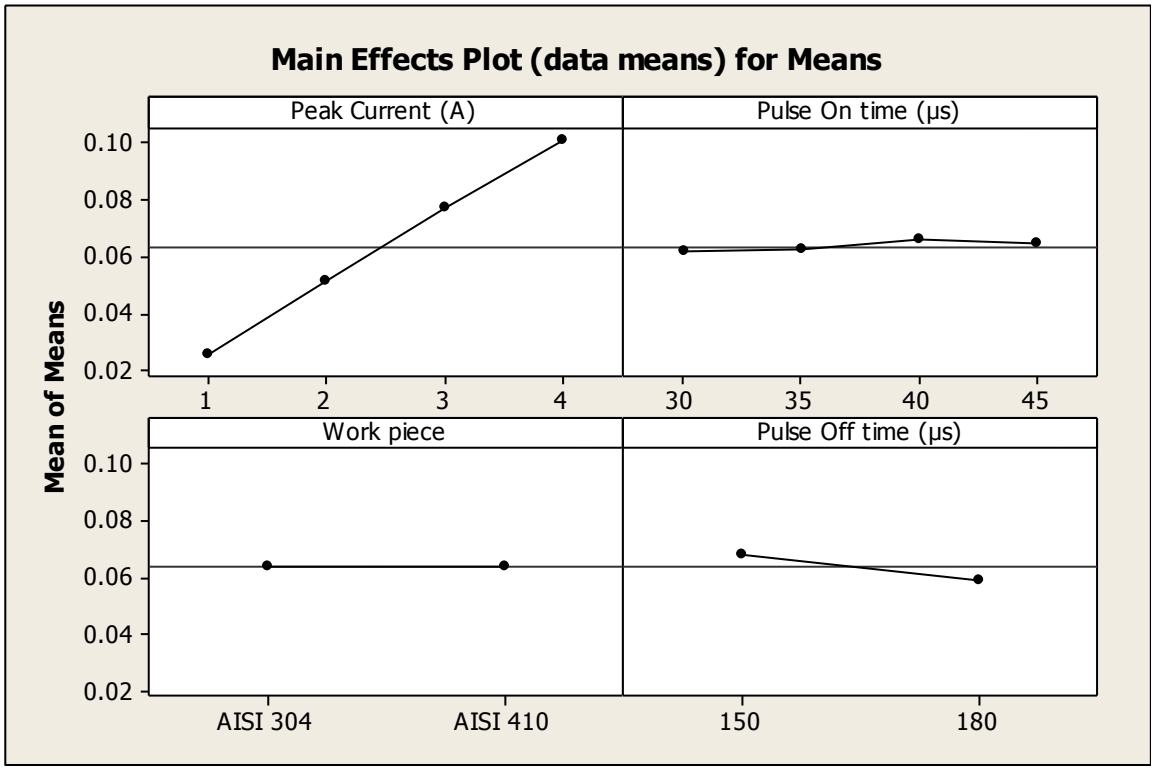

Figure 4.1 Main effects plot of MRR for Means

4.3 RESULTS AND ANALYSIS FOR SR (EXPERIMENT SET 1)

The results for surface roughness (SR) for each of the 16 treatment conditions for experiment 1 are given in table 4.4. Responses for surface roughness have been measured by using Mitutoyo surface-roughness measuring instrument.

Table 4.4 Results for Surface Roughness (Experiment Set 1)

Exp No.	Peak Current (A)	Pulse on time (µs)	Work piece	Pulse off time (µs)	SR Value '1'	SR Value '2'	SR 'Mean'	SN Ratio
1	1	30	AISI 304	150	2.97	3.21	3.09	-9.7992
2	1	35	AISI 304	150	3.32	2.36	2.84	-9.0664
3	1	40	AISI 410	180	3.53	3.05	3.29	-10.3439
4	1	45	AISI 410	180	3.31	3.43	3.37	-10.5526
5	2	30	AISI 410	180	3.25	3.59	3.42	-10.6805
6	2	35	AISI 410	180	2.97	3.99	3.48	-10.8316
7	2	40	AISI 304	150	4.28	3.90	4.09	-12.2345
8	2	45	AISI 304	150	4.73	4.79	4.76	-13.5521

9	3	30	AISI 304	180	4.04	4.42	4.23	-12.5268
10	3	35	AISI 304	180	4.01	3.75	3.88	-11.7766
11	3	40	AISI 410	150	3.86	4.54	4.2	-12.465
12	3	45	AISI 410	150	4.60	3.94	4.27	-12.6086
13	4	30	AISI 410	150	3.99	4.57	4.28	-12.6289
14	4	35	AISI 410	150	4.56	4.70	4.63	-13.3116
15	4	40	AISI 304	180	4.75	5.11	4.93	-13.8569
16	4	45	AISI 304	180	5.15	4.91	5.03	-14.0314

4.3.1 Analysis of Variance for Surface Roughness

The results for surface roughness were analyzed using ANOVA for identifying the significant factors affecting the performance measures. ANOVA for the mean surface roughness at 99% confidence interval is given in table 4.5. As principle of the F test is that the larger the F value for a particular parameter, the greater the effect on the performance characteristic due to the change in that process parameter. ANOVA table 4.5 for means of surface roughness shows that peak current (F value 31) and pulse on time (F value 7.08) are the factors that significantly affect the surface roughness. Table 4.6 shows the ranks of various factors in terms their relative significance. Current has the highest rank signifying highest contribution to surface roughness and pulse off has the lowest and was observed to be insignificant in affecting surface roughness.

Main effects plot for the MRR are shown in figure 4.2 which shows the variation of surface roughness with the input parameters. As can be seen surface roughness increases with increase in peak current and pulse on time from 1 Amp to 4 Amp and 30μs to 45μs respectively. As the peak current and pulse on time are increased, the discharge energy increases and this increase in discharge energy produces a larger crater, causing an increased value of surface roughness on the work piece. Also as the pulse off time decreases, the number of discharges increases, which causes poor surface finish.

Table 4.5 ANOVA for Means of Surface Roughness

Source	DF	Seq SS	Adj MS	F	P
Peak Current	3	5.06322	1.68774	31.00	0.00
Pulse On	3	1.15582	0.38527	7.08	0.00

Work Piece	1	0.22801	0.22801	4.19	0.80
Pulse Off	1	0.01756	0.01756	0.32	0.59
Residual Error	7	0.38114	0.05445		
Total	15	6.84574			

Table 4.6 Response Table for Means of Surface Roughness

Level	Peak Current	Pulse On	Work Piece	Pulse Off
1	3.148	3.755	4.106	4.020
2	3.938	3.708	3.868	3.954
3	4.145	4.128		
4	4.718	4.358		
Delta	1.570	0.650	0.239	0.066
Rank	1	2	3	4

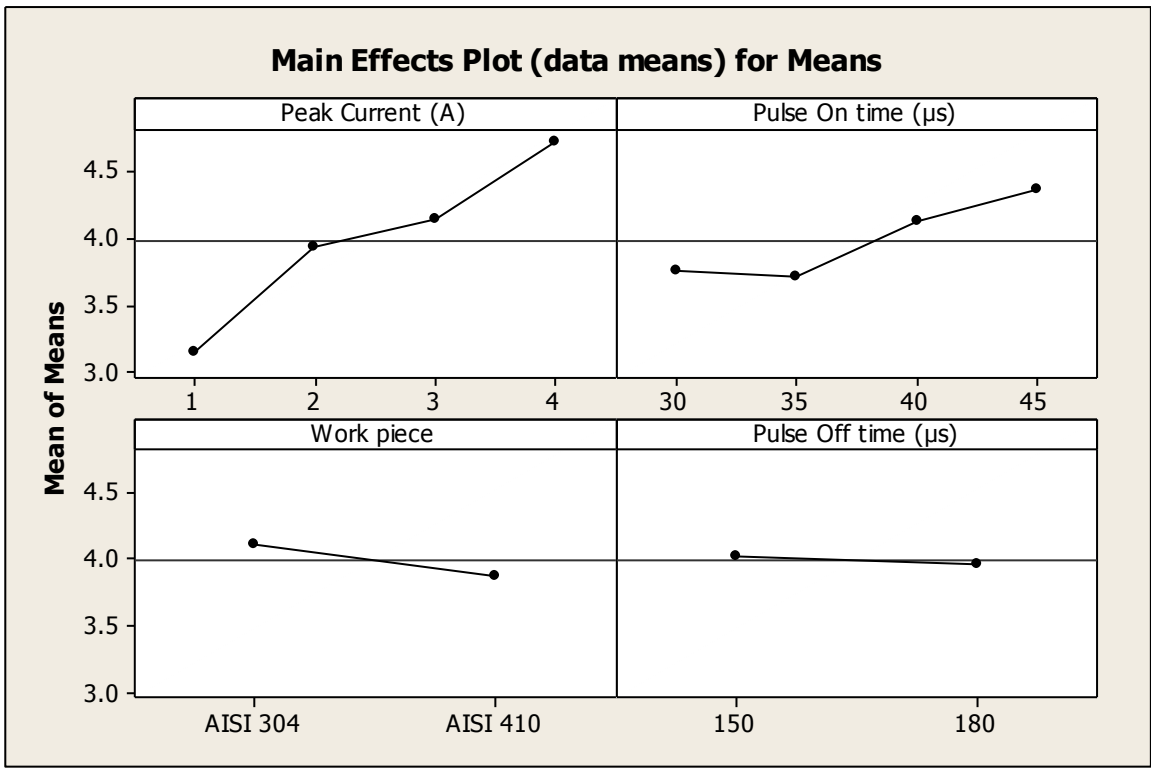

Figure 4.2 Main effects plot of Surface Roughness for Means

4.3.2 Results for SN Ratio of Surface Roughness

The SN ratio several repetitions into one value which reflects the amount of variation present. The values of all the results according to Taguchi array parameter design layout

are presented in this section. The SN ratios have been calculated to identify the major contributing factors and interactions for variation in the roughness values In this design situation, roughness is the type of 'lower is better', which is a logarithmic function based on the mean square deviation (MSD), given by

$$SN_{LB} = -10\log(MSD) = -10\log[(\frac{1}{r}\sum_{i=1}^{r} y^2{}_i)$$

Where $MSD_{LB} = \frac{1}{r}\sum_{j=1}^{r}\left(y_j{}^2\right)$

Table 4.7 shows the ANOVA for SN ratio for roughness at 99% confidence interval. Among all the factors current and pulse on time are the most significant which has highest contribution in roughness, pulse off being the insignificant factor. Main effects plot for the SN ratios are shown in figure 4.3 which shows the variation of surface roughness with the input parameters.

Table 4.7 ANOVA for SN ratios of Surface Roughness

Source	DF	Seq SS	Adj MS	F	P
Peak Current	3	25.8688	8.62294	29.64	0.00
Pulse On	3	5.5667	1.85557	6.38	0.00
Work Piece	1	0.7315	0.73155	2.51	0.16
Pulse Off	1	0.0710	0.07100	0.24	0.64
Residual Error	7	2.0363	0.29090		
Total	15	34.2744			

Table 4.8 Response Table for SN Ratios of Surface Roughness

Level	Peak Current	Pulse On	Work Piece	Pulse Off
1	-9.941	-11.409	-12.105	-11.958
2	-11.825	-11.247	-11.678	-11.825
3	-12.344	-12.225		
4	-13.457	-12.686		
Delta	3.517	1.440	0.428	0.133
Rank	1	2	3	4

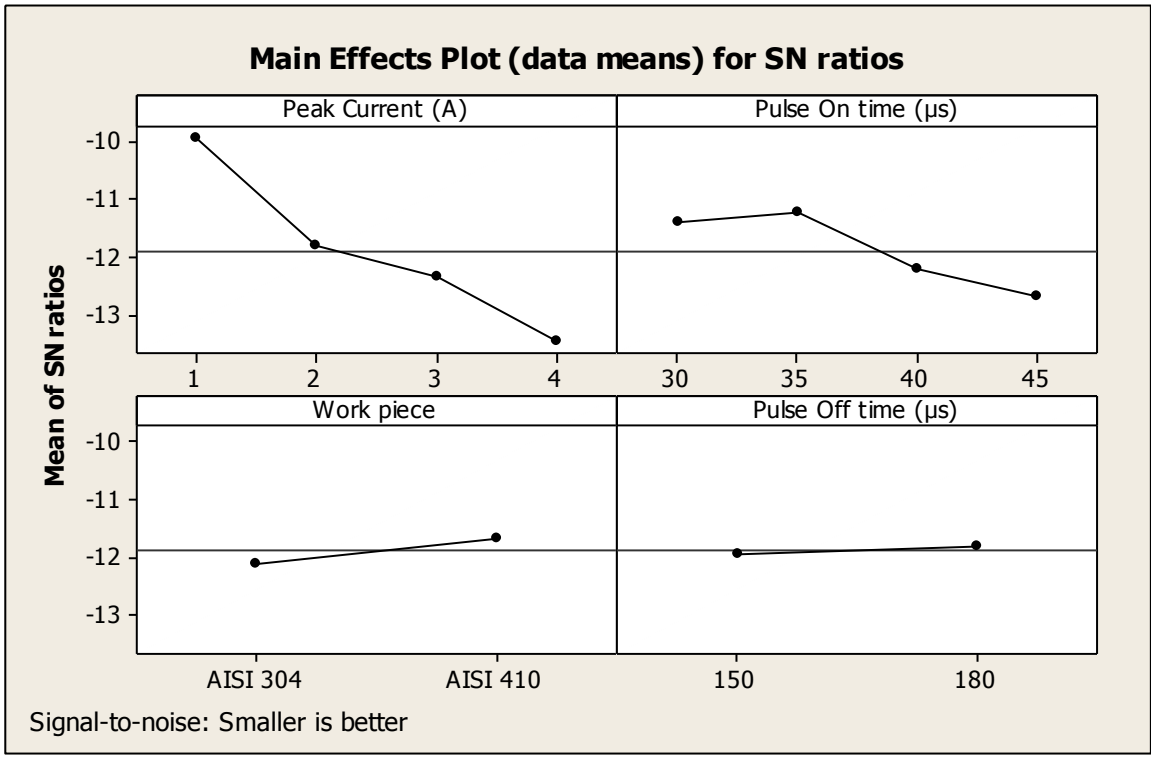

Figure 4.3 Main effects plot of Surface Roughness for SN Ratios

4.4 RESULTS AND ANALYSIS OF KERF WIDTH (EXPERIMENT SET 1)

The results for kerf width (KW) for each of the 16 treatment conditions for experiment 1 are given in table 4.9. Kerf width has been measured using Nikon profile projector. Three different values have been taken at three different points of the cut and average of these three values has been taken as the kerf width of the cut.

Table 4.9 Results for Kerf Width (Experiment Set 1)

Exp No.	Peak Current (A)	Pulse On Time (µs)	Work piece	Pulse Off Time (µs)	KW '1'	KW '2'	KW 'Mean'	SN Ratio
1	1	30	AISI 304	150	0.185	0.189	0.187	14.5627
2	1	35	AISI 304	150	0.189	0.190	0.190	14.4478
3	1	40	AISI 410	180	0.195	0.195	0.195	14.1993
4	1	45	AISI 410	180	0.196	0.197	0.197	14.1327
5	2	30	AISI 410	180	0.200	0.201	0.201	13.9577
6	2	35	AISI 410	180	0.201	0.205	0.203	13.8497

7	2	40	AISI 304	150	0.206	0.204	0.205	13.7648
8	2	45	AISI 304	150	0.202	0.205	0.204	13.8285
9	3	30	AISI 304	180	0.200	0.204	0.202	13.8925
10	3	35	AISI 304	180	0.205	0.203	0.204	13.8073
11	3	40	AISI 410	150	0.206	0.209	0.208	13.6594
12	3	45	AISI 410	150	0.208	0.210	0.209	13.597
13	4	30	AISI 410	150	0.203	0.205	0.204	13.8073
14	4	35	AISI 410	150	0.207	0.206	0.207	13.7016
15	4	40	AISI 304	180	0.210	0.209	0.210	13.5763
16	4	45	AISI 304	180	0.208	0.211	0.210	13.5761

4.4.1 Analysis of Variance for Kerf Width

The results for kerf width were analyzed using ANOVA for identifying the significant factors affecting the performance measures. ANOVA for the mean Kerf Width at 99% confidence interval is given in table 4.10. ANOVA table shows that peak current (F value 410.76) and pulse on (F value 76.55) are the factors that significantly affect the kerf width. Table 4.11 shows the ranks of various factors in terms their relative significance. Current has the highest rank signifying highest contribution to kerf width.

Main effects plot for the kerf width are shown in figure 4.4 which shows the variation of kerf width with the input parameters. Increased value for peak current and pulse on time leads to increased machining time. Longer machining time results in larger kerf values.

Table 4.10 ANOVA for Means of Kerf Width

Source	DF	Seq SS	Adj MS	F	P
Peak Current	3	0.000572	0.000191	410.76	0.00
Pulse On	3	0.000107	0.000036	76.55	0.00
Work Piece	1	0.000009	0.000009	19.38	0.003
Pulse Off	1	0.000004	0.000004	8.62	0.022

Residual Error	7	0.000003	0.000000		
Total	15	0.000695			

Table 4.11 Response Table for Means of Kerf Width

Level	Peak Current	Pulse On	Work Piece	Pulse Off
1	0.1920	0.1984	0.2013	0.2015
2	3.9050.2030	0.2008	0.2028	0.2025
3	0.2056	0.2043		
4	0.2074	0.2046		
Delta	0.0154	0.0062	0.0015	0.0010
Rank	1	2	3	4

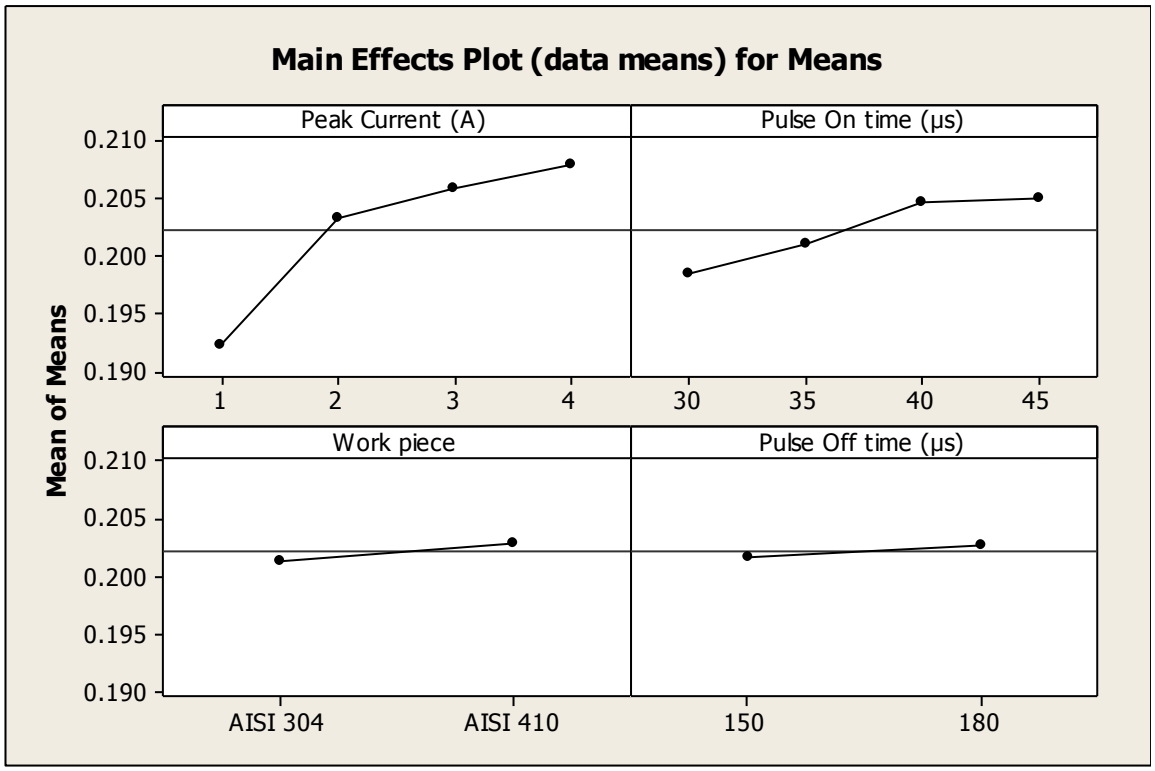

Figure 4.4 Main effects plot of Kerf Width for Means

4.4.2 Results for SN Ratio of Kerf Width

The SN ratio several repetitions into one value which reflects the amount of variation present. The values of all the results according to Taguchi array parameter design layout are presented in this section. The SN ratios have been calculated to identify the major contributing factors for variation in the kerf width values. In this design situation, kerf

width is the type of 'lower is better', which is a logarithmic function based on the mean square deviation (MSD), given by:

$$S/N_{LB} = -10\log(MSD) = -10\log[(\frac{1}{r}\sum_{i=1}^{r} y^2{}_i)$$

Where $MSD_{LB} = \frac{1}{r}\sum_{j=1}^{r}\left(y_j{}^2\right)$

Table 4.12 shows the ANOVA for SN ratio for roughness at 99% confidence interval. Among all current and work piece are the most significant which has highest contribution in kerf width, pulse on time being the lowest contributing factor. Main effects plot for the kerf width are shown in figure 4.5 which shows the variation of surface roughness with the input parameters.

Table 4.12 ANOVA for SN ratios of Kerf Width

Source	DF	Seq SS	Adj MS	F	P
Peak Current	3	1.09282	0.364275	396.31	0.00
Pulse On	3	0.20096	0.066988	72.88	0.00
Work Piece	1	0.01900	0.019000	20.67	0.003
Pulse Off	1	0.00890	0.008902	9.68	0.017
Residual Error	7	0.00643	0.000919		
Total	15	1.32812			

Table 4.13 Response Table for SN Ratios of Kerf Width

Level	Peak Current	Pulse On	Work Piece	Pulse Off
1	0.1920	0.1984	0.2013	0.2015
2	0.2030	0.2008	0.2028	0.2025
3	0.2056	0.2043		
4	0.2074	0.2046		
Delta	0.0154	0.0062	0.0015	0.0010
Rank	1	2	3	4

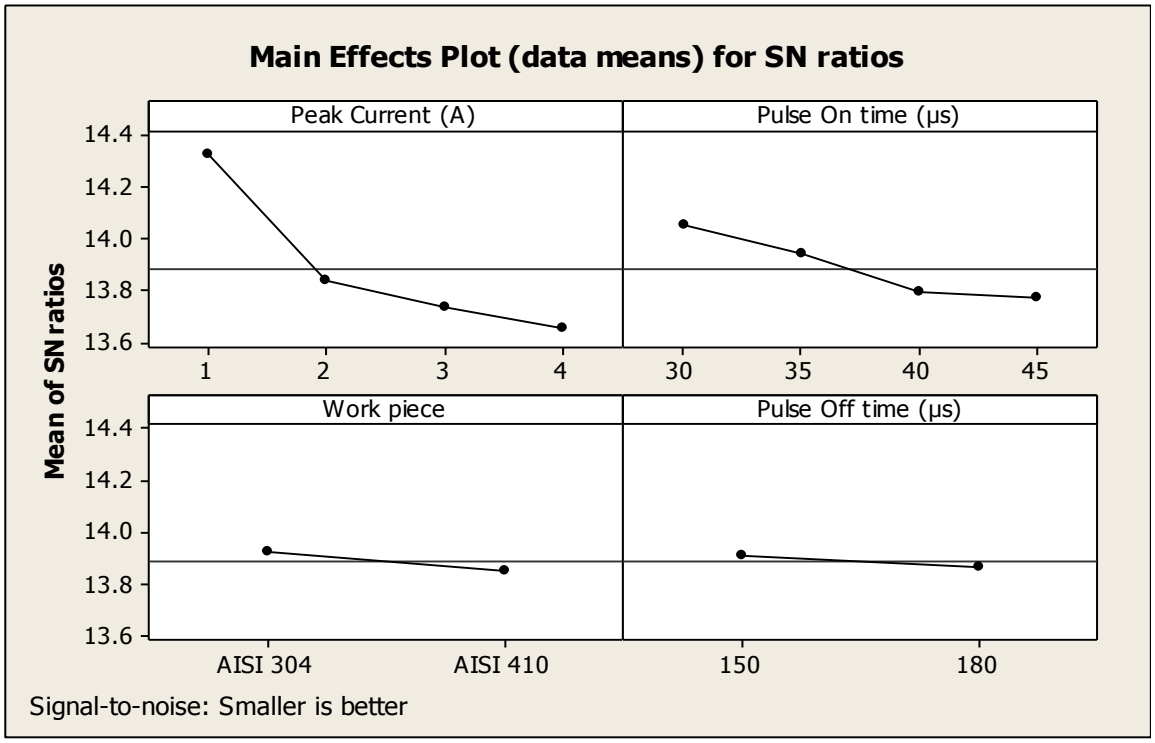

Figure 4.5 Main effects plot of Kerf Width for SN Ratios

4.5 RESULTS AND ANALYSIS FOR GAP CURRENT (EXPERIMENT SET 1)

The results for gap current for each of the 16 treatment conditions for experiment 1 are given in table 4.14. Gap current measurement was taken directly from the ampere meter in the control cabinet of the machine.

Table 4.14 Results for Gap Current (Experiment Set 1)

Exp No.	Peak Current (A)	Pulse On Time (µs)	Work piece	Pulse Off Time (µs)	Gap Current '1'	Gap Current '2'	Gap Current 'Mean'	SN Ratio
1	1	30	AISI 304	150	0.75	0.75	0.75	-2.49877
2	1	35	AISI 304	150	0.75	0.75	0.75	-2.49877
3	1	40	AISI 410	180	0.75	0.75	0.75	-2.49877
4	1	45	AISI 410	180	0.75	0.75	0.75	-2.49877
5	2	30	AISI 410	180	1	1	1	0
6	2	35	AISI 410	180	1	1	1	0
7	2	40	AISI 304	150	1.4	1.4	1.4	2.92256
8	2	45	AISI 304	150	1.4	1.4	1.4	2.92256

9	3	30	AISI 304	180	1.5	1.5	1.5	3.52183
10	3	35	AISI 304	180	1.5	1.5	1.5	3.52183
11	3	40	AISI 410	150	1.75	1.75	1.75	4.86076
12	3	45	AISI 410	150	1.75	1.75	1.75	4.86076
13	4	30	AISI 410	150	2	2	2	6.0206
14	4	35	AISI 410	150	2	2	2	6.0206
15	4	40	AISI 304	180	1.75	1.75	1.75	4.86076
16	4	45	AISI 304	180	1.75	1.75	1.75	4.86076

4.5.1 Analysis of Variance for Gap Current

The results for gap current were analyzed using ANOVA for identifying the significant factors affecting the performance measures. ANOVA for the mean gap current at 99% confidence interval is given in table 4.15. ANOVA table shows that peak current (F value 171.06) and pulse off time (F value 35.44) are the factors that significantly affect the gap current. However work piece (F value 0.44) is least significant to affect the gap current. Table 4.16 shows the ranks of various factors in terms their relative significance. Current has the highest rank signifying highest contribution to gap current and workpiece has the lowest rank in affecting gap current.

Main effects plot for the gap current are shown in figure 4.6 which shows the variation of gap current with the input parameters. As can be seen gap current increases with increase in peak current and increases with decrease in pulse off time.

Table 4.15 Analysis of Variance for Means of Gap Current

Source	DF	Seq SS	Adj MS	F	P
Peak Current	3	2.93250	0.977500	171.06	0.00
Pulse On	3	0.04000	0.013333	2.33	0.16
Work Piece	1	0.00250	0.002500	0.44	0.53
Pulse Off	1	0.20250	0.202500	35.44	0.00
Residual Error	7	0.04000	0.005714		
Total	15	3.21750			

Table 4.16 Response Table for Means of Gap Current

Level	Peak Current	Pulse On	Work Piece	Pulse Off
1	0.7500	1.3125	1.3500	1.4750
2	1.2000	1.3125	1.3750	1.2500
3	1.6250	1.4125		
4	1.8750	1.4125		
Delta	1.1250	0.1000	0.0250	0.2250
Rank	1	3	4	2

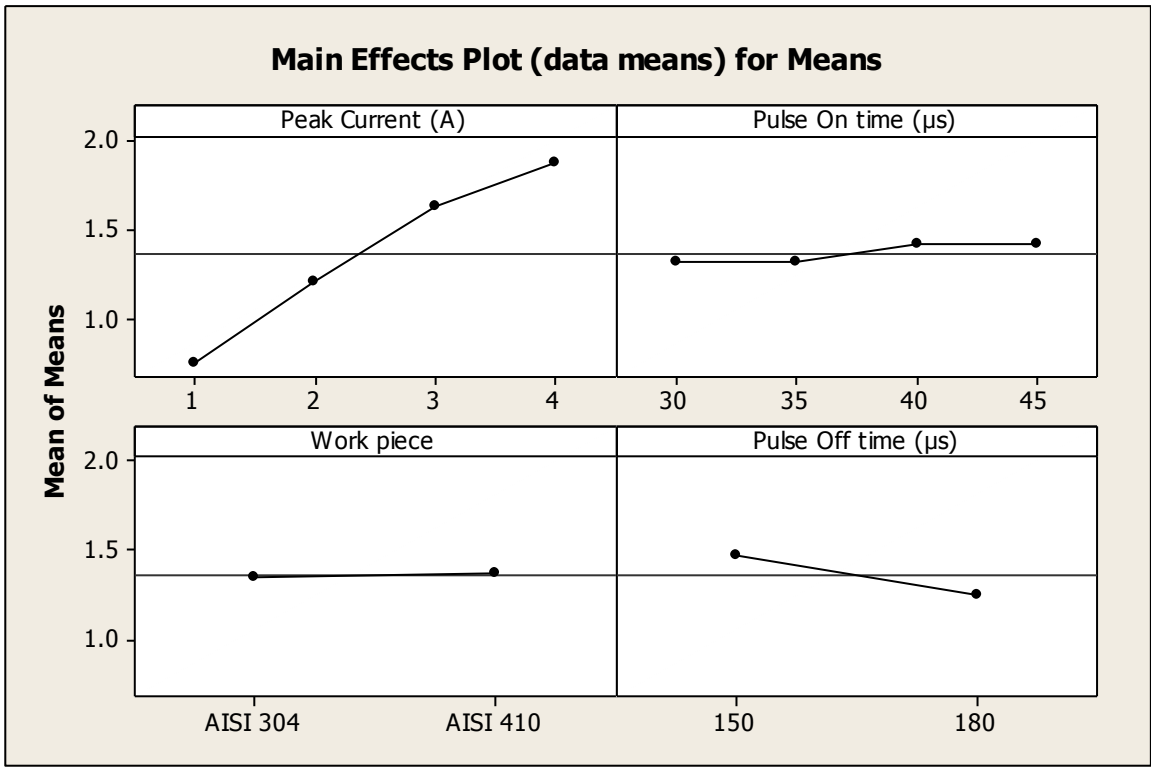

Figure 4.6 Main effects plot of Gap Current for Means

4.5.2 Results for SN Ratio of Gap Current

The SN ratio consolidates several repetitions into one value and is an indication of the amount of variation present. The SN ratios have been calculated to identify the major contributing factors and interactions that cause variation in the gap current. Gap current is "Higher is better" type response which is given by:

$(SN)_{HB} = -10 \log (MSD_{HB})$

Where $MSD_{HB} = \frac{1}{r}\sum_{j=1}^{r}\left(\frac{1}{y_j^{\,2}}\right)$

MSD_{HB} = Mean Square Deviation for higher-the-better response.

Table 4.17 shows the ANOVA results for SN ratio of MRR at 99% confidence interval. Current was observed to be the most significant factor affecting the gap current, followed by pulse off time and pulse on time according to F test. Although workpiece seems to be insignificant table 4.18 shows the ranks of various factors in terms their relative significance. Current has the highest rank signifying highest contribution to gap current and workpiece has the lowest rank and was observed to be insignificant in affecting gap current. Main effects plot of SN ratio for MRR are shown in the figure 4.7.

Table 4.17 Analysis of Variance for SN ratios of Gap Current

Source	DF	Seq SS	Adj MS	F	P
Peak Current	3	148.324	49.4412	183.93	0.00
Pulse On	3	2.405	0.8017	2.98	0.11
Work Piece	1	0.045	0.0449	0.17	0.70
Pulse Off	1	7.348	7.3477	27.33	0.00
Residual Error	7	1.882	0.2688		
Total	15	160.003			

Table 4.18 Response Table for SN Ratios of Gap Current

Level	Peak Current	Pulse On	Work Piece	Pulse Off
1	-2.499	1.761	2.202	2.826
2	1.461	1.761	2.096	1.471
3	4.191	2.536		
4	5.441	2.536		
Delta	7.939	0.775	0.106	1.355
Rank	1	3	4	2

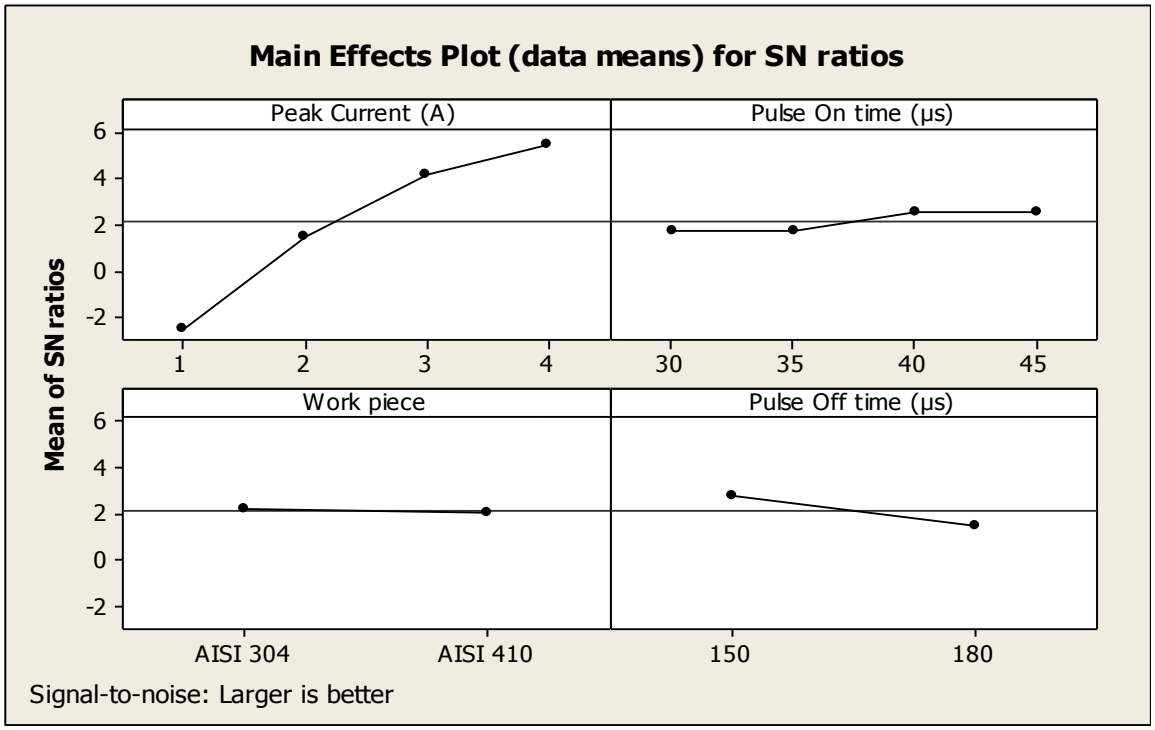

Figure 4.7 Main effects plot of Gap Current for SN Ratios

4.6 OPTIMAL DESIGN FOR EXPERIMENT SET 1

In this experimental analysis, the main effect plots for different parameters studied and it was observed that workpiece is the least significant factor in WEDM process. As the response variable MRR is higher the better response, surface roughness and kerf width are lower the better response variables. In WEDM process it is desired that machined workpiece should have good surface finish and smaller kerf width, however it is necessary to have higher material removal rates. In order to optimize the WEDM process for the current experimental set, The Analytic Hierarchy Process, commonly known as AHP has been chosen.

4.6.1 The Analytic Hierarchy Process

Analytic Hierarchy Process is a one of the very popular decision-making methods used to solve complicated problems that include multiple criteria. AHP allows decision-makers to model the complicated problems in a hierarchical structure having the main target, criteria, sub-criteria and alternatives and the relationships among these. The most important characteristic of AHP is combining knowledge, experience, individual opinions and foresights in a logical way. The Analytic Hierarchy Process is a well-known technique that breaks down a decision-making problem into several levels in such a way

that they form a hierarchy with unidirectional hierarchical relationships between levels. The top level of the hierarchy is the main goal of the decision problem. The lower levels are the tangible and/or intangible criteria and subcriteria that contribute to the goal. The bottom level is formed by the alternatives to evaluate in terms of the criteria. AHP uses pairwise comparison to allocate weights to the elements of each level, measuring their relative importance with pairwise comparison table and finally global weights are calculated for assessment at the bottom level [56].

4.6.2 Steps Involved In AHP

Basic steps that are generally involved in a standard AHP are

- Represent the problem as thoroughly as possible.
- Broaden the objectives of the problem or consider all factors, objectives and its outcome.
- Identify the factors/criteria that will have direct or indirect impact on the process of decision making.
- Arrange the problem in a hierarchy of different levels constituting goal, criteria, sub-criteria and alternatives. Goal or the objective of the decision is the top level of the hierarchy, while the criteria, subcriteria or sub-sub-criteria (if any) are placed in the subsequent descending levels with the lowest level in the hierarchy constructed by picking the available alternatives as shown in figure 4.8.

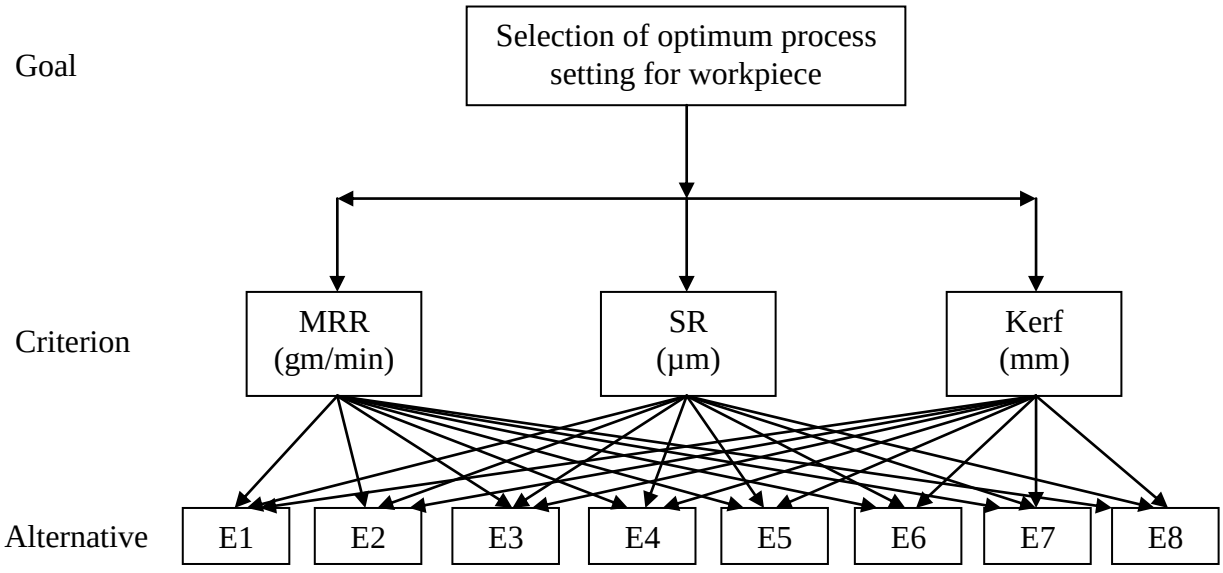

Figure 4.8 Hierarchy structure of the present analysis procedure

- After deciding the objective, criteria and sub criteria and constructing the hierarchy structure, a pairwaise comparison matrix formed for criteria and subcriteria by comparing each criteria with other criteria and subcriteria with other higher level sub criteria. For assigning rating for comparing one criteria over other, a scale for pair wise comparison is used as given in table 4.19 A typical pairwise comparison matrix (A) can be expressed as

$$[A] = \begin{bmatrix} a_{11} & a_{12} & \ldots\ldots & a_{1n} \\ a_{21} & a_{22} & \ldots\ldots & a_{2n} \\ . & . & \ldots\ldots & . \\ . & . & \ldots\ldots & . \\ . & . & \ldots\ldots & . \\ a_{n1} & a_{n2} & \ldots\ldots & a_{nn} \end{bmatrix}$$

where aij (for i, j = 1, 2, 3,. . ., n) is the strength of preferences of the a_i over a_j corresponding to the criterion ($a_{ij} = a_i/a_j$), also $a_{ji} = 1/a_{ij}$ and $a_{ii} = 1$ for all values of i and j.

Values of a_i and a_j were taken from the ratio scale for pairwise comparison as shown in table 4.19.

Table 4.19 Scale for pairwise comparison [56]

Rating	Preferential judgment/explanation
9	Extremely preferred
8	Between very strongly to extremely preferred
7	Very strongly preferred
6	Between strongly to very strongly preferred
5	Strongly preferred
4	Between moderately to strongly preferred
3	Moderately preferred
2	Between equally to moderately preferred
1	Equally preferred

- After completing the pairwise comparison matrices, sum of each columns of matrix is calculated. Once the column totals have been determined, the numbers in

the respective matrix are divided by their respective column totals to produce the normalized matrix. Once the matrix is normalized, the numbers in each column will sum to one**.** Now priority weight of each criteria is calculated by averaging the rows of the normalized matrix.

- To determine whether our responses are consistent or not, we need to find out the consistency ratio. In order to find out consistency ratio, a weighted sum vector is calculated. The original pairwise comparison matrix is multiplied with the column of row averages of the normalized matrix (i.e. priority weight column). Than a consistency vector is calculated by dividing weighted vector by the priority weight for each factor.

- After computing the consistency vector, eigen value λ_m and consistency index (CI) for pairwise matrix is calculated. Value of λ_m is calculated by averaging the values of consistency vector. Value of $\lambda_m \geq n$. Value of CI can be calculated by equation 4.1.

$$CI = \frac{\lambda_m - n}{n - 1} \qquad \text{(Equation 4.1)}$$

where n is the order of the pairwise comparison matrix.

- The degree of inconsistency is measured by the parameter called the consistency ratio (CR). A random index (RI) is also generated picking the values for order of the matrix (n) as can be found from table 4.20.

Table 4.20 Random Index (RI) for different matrix order (n) [56]

n	2	3	4	5	6	7	8	9	10
RI	0	0.56	0.9	0.12	1.25	1.34	1.42	1.45	1.51

The CR is defined by equation 4.2 and should be 10 per cent or less ($CR \leq 0.1$) for it to be acceptable

$$CR = \frac{CI}{RI} \qquad \text{(Equation 4.2)}$$

- If the maximum Eigenvalue λ_m , CI and CR are satisfactory then decision is taken based on the normalized values; else the procedure is repeated till these values lie in the desired range.

- Finally, the global weight is calculated by multiplying the priority weights of each alternative for different criteria with the pairwise comparison matrix of the criteria, i.e. criteria weight. The maximum value of the global weight is generally considered the optimum value and the corresponding alternative is selected for the optimum process setting [56].

4.6.3 Implementation of AHP

In the present experiment, WEDM process parameters are being optimized by following step-by-step AHP procedure that will maximize the MRR, lower the kerf width (KW) and improve the surface finish. It has been found by experimentation and ANOVA results that three responses (MRR, SR and KW) varied significantly for each of the workpiece material for similar machining conditions and thus workpiece is concluded as one of the control factors. Thus there are two alternatives available for optimizing the process parameters, one for each type of workpiece material (i.e for AISI 304 and AISI 410). The experimental design chosen for the present study is L16, it has 16 trials, with eight trials for each of the two workpiece materials as given in table 4.21. Thus, for each workpiece, eight different alternatives depicted by E1 to E8 were available in the present experimental design leading to two optimum solutions, one each for each workpiece.

Table 4.21 Results of MRR, SR and KW (Experiment Set 1)

Trial No.	Work piece	MRR	SR 'Mean'	KW 'Mean'
1	AISI 304	0.029	3.09	0.187
2	AISI 304	0.029	2.84	0.19
3	AISI 410	0.022	3.29	0.195
4	AISI 410	0.022	3.37	0.197
5	AISI 410	0.046	3.42	0.201
6	AISI 410	0.045	3.48	0.203

7	AISI 304	0.059	4.09	0.205
8	AISI 304	0.056	4.76	0.204
9	AISI 304	0.070	4.23	0.202
10	AISI 304	0.071	3.88	0.204
11	AISI 410	0.084	4.2	0.208
12	AISI 410	0.082	4.27	0.209
13	AISI 410	0.102	4.28	0.204
14	AISI 410	0.105	4.63	0.207
15	AISI 304	0.099	4.93	0.21
16	AISI 304	0.097	5.03	0.21

The hierarchy structure for the AHP solution for the present study is shown in figure 4.8. Selecting the alternatives from the experimental array leads to advantages like the alternatives and the optimum solution will involve all control parameters. Since the orthogonality was maintained during the L16 experimental design, obtaining the level setting for optimum solution was possible with a minimum number of experiments.

In order to decide the relative rating between two criteria, table 4.19 is used and for alternatives the decision for rating was made using the experimental results obtained for each response variable as given in table 4.21. Choosing and comparing two alternatives from experimental results eliminates the subjectivity and leads to objective evaluation of the two alternatives. By following the step by step procedure as mentioned in section 4.6.2, a pairwise comparison matrix for criteria, i.e. MRR, SR and KW (a 3×3 matrix), was established and is shown in table 4.22. The last column of table 4.22 shows the criteria weight (i.e. relative importance of each criteria) as obtained from the normalized eigen vector corresponding to maximum eigen value ($\lambda_{m} = 3.0183$).

Subsequently, the pairwise comparison matrices of alternatives for each workpiece material (AISI 304 and AISI 410) were developed for MRR, SR and kerf width using the experimental results. Trial numbers 1, 2, 7 to 10, 15 and 16 were used as the eight alternatives for AISI 304 workpiece. Similarly, trial numbers 3 to 6 and 11 to 14 were used as alternatives for AISI 410 respectively. Using this method, the pairwise comparison of each alternative for MRR using the two different workpiece materials are

given in tables 4.23 and 4.24. The last column of these tables show the priority weight of the alternatives as calculated by normalized eigen vector for maximum eigen value (λ_m). The CR value was also calculated and was observed to be less than 0.1, thus depicting consistency in the results. Similarly, tables 4.25 & 4.26 and tables 4.27 & 4.28 show the pairwise comparison matrices for SR and kerf width respectively for each of the two workpiece materials. The priority weights of the alternatives (E_i) for each of the three criteria (MRR, SR and kerf width) were assigned to the three columns of a priority matrix (P). The eight alternatives and three criteria resulted in a priority matrix of dimension 8×3. A column matrix C which was named as the criteria matrix (dimension 3×1), contained the criteria weight of MRR, SR and kerf width as obtained from the last column of table 4.21. Global weight matrix G, a column matrix, was then obtained (dimension 9×1), by multiplying the P matrix and C matrix and is given by $[G_{8\times1}] = [P_{8\times3}][C_{3\times1}]$.

Table 4.22 Pairwise comparison matrix for different criteria

	MRR	SR	KW	Criteria weight
MRR	1	1/6	1/2	0.1111
SR	6	1	3	0.6667
KW	2	1/3	1	0.2222
λ_m= 3			CR= 0.0000	

Table 4.23 Pairwise comparison matrix for alternatives on MRR of AISI 304

	E1	E2	E3	E4	E5	E6	E7	E8	Priority weight
E1	1	1	1/3	1/3	1/4	1/4	1/6	1/6	0.0331
E2	1	1	1/3	1/3	1/4	1/4	1/6	1/6	0.0331
E3	3	3	1	1	1/2	1/2	1/4	1/4	0.0748
E4	3	3	1	1	1/2	1/2	1/4	1/4	0.0748
E5	4	4	2	2	1	1	1/3	1/3	0.1199
E6	4	4	2	2	1	1	1/3	1/3	0.1199
E7	6	6	4	4	3	3	1	1	0.2721
E8	6	6	4	4	3	3	1	1	0.2721
λ_m= 8.1636						CR= 0.0165			

Table 4.24 Pairwise comparison matrix for alternatives on MRR of AISI 410

	E1	E2	E3	E4	E5	E6	E7	E8	Priority weight
E1	1	1	1/2	1/2	1/4	1/4	1/5	1/5	0.0393
E2	1	1	1/2	1/2	1/4	1/4	1/5	1/5	0.0393
E3	2	2	1	1	1/3	1/3	1/4	1/4	0.0632
E4	2	2	1	1	1/3	1/3	1/4	1/4	0.0632
E5	4	4	3	3	1	1	1/2	1/2	0.1527
E6	4	4	3	3	1	1	1/2	1/2	0.1527
E7	5	5	4	4	2	2	1	1	0.2448
E8	5	5	4	4	2	2	1	1	0.2448

$\lambda_{m=}$ 8.0971 CR= 0.0098

Table 4.25 Pairwise comparison matrix for alternatives on SR of AISI 304

	E1	E2	E3	E4	E5	E6	E7	E8	Priority weight
E1	1	1/2	3	4	3	2	5	5	0.2191
E2	2	1	4	5	4	3	6	6	0.3203
E3	1/3	1/4	1	2	1	1/2	3	3	0.0920
E4	1/4	1/5	1/2	1	1/2	1/3	2	2	0.0577
E5	1/3	1/4	1	2	1	1/2	3	3	0.0920
E6	1/2	1/3	2	3	2	1	4	4	0.1454
E7	0.2	1/6	1/3	1/2	1/3	1/4	1	1	0.0368
E8	0.2	1/6	1/3	1/2	1/3	1/4	1	1	0.0368

$\lambda_{m=}$ 8.1592 CR= 0.0160

Table 4.26 Pairwise comparison matrix for alternatives on SR of AISI 410

	E1	E2	E3	E4	E5	E6	E7	E8	Priority weight
E1	1	1	1	1	4	4	4	5	0.2011
E2	1	1	1	1	4	4	4	5	0.2011
E3	1	1	1	1	4	4	4	5	0.2011
E4	1	1	1	1	4	4	4	5	0.2011
E5	1/4	1/4	1/4	1/4	1	1	1	2	0.0537
E6	1/4	1/4	1/4	1/4	1	1	1	2	0.0537
E7	1/4	1/4	1/4	1/4	1	1	1	2	0.0537
E8	1/5	1/5	1/5	1/5	1/2	1/2	1/2	1	0.0344

$\lambda_{m=}$ 8.0420 CR= 0.0042

Table 4.27 Pairwise comparison matrix for alternatives on KW of AISI 304

	E1	E2	E3	E4	E5	E6	E7	E8	Priority weight
E1	1	1	2	2	2	2	2	2	0.2000
E2	1	1	2	2	2	2	2	2	0.2000
E3	1/2	1/2	1	1	1	1	1	1	0.1000
E4	1/2	1/2	1	1	1	1	1	1	0.1000
E5	1/2	1/2	1	1	1	1	1	1	0.1000
E6	1/2	1/2	1	1	1	1	1	1	0.1000
E7	1/2	1/2	1	1	1	1	1	1	0.1000
E8	1/2	1/2	1	1	1	1	1	1	0.1000
$\lambda_{m=}$ 8.0000						CR= 0.0000			

Table 4.28 Pairwise comparison matrix for alternatives on KW of AISI 410

	E1	E2	E3	E4	E5	E6	E7	E8	Priority weight
E1	1	1	1	2	2	2	2	2	0.1818
E2	1	1	1	2	2	2	2	2	0.1818
E3	1	1	1	2	2	2	2	2	0.1818
E4	1/2	1/2	1/2	1	1	1	1	1	0.0909
E5	1/2	1/2	1/2	1	1	1	1	1	0.0909
E6	1/2	1/2	1/2	1	1	1	1	1	0.0909
E7	1/2	1/2	1/2	1	1	1	1	1	0.0909
E8	1/2	1/2	1/2	1	1	1	1	1	0.0909
$\lambda_{m=}$ 8.0000						CR= 0.0000			

- *Calculation of global weights for AISI 304 and AISI 410*

In order to calculate the global weight of each alternative of AISI 304 and AISI 410, equation 4.4 is used. Each column of priority matrix P is the priority weight of alternatives (three columns for MRR, SR and KW respectively of AISI 304 from tables 4.23, 4.25 and 4.27 respectively) and criteria weight, C = $\{0.1111\ 0.6667\ 0.2222\}^T$ as mentioned in the table 4.21.

$$[P_{8\times3}][C_{3\times1}] = [G_{8\times1}] \qquad \text{(Equation 4.4)}$$

Solution of equation in matrix form for each alternative of AISI 304 is given below:

$$\begin{bmatrix} 0.0331 & 0.2191 & 0.2 \\ 0.0331 & 0.3203 & 0.2 \\ 0.0748 & 0.0920 & 0.1 \\ 0.0748 & 0.0577 & 0.1 \\ 0.1199 & 0.0920 & 0.1 \\ 0.1199 & 0.1454 & 0.1 \\ 0.2721 & 0.0368 & 0.1 \\ 0.2721 & 0.0368 & 0.1 \end{bmatrix} \times \begin{bmatrix} 0.1111 \\ 0.6667 \\ 0.2222 \end{bmatrix} = \begin{bmatrix} 0.194191 \\ 0.261661 \\ 0.091867 \\ 0.068999 \\ 0.096877 \\ 0.132479 \\ 0.076985 \\ 0.076985 \end{bmatrix}$$

Priority weight for each factor and calculated global weight for each alternative of AISI 304 is given in table 4.29.

Table 4.29 Global weight for alternatives of AISI 304

Alternatives for AISI 304 (Trial No.)	MRR priority weight	SR priority weight	KW priority weight	Global Weight
E1(1)	0.0331	0.2191	0.2	0.194191
E2(2)	0.0331	0.3203	0.2	**0.261661**
E3(7)	0.0748	0.0920	0.1	0.091867
E4(8)	0.0748	0.0577	0.1	0.068999
E5(9)	0.1199	0.0920	0.1	0.096877
E6(10)	0.1199	0.1454	0.1	0.132479
E7(15)	0.2721	0.0368	0.1	0.076985
E8(16)	0.2721	0.0368	0.1	0.076985

The global weight matrix shows that the second alternative has the maximum global weight (0.261661), therefore the second alternative will be the optimum solution for the AISI 304 workpiece. Thus the process conditions used in the second trial were selected as the optimal solution for AISI 304 material which will globally optimize the three responses. It can be seen that in WEDM process good surface finish alongwith smaller kerf can be obtained by using lower value of peak current and pulse on.

Solution of equation in matrix form for each alternative of AISI 410 is given below:

$$\begin{bmatrix} 0.0393 & 0.2011 & 0.1818 \\ 0.0393 & 0.2011 & 0.1818 \\ 0.0632 & 0.2011 & 0.1818 \\ 0.0632 & 0.2011 & 0.0909 \\ 0.1527 & 0.0537 & 0.0909 \\ 0.1527 & 0.0537 & 0.0909 \\ 0.2448 & 0.0537 & 0.0909 \\ 0.2448 & 0.0344 & 0.0909 \end{bmatrix} \times \begin{bmatrix} 0.1111 \\ 0.6667 \\ 0.2222 \end{bmatrix} = \begin{bmatrix} 0.178836 \\ 0.178836 \\ 0.181491 \\ 0.161293 \\ 0.072965 \\ 0.072965 \\ 0.083197 \\ 0.070330 \end{bmatrix}$$

Priority weight for each factor and calculated global weight for each alternative of AISI 410 is given in table 4.30.

Table 4.30 Global weight for alternatives of AISI 410

Alternatives for AISI 410 (Trial No.)	MRR priority weight	SR priority weight	KW priority weight	Global Weight
E1(3)	0.0393	0.2011	0.1818	0.178836
E2(4)	0.0393	0.2011	0.1818	0.178836
E3(5)	0.0632	0.2011	0.1818	**0.181491**
E4(6)	0.0632	0.2011	0.0909	0.161293
E5(11)	0.1527	0.0537	0.0909	0.072965
E6(12)	0.1527	0.0537	0.0909	0.072965
E7(13)	0.2448	0.0537	0.0909	0.083197
E8(14)	0.2448	0.0344	0.0909	0.070330

The global weight matrix shows that the second alternative has the maximum global weight (0.181491), therefore the third alternative will be the optimum solution for the AISI 410 workpiece. Thus the process conditions used in the third trial were selected as the optimal solution for AISI 410 material which will globally optimize the three responses. It can be seen that in WEDM process good surface finish alongwith smaller kerf can be obtained by using lower value of peak current and pulse on time.

4.7 RESULTS AND ANALYSIS FOR MRR (EXPERIMENT SET 2)

The results for MRR for each of the 16 treatment conditions for experiment 2 are given in table 4.31. MRR of each sample is calculated from weight difference of workpiece before and after the performance trial, which is given by:

$$\text{MRR} = \frac{(\text{Wi} - \text{Wf})}{\text{t}}$$

Where W_i = Initial weight of workpiece material (grams)

W_f = Final weight of workpiece material (grams)

t = Time period of each trials in minutes

Table 4.31 Results for MRR (experiment set 2)

Exp. No.	Peak Current (A)	Pulse on time (µs)	Work piece	Pulse off time (µs)	MRR (g/min)
1	1	30	EN 31	150	0.026
2	1	35	EN 31	150	0.03
3	1	40	H21	180	0.021
4	1	45	H21	180	0.019
5	2	30	H21	180	0.048
6	2	35	H21	180	0.047
7	2	40	EN 31	150	0.057
8	2	45	EN 31	150	0.055
9	3	30	EN 31	180	0.064
10	3	35	EN 31	180	0.068
11	3	40	H21	150	0.084
12	3	45	H21	150	0.082
13	4	30	H21	150	0.097
14	4	35	H21	150	0.097
15	4	40	EN 31	180	0.086
16	4	45	EN 31	180	0.085

4.7.1 Analysis of Variance for MRR

The results for MRR were analyzed using ANOVA for identifying the significant factors affecting the performance measures. The Analysis of Variance (ANOVA) for the mean MRR at 99% confidence interval is given in table 4.32. F-test was performed on the variance data for each factor to find significance of each. The principle of the F test is that the larger the F value for a particular parameter, the greater the effect on the performance characteristic due to the change in that process parameter. ANOVA table shows that current (F value 1400.17) and pulse off time (F value 208.46) are the significant factors which affect the MRR. Table 4.33 shows the ranks of various factors in terms their

relative significance. Current has the highest rank signifying highest contribution to MRR and workpiece has the lowest and was observed to be insignificant in affecting MRR.

Main effects plot for the MRR are shown in figure 4.9 which shows the variation of MRR with the input parameters. As can be seen MRR increases with increase in current from 1 Amp to 4 Amp. MRR is decreased with increase in pulse off time from 150µs to 180µs. This is due the fact that discharge energy increases with peak current and pulse on time resulting in faster material removal rate. Also as the pulse off time decreases, the amount of current discharges within a given period becomes more which results in higher material rate.

Table 4.32 ANOVA for Means of MRR

Source	DF	Seq SS	Adj MS	F	P
Peak Current	3	0.010201	0.003400	1400.17	0.00
Pulse On	3	0.000021	0.000007	2.92	0.11
Work Piece	1	0.000036	0.000036	14.82	0.01
Pulse Off	1	0.000506	0.000506	208.46	0.00
Residual Error	7	0.000017	0.000002		
Total	15	0.010758			

Table 4.33 Response Table for Means of MRR

Level	Peak Current	Pulse On	Work Piece	Pulse Off
1	0.02400	0.05875	0.05888	0.06600
2	0.05175	0.06050	0.06188	0.05475
3	0.07450	0.06200		
4	0.09125	0.06025		
Delta	0.06725	0.00325	0.00300	0.01125
Rank	1	3	4	2

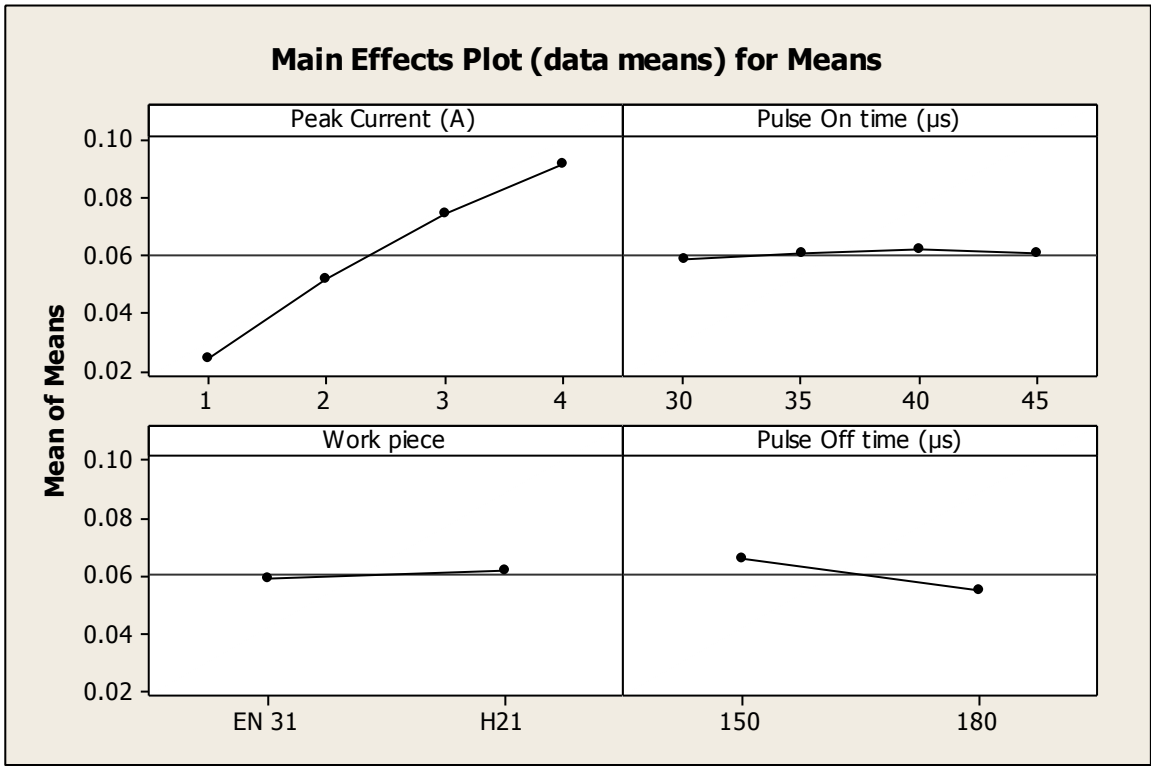

Figure 4.9 Main effects plot of MRR for Means

4.8 RESULTS AND ANALYSIS FOR SR (EXPERIMENT SET 2)

The results for surface roughness for each of the 16 treatment conditions for experiment 2 are given in table 4.34. Responses for surface roughness have been measured by using Mitutoyo surface-roughness measuring instrument.

Table 4.34 Results for Surface Roughness (Experiment Set 2)

Exp No.	Peak Current (A)	Pulse on time (µs)	Work piece	Pulse off time (µs)	SR Value '1'	SR Value '2'	SR 'Mean'	SN Ratio
1	1	30	EN 31	150	3.37	2.91	3.14	-9.9386
2	1	35	EN 31	150	2.79	3.71	3.25	-10.2377
3	1	40	H21	180	3.11	3.75	3.43	-10.7059
4	1	45	H21	180	3.63	3.35	3.49	-10.8565
5	2	30	H21	180	3.34	3.22	3.58	-11.0777
6	2	35	H21	180	4.47	3.99	4.23	-12.5268
7	2	40	EN 31	150	3.74	4.18	3.96	-11.9539

8	2	45	EN 31	150	3.61	4.09	3.85	-11.7092
9	3	30	EN 31	180	4.12	4.48	4.3	-12.6694
10	3	35	EN 31	180	3.98	4.52	4.25	-12.5678
11	3	40	H21	150	4.46	4.32	4.39	-12.8493
12	3	45	H21	150	3.90	4.02	3.96	-11.9539
13	4	30	H21	150	3.49	4.25	3.87	-11.7542
14	4	35	H21	150	4.28	4.58	4.43	-12.9281
15	4	40	EN 31	180	4.83	4.53	4.68	-13.4049
16	4	45	EN 31	180	4.02	4.46	4.24	-12.5473

4.8.1 Analysis of Variance for Surface Roughness

The results for surface roughness were analyzed using ANOVA for identifying the significant factors affecting the performance measures. ANOVA for the mean surface roughness at 99% confidence interval is given in table 4.35. The principle of the F test is that the larger the F value for a particular parameter, the greater the effect on the performance characteristic due to the change in that process parameter. ANOVA table shows that current (F value 20.75) and pulse on time (F value 3.19) are the factors that significantly affect the MRR, however workpiece (F value 0.14) is least significant to affect the surface roughness. Table 4.36 shows the ranks of various factors in terms their relative significance. Current has the highest rank signifying highest contribution to surface roughness and workpiece has the lowest and was observed to be insignificant in affecting surface roughness.

Main effects plot for the MRR are shown in figure 4.10 which shows the variation of surface roughness with the input parameters. As the peak current and pulse on time are increased, the discharge energy increases and this increase in discharge energy produces a larger crater, causing an increased value of surface roughness on the work piece. Also as the pulse off time decreases, the number of discharges increases which causes poor surface finish.

Table 4.35 ANOVA for Means of Surface Roughness

Source	DF	Seq SS	Adj MS	F	P
Peak Current	3	2.36332	0.787773	20.75	0.00
Pulse On	3	0.36382	0.121273	3.19	0.00
Work Piece	1	0.00526	0.005256	0.14	0.72
Pulse Off	1	0.11391	0.113906	3.00	0.13
Residual Error	7	0.26579	0.037971		
Total	15	3.11209			

Table 4.36 Response Table for Means of Surface Roughness

Level	Peak Current	Pulse On	Work Piece	Pulse Off
1	3.328	3.723	3.959	3.86
2	3.905	4.040	3.923	4.03
3	4.225	4.115		
4	4.305	3.885		
Delta	0.978	0.393	0.036	0.17
Rank	1	2	4	3

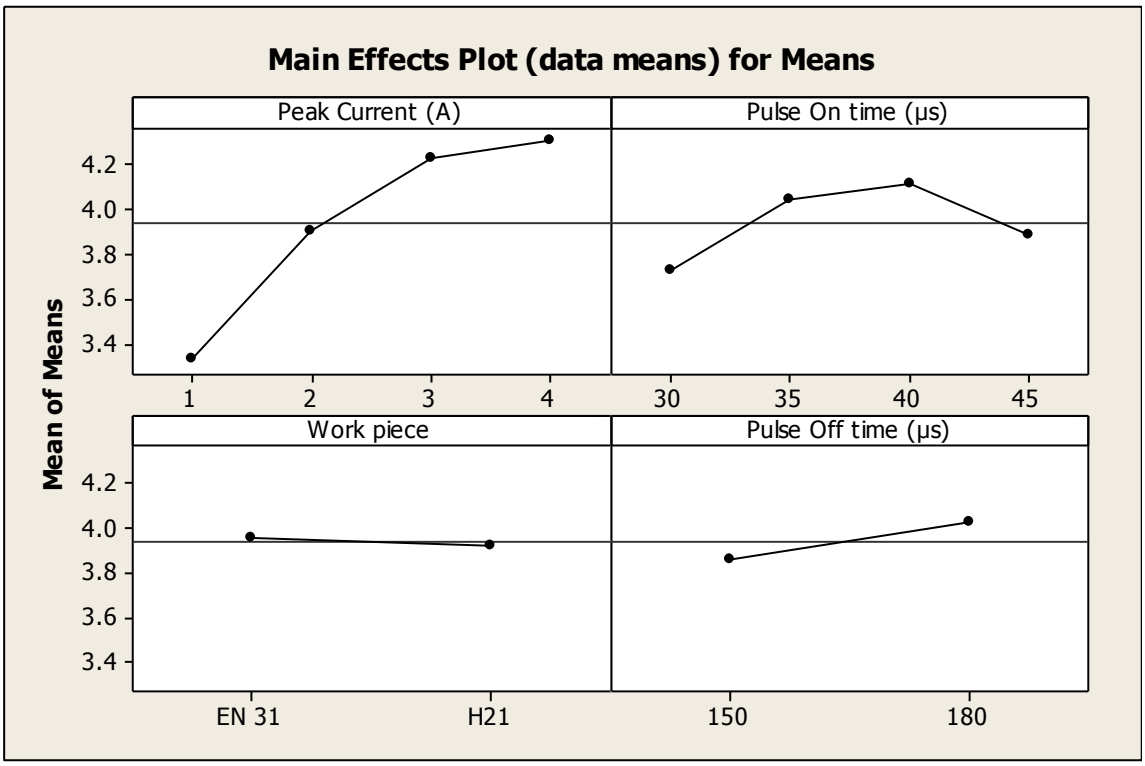

Figure 4.10 Main effects plot of Surface Roughness for Means

4.8.2 Results for SN Ratio of Surface Roughness

The SN ratio several repetitions into one value which reflects the amount of variation present. The values of all the results according to Taguchi array parameter design layout are presented in this section. The SN ratios have been calculated to identify the major contributing factors and interactions for variation in the roughness values In this design situation, roughness is the type of 'lower is better', which is a logarithmic function based on the mean square deviation (MSD), given by

$$S/N_{LB} = -10\log(MSD) = -10\log[(\frac{1}{r}\sum_{i=1}^{r} y^2{}_i)$$

Where $MSD_{LB} = \frac{1}{r}\sum_{j=1}^{r}\left(y_j{}^2\right)$

Table 4.37 shows the ANOVA for SN ratio for roughness at 99% confidence interval. Current, pulse on time and pulse off time are the most significant factors while workpiece being the insignificant factor. Main effects plot for the surface roughness are shown in Figure 4.11 which shows the variation of surface roughness with the input parameters.

Table 4.37 ANOVA for SN ratios of Surface Roughness

Source	DF	Seq SS	Adj MS	F	P
Peak Current	3	12.3751	4.12503	24.04	0.00
Pulse On	3	1.7460	0.58199	3.39	0.00
Work Piece	1	0.0089	0.0086	0.05	0.83
Pulse Off	1	0.5743	0.57433	3.35	0.11
Residual Error	7	1.2011	0.17158		
Total	15	15.9053			

Table 4.38 Response Table for SN Ratios of Surface Roughness

Level	Peak Current	Pulse On	Work Piece	Pulse Off
1	-10.43	-11.36	-11.88	-11.67
2	-11.82	-12.07	-11.83	-12.04
3	-12.51	-12.23		
4	-12.66	-11.77		
Delta	2.22	0.87	0.05	0.38
Rank	1	2	4	3

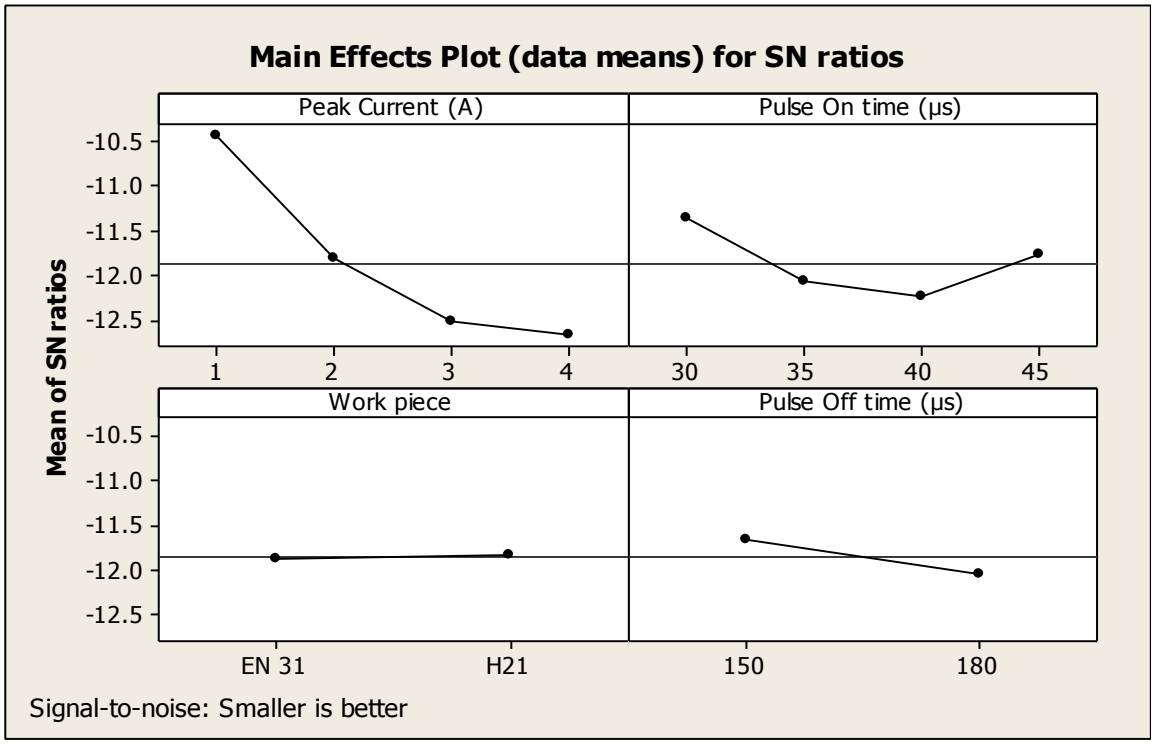

Figure 4.11 Main effects plot of Surface Roughness for SN Ratios

4.9 RESULTS AND ANALYSIS OF KERF WIDTH (EXPERIMENT SET 2)

The results for kerf width for each of the 16 treatment conditions for experiment 2 are given in table 4.39. Kerf width has been measured using Nikon profile projector. Three different values have been taken at three different points of the cut and average of these three values has been taken as the kerf width of the cut.

Table 4.39 Results for Kerf Width (Experiment Set 2)

Exp. No.	Peak Current (A)	Pulse on time (µs)	Work piece	Pulse off time (µs)	KW '1'	KW '2'	KW 'Mean'	SN Ratio
1	1	30	EN 31	150	0.191	0.195	0.193	14.2889
2	1	35	EN 31	150	0.194	0.196	0.195	14.1993
3	1	40	H21	180	0.194	0.192	0.193	14.2889
4	1	45	H21	180	0.192	0.196	0.194	14.244
5	2	30	H21	180	0.196	0.198	0.202	13.893
6	2	35	H21	180	0.211	0.213	0.212	13.4733
7	2	40	EN 31	150	0.212	0.21	0.211	13.5144

8	2	45	EN 31	150	0.211	0.215	0.213	13.4324
9	3	30	EN 31	180	0.204	0.2	0.202	13.893
10	3	35	EN 31	180	0.206	0.208	0.207	13.6806
11	3	40	H21	150	0.214	0.21	0.212	13.4733
12	3	45	H21	150	0.209	0.207	0.208	13.6387
13	4	30	H21	150	0.212	0.214	0.213	13.4324
14	4	35	H21	150	0.209	0.211	0.210	13.5556
15	4	40	EN 31	180	0.211	0.209	0.210	13.5556
16	4	45	EN 31	180	0.217	0.213	0.215	13.3512

4.9.1 Analysis of Variance for Kerf Width

The results for kerf width were analyzed using ANOVA for identifying the significant factors affecting the performance measures. ANOVA for the mean Kerf Width at 99% confidence interval is given in table 4.40. ANOVA table shows that peak current (F value 27.97) is the factor that significantly affects the kerf width. However workpiece (F value 0.03) is least significant to affect the kerf width. Table 4.41 shows the ranks of various factors in terms their relative significance. Current has the highest rank signifying highest contribution to surface roughness and workpiece has the lowest rank in affecting kerf width.

Main effects plot for the kerf width are shown in figure 4.12 which shows the variation of kerf width with the input parameters. Increased value for peak current and pulse on time leads to increased machining time. Longer machining time results in larger kerf values.

Table 4.40 ANOVA for Means of Kerf Width

Source	DF	Seq SS	Adj MS	F	P
Peak Current	3	0.000797	0.000266	27.97	0.00
Pulse On	3	0.000057	0.000019	1.99	0.20
WorkPiece	1	0.000000	0.000000	0.03	0.88
Pulse Off	1	0.000025	0.000025	2.63	0.15
Residual Error	7	0.000066	0.000009		
Total	15	0.000946			

Table 4.41 Response Table for Means of Kerf Width

Level	Peak Current	Pulse On	Work Piece	Pulse Off
1	0.1938	0.2025	0.2058	0.2069
2	0.2095	0.2060	0.2055	0.2044
3	0.2073	0.2065		
4	0.2120	0.2075		
Delta	0.0182	0.0050	0.0003	0.0025
Rank	1	2	4	3

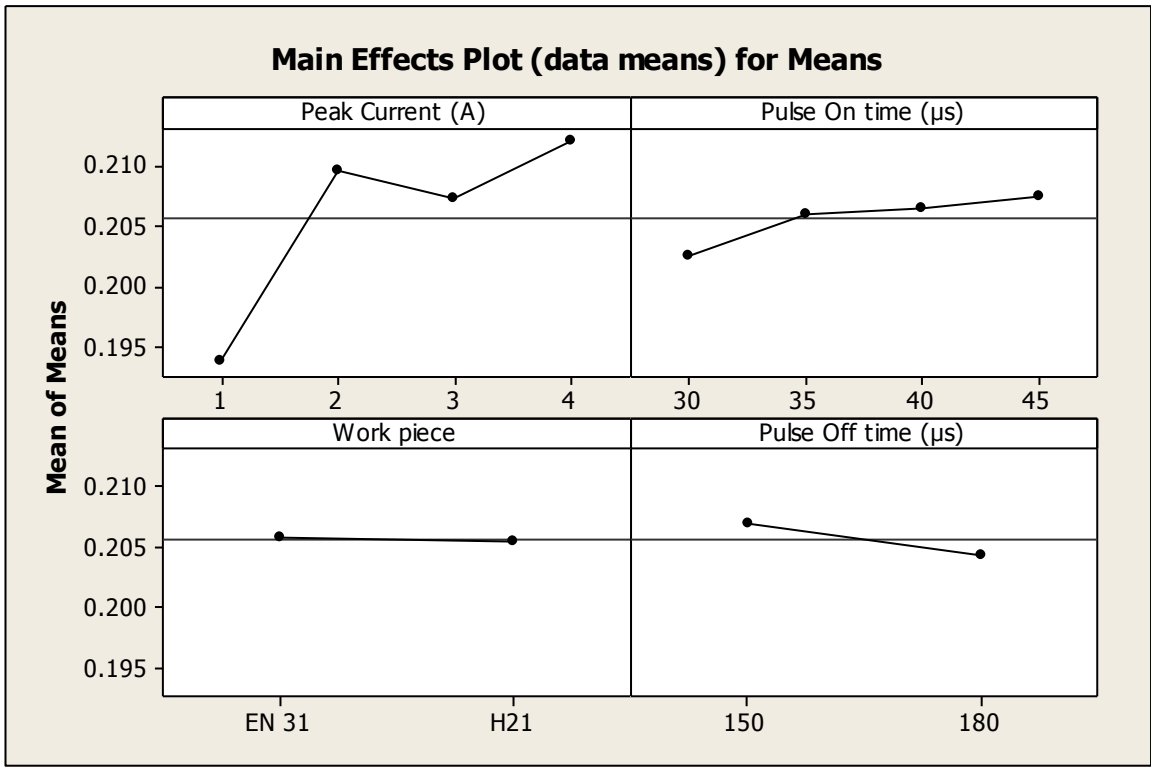

Figure 4.12 Main effects plot of Kerf Width for Means

4.9.2 Results for SN Ratio of Kerf Width

The SN ratio several repetitions into one value which reflects the amount of variation present. The values of all the results according to Taguchi array parameter design layout are presented in this section. The SN ratios have been calculated to identify the major contributing factors for variation in the kerf width values. In this design situation, kerf width is the type of 'lower is better', which is a logarithmic function based on the mean square deviation (MSD), given by

$$S/N_{LB} = -10\log(MSD) = -10\log[(\frac{1}{r}\sum_{i=1}^{r} y^2{}_i)$$

Where $MSD_{LB} = \frac{1}{r}\sum_{j=1}^{r}\left(y_j{}^2\right)$

Table 4.42 shows the ANOVA for SN ratio for roughness at 99% confidence interval. Among all the factors current, pulse on and powder are significant factor. Current and pulse off are the most significant which has highest contribution in kerf width, workpiece being the lowest contributing factor. Main effects plot for the kerf width are shown in figure 4.13 which shows the variation of kerf width with the input parameters.

Table 4.42 ANOVA for SN ratios of Kerf Width

Source	DF	Seq SS	Adj MS	F	P
Peak Current	3	1.46867	0.489555	29.87	0.00
Pulse On	3	0.10082	0.033606	2.05	0.19
Work Piece	1	0.00044	0.000439	0.03	0.86
Pulse Off	1	0.04458	0.044577	2.72	0.14
Residual Error	7	0.11472	0.016839		
Total	15	1.72922			

Table 4.43 Response Table for Signal to Noise Ratios of Kerf Width

Level	Peak Current	Pulse On	Work Piece	Pulse Off
1	14.26	13.88	13.74	13.69
2	13.58	13.73	13.75	13.80
3	13.67	13.71		
4	13.47	13.67		
Delta	0.78	0.21	0.01	0.11
Rank	1	2	4	3

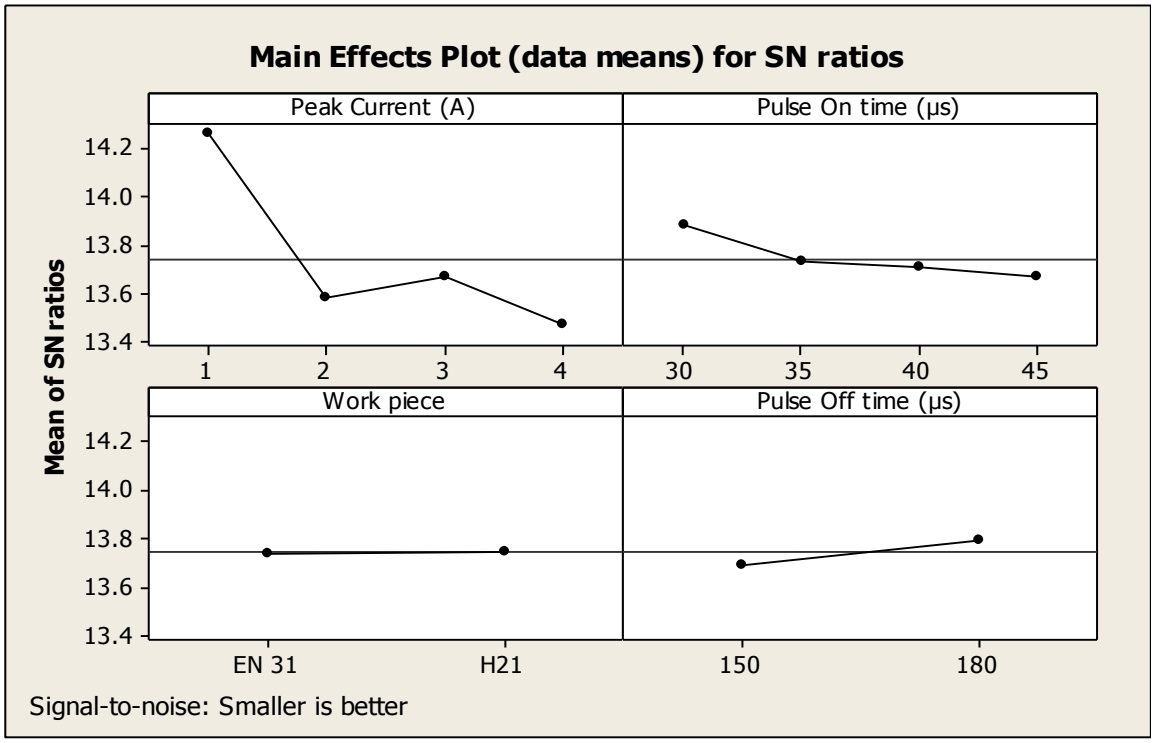

Figure 4.13 Main effects plot of Kerf Width for SN Ratios

4.10 RESULTS AND ANALYSIS FOR GAP CURRENT (EXPERIMENT SET 2)

The results for gap current for each of the 16 treatment conditions for experiment 2 are given in table 4.44. Gap current measurement was taken directly from the ampere meter in the control cabinet of the machine.

Table 4.44 Results for Gap Current (Experiment Set 2)

Exp No.	Peak Current (A)	Pulse On Time (µs)	Work piece	Pulse Off Time (µs)	Gap Current '1'	Gap Current '2'	Gap Current 'Mean'	SN Ratio
1	1	30	EN 31	150	0.75	0.75	0.75	-2.49877
2	1	35	EN 31	150	0.75	0.75	0.75	-2.49877
3	1	40	H21	180	0.75	0.75	0.75	-2.49877
4	1	45	H21	180	0.75	0.75	0.75	-2.49877
5	2	30	H21	180	1	1	1	0
6	2	35	H21	180	1	1	1	0
7	2	40	EN 31	150	1.4	1.4	1.4	2.92256

8	2	45	EN 31	150	1.4	1.4	1.4	2.92256
9	3	30	EN 31	180	1.5	1.5	1.5	3.52183
10	3	35	EN 31	180	1.5	1.5	1.5	3.52183
11	3	40	H21	150	1.75	1.75	1.75	4.86076
12	3	45	H21	150	1.75	1.75	1.75	4.86076
13	4	30	H21	150	2	2	2	6.0206
14	4	35	H21	150	2	2	2	6.0206
15	4	40	EN 31	180	1.75	1.75	1.75	4.86076
16	4	45	EN 31	180	1.75	1.75	1.75	4.86076

4.10.1 Analysis of Variance for Gap Current

The results for gap current were analyzed using ANOVA for identifying the significant factors affecting the performance measures. ANOVA for the mean gap current at 99% confidence interval is given in table 4.45. ANOVA table shows that current (F value 171.06) and pulse off time (F value 35.44) are the factors that significantly affect the gap current. However work piece (F value 0.44) is least significant to affect the gap current. Table 4.46 shows the ranks of various factors in terms their relative significance. Current has the highest rank signifying highest contribution to gap current and workpiece has the lowest rank in affecting gap current.

Main effects plot for the gap current are shown in figure 4.14 which shows the variation of gap current with the input parameters. As can be seen gap current increases with increase in peak current and increases with decrease in pulse off time.

Table 4.45 Analysis of Variance for Means of Gap Current

Source	DF	Seq SS	Adj MS	F	P
Peak Current	3	2.93250	0.977500	171.06	0.00
Pulse On	3	0.04000	0.013333	2.33	0.16
Work Piece	1	0.00250	0.002500	0.44	0.53
Pulse Off	1	0.20250	0.202500	35.44	0.00
Residual Error	7	0.04000	0.005714		
Total	15	3.21750			

Table 4.46 Response Table for Means of Gap Current

Level	Peak Current	Pulse On	Work Piece	Pulse Off
1	0.7500	1.3125	1.3500	1.4750
2	1.2000	1.3125	1.3750	1.2500
3	1.6250	1.4125		
4	1.8750	1.4125		
Delta	1.1250	0.1000	0.0250	0.2250
Rank	1	3	4	2

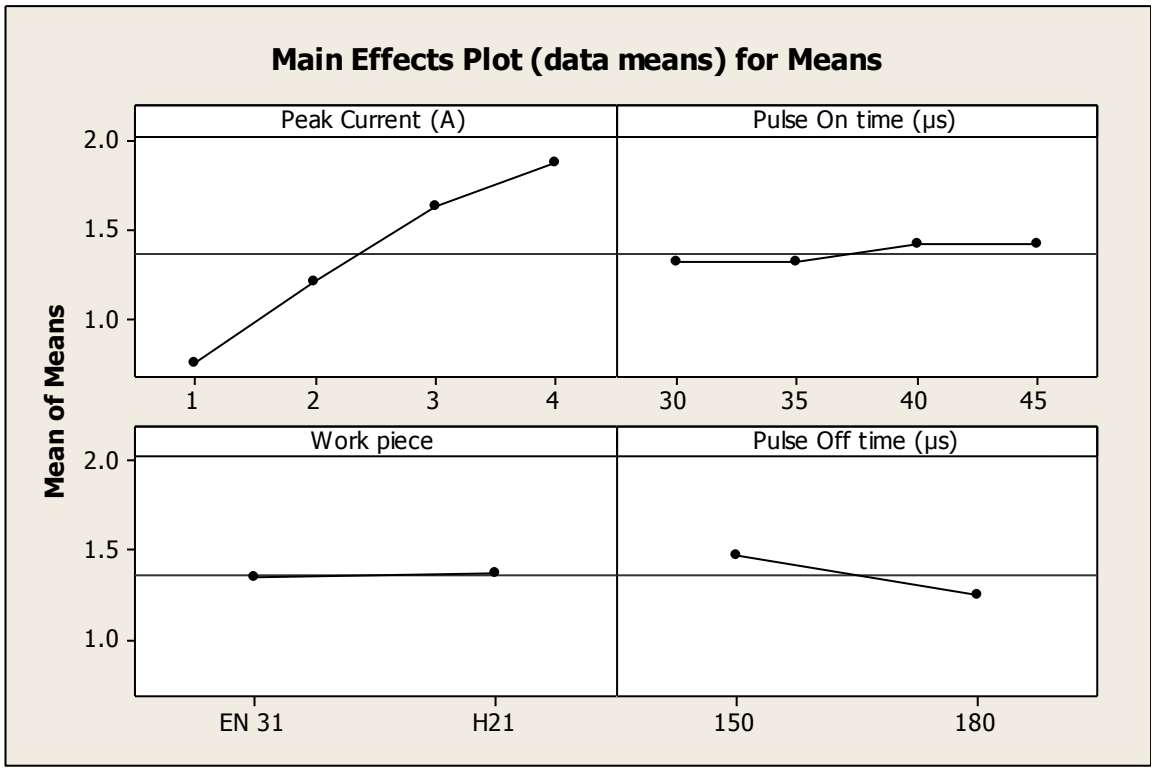

Figure 4.14 Main effects plot of Gap Current for Means

4.10.2 Results for SN Ratio of Gap Current

The SN ratio consolidates several repetitions into one value and is an indication of the amount of variation present. The SN ratios have been calculated to identify the major contributing factors and interactions that cause variation in the gap current. Gap current is "Higher is better" type response which is given by:

$(SN)_{HB} = -10 \log (MSD_{HB})$

Where $MSD_{HB} = \frac{1}{r}\sum_{j=1}^{r}\left(\frac{1}{y_j^{\,2}}\right)$

MSD_{HB} = Mean Square Deviation for higher-the-better response.

Table 4.47 shows the ANOVA results for SN ratio of MRR at 99% confidence interval. Current was observed to be the most significant factor affecting the gap current, followed by pulse off time and pulse on time according to F test. Although workpiece seems to be insignificant, table 4.48 shows the ranks of various factors in terms their relative significance. Current has the highest rank signifying highest contribution to gap current and workpiece has the lowest rank and was observed to be insignificant in affecting gap current. Main effects plot of SN ratio for MRR are shown in the figure 4.15.

Table 4.47 Analysis of Variance for SN ratios of Gap Current

Source	DF	Seq SS	Adj MS	F	P
Peak Current	3	148.324	49.4412	183.93	0.00
Pulse On	3	2.405	0.8017	2.98	0.11
Work Piece	1	0.045	0.0449	0.17	0.70
Pulse Off	1	7.348	7.3477	27.33	0.00
Residual Error	7	1.882	0.2688		
Total	15	160.003			

Table 4.48 Response Table for Signal to Noise Ratios of Gap Current

Level	Peak Current	Pulse On	Work Piece	Pulse Off
1	-2.499	1.761	2.202	2.826
2	1.461	1.761	2.096	1.471
3	4.191	2.536		
4	5.441	2.536		
Delta	7.939	0.775	0.106	1.355
Rank	1	3	4	2

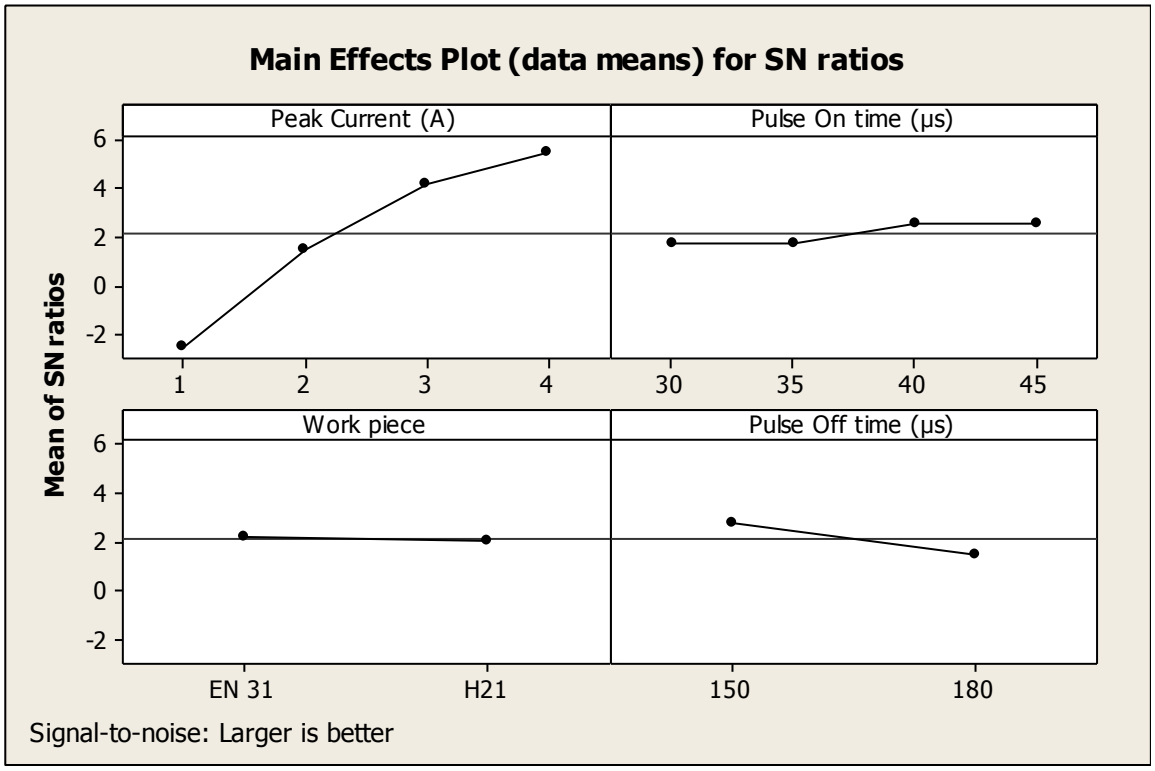

Figure 4.15 Main effects plot of Gap Current for SN Ratios

4.11 OPTIMAL DESIGN FOR EXPERIMENT SET 2

In this experimental analysis, the main effect plots for different parameters studied and it was observed that workpiece is the least significant factor in WEDM process. As the response variable MRR is higher the better response, surface roughness and kerf width are lower the better response variables. In WEDM process it is desired that machined workpiece should have good surface finish and smaller kerf width, however it is sometimes necessary to have higher material removal rates. In order to optimize the WEDM process for the current experimental set, The Analytic Hierarchy Process, commonly known as AHP has been chosen.

4.11.1 Steps Involved In AHP

The steps involved for AHP are same as discussed for experimental set 1 under section 4.6.2.

4.11.2 Implementation of AHP

In the present experiment, WEDM process parameters are being optimized by following step-by-step AHP procedure that will maximize the MRR, lower the kerf width (KW) and

improve the surface finish. It has been found by experimentation and ANOVA results that three responses (MRR, SR and KW) varied significantly for each of the workpiece material for similar machining conditions and thus workpiece is concluded as one of the control factors. Thus there are two alternatives available for optimizing the process parameters, one for each type of workpiece material (i.e for EN 31 and H21). The experimental design chosen for the present study is L16, it has 16 trials, with eight trials for each of the two workpiece materials as given in table 4.49. Thus, for each workpiece, eight different alternatives depicted by E1 to E8 were available in the present experimental design leading to two optimum solutions, one each for each workpiece.

Table 4.49 Results of MRR, SR and KW (Experiment Set 2)

Trial No.	Work piece	MRR (g/min)	SR 'Mean'	KW 'Mean'
1	EN 31	0.026	3.14	0.193
2	EN 31	0.030	3.25	0.195
3	H21	0.021	3.43	0.193
4	H21	0.019	3.49	0.194
5	H21	0.048	3.58	0.202
6	H21	0.047	4.23	0.212
7	EN 31	0.057	3.96	0.211
8	EN 31	0.055	3.85	0.213
9	EN 31	0.064	4.30	0.202
10	EN 31	0.068	4.25	0.207
11	H21	0.084	4.39	0.212
12	H21	0.082	3.96	0.208
13	H21	0.097	3.87	0.213
14	H21	0.097	4.43	0.210
15	EN 31	0.086	4.68	0.210
16	EN 31	0.085	4.24	0.215

In order to decide the relative rating between two criteria, table 4.19 is used and for alternatives the decision for rating was made using the experimental results obtained for each response variable as given in table 4.49. Choosing and comparing two alternatives

from experimental results eliminates the subjectivity and leads to objective evaluation of the two alternatives. By following the step by step procedure as mentioned in section 4.6.2, a pairwise comparison matrix for criteria, i.e. MRR, SR and KW (a 3×3 matrix), was established and is shown in table 4.50. The last column of table 4.50 shows the criteria weight (i.e. relative importance of each criteria) as obtained from the normalized eigen vector corresponding to maximum eigen value (λ_m = 3.0183).

Subsequently, the pairwise comparison matrices of alternatives for each workpiece material (EN 31 and H21) were developed for MRR, SR and kerf width using the experimental results. Trial numbers 1, 2, 7 to 10, 15 and 16 were used as the eight alternatives for EN 31workpiece. Similarly, trial numbers 3 to 6 and 11 to 14 were used as alternatives for H21 respectively. Using this method, the pairwise comparison of each alternative for MRR using the two different workpiece materials are given in tables 4.51 and 4.52. The last column of these tables show the priority weight of the alternatives as calculated by normalized eigen vector for maximum eigen value (λ_m). The CR value was also calculated and was observed to be less than 0.1, thus depicting consistency in the results. Similarly, tables 4.53 & 4.54 and tables 4.55 & 4.56 show the pairwise comparison matrices for SR and kerf width respectively for each of the two workpiece materials. The priority weights of the alternatives (E_i) for each of the three criteria (MRR, SR and kerf width) were assigned to the three columns of a priority matrix (P). The eight alternatives and three criteria resulted in a priority matrix of dimension 8×3. A column matrix C which was named as the criteria matrix (dimension 3×1), contained the criteria weight of MRR, SR and kerf width as obtained from the last column of table 4.21. Global weight matrix G, a column matrix, was then obtained (dimension 9×1), by multiplying the P matrix and C matrix and is given by $[G_{8\times1}] = [P_{8\times3}][C_{3\times1}]$

Table 4.50 Pairwise comparison matrix for different criteria

	MRR	SR	KW	Criteria weight
MRR	1	1/6	1/2	0.1111
SR	6	1	3	0.6667
KW	2	1/3	1	0.2222
λ_m= 3		CR= 0.0000		

Table 4.51 Pairwise comparison matrix for alternatives on MRR of EN 31

	E1	E2	E3	E4	E5	E6	E7	E8	Priority weight
E1	1	1	1/3	1/3	1/4	1/4	1/5	1/5	0.0368
E2	1	1	1/3	1/3	1/4	1/4	1/5	1/5	0.0368
E3	3	3	1	1	1/2	1/2	1/3	1/3	0.0857
E4	3	3	1	1	1/2	1/2	1/3	1/3	0.0857
E5	4	4	2	2	1	1	1/2	1/2	0.1420
E6	4	4	2	2	1	1	1/2	1/2	0.1420
E7	5	5	3	3	2	2	1	1	0.2354
E8	5	5	3	3	2	2	1	1	0.2354
$\lambda_{m=}$ 8.1027						CR= 0.0103			

Table 4.52 Pairwise comparison matrix for alternatives on MRR of H21

	E1	E2	E3	E4	E5	E6	E7	E8	Priority weight
E1	1	1	1/3	1/3	1/5	1/5	1/6	1/6	0.0313
E2	1	1	1/3	1/3	1/5	1/5	1/6	1/6	0.0313
E3	3	3	1	1	1/3	1/3	1/4	1/4	0.0681
E4	3	3	1	1	1/3	1/3	1/4	1/4	0.0681
E5	5	5	3	3	1	1	1/2	1/2	0.1547
E6	5	5	3	3	1	1	1/2	1/2	0.1547
E7	6	6	4	4	2	2	1	1	0.2460
E8	6	6	4	4	2	2	1	1	0.2460
$\lambda_{m=}$ 8.1593						CR= 0.0160			

Table 4.53 Pairwise comparison matrix for alternatives on SR of EN 31

	E1	E2	E3	E4	E5	E6	E7	E8	Priority weight
E1	1	1	3	3	4	4	5	4	0.2693
E2	2	1	3	3	4	4	5	4	0.2693
E3	1/3	1/3	1	1	2	2	3	2	0.1132
E4	1/3	1/3	1	1	2	2	3	2	0.1132
E5	1/4	1/4	1/2	1/2	1	1	2	1	0.0651
E6	1/4	1/4	1/2	1/2	1	1	2	1	0.0651
E7	1/5	1/5	1/3	1/3	1/2	1/2	1	1/2	0.0398
E8	1/4	1/4	1/2	1/2	1	1	2	1	0.0651
$\lambda_{m=}$ 8.0816						CR= 0.0082			

Table 4.54 Pairwise comparison matrix for alternatives on SR of H21

	E1	E2	E3	E4	E5	E6	E7	E8	Priority weight
E1	1	1	1	3	3	2	2	3	0.1979
E2	1	1	1	3	3	2	2	3	0.1979
E3	1	1	1	3	3	2	2	3	0.1979
E4	1/3	1/3	1/3	1	1	1/2	1/2	1	0.0616
E5	1/3	1/3	1/3	1	1	1/2	1/2	1	0.0616
E6	1/2	1/2	1/2	2	2	1	1	2	0.1107
E7	1/2	1/2	1/2	2	2	1	1	2	0.1107
E8	1/3	1/3	1/3	1	1	1/2	1/2	1	0.0616

$\lambda_{m=}$ 8.0233 CR= 0.0023

Table 4.55 Pairwise comparison matrix for alternatives on KW of EN 31

	E1	E2	E3	E4	E5	E6	E7	E8	Priority weight
E1	1	1	2	2	1	2	2	2	0.1818
E2	1	1	2	2	1	2	2	2	0.1818
E3	1/2	1/2	1	1	1/2	1	1	1	0.0909
E4	1/2	1/2	1	1	1/2	1	1	1	0.0909
E5	1	1	2	2	1	2	2	2	0.1818
E6	1/2	1/2	1	1	1/2	1	1	1	0.0909
E7	1/2	1/2	1	1	1/2	1	1	1	0.0909
E8	1/2	1/2	1	1	1/2	1	1	1	0.0909

$\lambda_{m=}$ 8.0000 CR= 0.0000

Table 4.56 Pairwise comparison matrix for alternatives on KW of H21

	E1	E2	E3	E4	E5	E6	E7	E8	Priority weight
E1	1	1	1	2	2	2	2	2	0.1818
E2	1	1	1	2	2	2	2	2	0.1818
E3	1	1	1	2	2	2	2	2	0.1818
E4	1/2	1/2	1/2	1	1	1	1	1	0.0909
E5	1/2	1/2	1/2	1	1	1	1	1	0.0909
E6	1/2	1/2	1/2	1	1	1	1	1	0.0909
E7	1/2	1/2	1/2	1	1	1	1	1	0.0909
E8	1/2	1/2	1/2	1	1	1	1	1	0.0909

$\lambda_{m=}$ 8.0000 CR= 0.0000

- *Calculation of Global Weights for EN 31 and H21*

In order to calculate the global weight of each alternative of EN 31 and H21, equation 4.4 is used. Each column of priority matrix P is the priority weight of alternatives (three columns for MRR, SR and KW respectively of AISI 304 from tables 4.51, 4.53 and 4.55 respectively) and criteria weight, C = $\{0.1111\ 0.6667\ 0.2222\}^T$ as mentioned in the table 4.50

$$[P_{8\times3}][C_{3\times1}] = [G_{8\times1}] \qquad \text{(Equation 4.4)}$$

Solution of equation 4.4 in matrix form for each alternative of EN 31 is given below:

$$\begin{bmatrix} 0.0368 & 0.2693 & 0.1818 \\ 0.0368 & 0.2693 & 0.1818 \\ 0.0857 & 0.1132 & 0.0909 \\ 0.0857 & 0.1132 & 0.0909 \\ 0.1420 & 0.0651 & 0.1818 \\ 0.1420 & 0.0651 & 0.0909 \\ 0.2354 & 0.0398 & 0.0909 \\ 0.2354 & 0.0651 & 0.0909 \end{bmatrix} \times \begin{bmatrix} 0.1111 \\ 0.6667 \\ 0.2222 \end{bmatrix} = \begin{bmatrix} 0.222612 \\ 0.222612 \\ 0.103851 \\ 0.103851 \\ 0.110144 \\ 0.079802 \\ 0.072096 \\ 0.087040 \end{bmatrix}$$

Priority weight for each factor and calculated global weight for each alternative of EN 31 is given in table 4.57.

Table 4.57 Global weight for alternatives of EN 31

Alternatives for EN 31 (Trial No.)	MRR priority weight	SR priority weight	KW priority weight	Global Weight
E1(1)	0.0368	0.2693	0.1818	**0.222612**
E2(2)	0.0368	0.2693	0.1818	**0.222612**
E3(7)	0.0857	0.1132	0.0909	0.103851
E4(8)	0.0857	0.1132	0.0909	0.103851
E5(9)	0.1420	0.0651	0.1818	0.110144
E6(10)	0.1420	0.0651	0.0909	0.079802
E7(15)	0.2354	0.0398	0.0909	0.072096
E8(16)	0.2354	0.0651	0.0909	0.087040

The global weight matrix shows that the first and second alternative has the maximum global weight (0.222612), therefore the first and second alternative will be the optimum solution for the EN 31 workpiece. Thus the process conditions used in the first and second trial were selected as the optimal solution for EN 31 material which will globally

optimize the three responses. It can be seen that in WEDM process good surface finish alongwith smaller kerf can be obtained by using lower value of peak current and pulse on.

Solution of equation 4.4 in matrix form for each alternative is given below. Each column of priority matrix P is the priority weight of alternatives (three columns for MRR, SR and KW respectively of H21 from tables 4.52, 4.54 and 4.56 respectively) and criteria weight, C = {0.1111 0.6667 0.2222}^{T} as mentioned in the table 4.50

$$\begin{bmatrix} 0.0313 & 0.1979 & 0.1818 \\ 0.0313 & 0.1979 & 0.1818 \\ 0.0681 & 0.1979 & 0.1818 \\ 0.0681 & 0.0616 & 0.0909 \\ 0.1547 & 0.1107 & 0.0909 \\ 0.1547 & 0.1107 & 0.0909 \\ 0.2460 & 0.1107 & 0.0909 \\ 0.2460 & 0.0616 & 0.0909 \end{bmatrix} \times \begin{bmatrix} 0.1111 \\ 0.6667 \\ 0.2222 \end{bmatrix} = \begin{bmatrix} 0.18001 \\ 0.18001 \\ 0.182862 \\ 0.072007 \\ 0.078719 \\ 0.107722 \\ 0.114798 \\ 0.085795 \end{bmatrix}$$

Priority weight for each factor and calculated global weight for each alternative of AISI H21 is given in table 4.58.

Table 4.58 Global weight for alternatives of H21

Alternatives for H21 (Trial No.)	MRR priority weight	SR priority weight	KW priority weight	Global Weight
E1(3)	0.0313	0.1979	0.1818	0.18001
E2(4)	0.0313	0.1979	0.1818	0.18001
E3(5)	0.0681	0.1979	0.1818	**0.182862**
E4(6)	0.0681	0.0616	0.0909	0.072007
E5(11)	0.1547	0.0616	0.0909	0.078719
E6(12)	0.1547	0.1107	0.0909	0.107722
E7(13)	0.2460	0.1107	0.0909	0.114798
E8(14)	0.2460	0.0616	0.0909	0.085795

The global weight matrix shows that the third alternative has the maximum global weight (0.182862), therefore the third alternative will be the optimum solution for the H21 workpiece. Thus the process conditions used in the third trial were selected as the optimal solution for H21 material which will globally optimize the three responses. It can be seen

that in WEDM process good surface finish alongwith smaller kerf can be obtained by using lower value of peak current and pulse on time.

CHAPTER 5
CONCLUSIONS AND RECOMMENDATIONS

5.1 CONCLUSIONS

In the previous chapters, the effect of machining parameters of WEDM on response variables such as material removal rate (MRR), surface finish, kerf width and gap current on different materials (AISI 304, AISI 410, EN 31 and H21) has been discussed. Also the levels of importance of machining parameters for each of response variables has been found out using ANOVA. An optimal set of process variables for each workpiece which gives optimum performance has been investigated using Analytic Hierarchy Process (AHP). The important conclusions drawn from the present study are summarized below:

- The process parameters and their ranges are chosen for the present study. Also two different set of experiments have been performed using two different materials for each experiment set.

- Thus the orthogonal array has been selected for four variables (namely peak current, pulse on-time, pulse off-time and material) and L16 has been chosen as orthogonal array for current experimentation.

- The effect of process parameters i.e. peak current, pulse on time, pulse off time and different materials) on response variables such as material removal rate, surface roughness, kerf width and gap current has been thoroughly studied. The levels of significance of process parameters for each response variable has been investigated using ANOVA.

- Peak current and pulse on time were found to be the most significant factors influencing all responses investigated for both the experiment sets. Increased values of peak current and pulse on time leads to the low quality of machining responses such as surface finish and kerf width.

- As the value of peak current and pulse on time are increased, material removal rate and gap current are also increased. Also if value of pulse off is decreased, better material removal rate and better gap current are achieved.

- The optimal sets of process parameters were obtained for each work piece using Analytic Hierarchy Process (AHP). The optimal values of process parameters for each work piece material are given in table 5.1.

Table 5.1 Optimal process parameter settings for different workpiece

Workpiece	Optimal process setting
AISI 304	Trial 02; Peak current 1 A, Pulse on time 35 µs, Pulse off time 150 µs
AISI 410	Trial 05; Peak current 2 A, Pulse on time 30 µs, Pulse off time 180 µs
EN 31	Trial 01 and Trial 02; Peak current 1 A, Pulse on time 30 µs & 35 µs, Pulse off time 150 µs
H21	Trial 05; Peak current 2 A, Pulse on time 30 µs, Pulse off time 180 µs

5.2 RECOMMENDATIONS FOR FUTURE WORK

Based on the observations and findings in this study, the future work might attempt to consider the other criteria proposed as follows:

- The effect of process parameters on response variables for materials namely AISI 304, AISI 410, EN 31 and H21 has been investigated using WEDM, still there is scope of further investigation for other materials.

- Molybdenum wire electrode (0.18 mm diameter) has been used for present investigation, however different types of wire materials as electrode need to be investigated for better understanding of WEDM.

- The effect of process parameters such as flushing pressure, conductivity of dielectric, wire diameter, workpiece height etc. may also be investigated.

- The effect of process parameters on response variables in different cutting environment may also be investigated.

- Priority weights assigned to different response variable for optimization of the process parameters should be based upon as per the requirement of the industry.

REFERENCES

1. H. A.-G. El-Hofy, "Advanced Machining Processes", McGraw-Hill, Production Engineering Department, Alexandria University, Egypt,
2. P. K. Mishra, "Non-Conventional Machining", Narosa Publishing House, Edition 2005.
3. S. Kim (2005), "Determination of Wall Thickness and Height Limits When Cutting Various Materials with Wire Electric Discharge Machining", Brigham Young University, Utah. http://contentdm.lib.byu.edu/ETD/image/etd757.pdf
4. "Study of EDM wire cutting precision", http://www.scribd.com/doc/28304019/EDM-wire-cuting
5. R. Agarwal (2010), "Optimization of Process Parameters of Micro Wire EDM", Department of Mechanical Engineering, National Institute of Technology, Rourkela http://ethesis.nitrkl.ac.in/1937/1/ricky's_project2.pdf
6. C. Sommer and S. Sommer**,** "The Wire EDM handbook", www.reliableedm.com.
7. P. C. Pandey and H. S. Shan, "Modern Machining Processes", Tata Mcgraw-Hill, New Delhi.
8. J. Proshka, A. G Mamalis and N. M. Vaxevanidis (1997), "The Effect of Electrode Material on Machinability in Wire Electro Discharge Machining", Journal of Material Processing Technology, 69, 233-237.
9. J. Kozak, K. P. Rajurkar and N. Chandarana, N. (2004), "Machining of Low Electrical Conductive Materials by Wire Electrical Discharge Machining (WEDM) Process", Journal of Materials Processing Technology, 149, 266-276.
10. Y. K. Lok and T. C. Lee (1997), "Processing of Advanced Ceramics using the Wire-Cut EDM Process", Journal of Materials Processing Technology, 63 (1-3), 839-843.
11. Y. C. Lin, B. H. Yan and Y. S. Chang (2000). "Machining Characteristics of Titanium Alloy (Ti-6Al-4V) Using a Combination Process of EDM and USM", Journal of Material Processing Technology, 104, 171-177.
12. A. Pandey and S. Singh (2010), "Current Research Trends in Variants of Electrical Discharge Machining: A Review", International Journal of Engineering Science and Technology, 2 (6), 2172-2191.
13. G. F. Schrader, A. K. Elshennawy, E. Lawrence (2000). "Manufacturing Processes & Materials", Society of Manufacturing Engineers, Edition 4.

14. A. R. Machado and J. Wallbank (1990), “Machining of Titanium and its Alloys – A Review”, Proc. Instn. Mech. Engrs., 204, 53-60.
15. G. F. Benedict (1987), “Electrical Discharge Machining (EDM), Non Traditional Manufacturing Process”, Marcel Dekker, Inc, New York & Basel, 231-232.
16. R. C. Stephenson (2007), “Comparing the Feasibility of Cutting Thin-Walled Sections From Five Commonly Used Metals Utilizing WEDM”, Brigham Young University, Utah. http://contentdm.lib.byu.edu/ETD/image/etd1948.pdf
17. Intech EDM, “A Reference to Understanding, Selecting and Using Wire on Wire-cut EDM Machines”, Edition 2, http://us.gfac.com/intech/shop/documents/wirebook.pdf
18. J. Kapoor, S. Singh and J. S. Khamba (2010), “Recent Developments in Wire Electrodes for High Performance WEDM”, Proceedings of the World Congress on Engineering, 2.
19. J. T. Huang, Y. S. Liao and W. J. Hsue (1999), “Determination of Finish-Cutting Operation Number and Machining-Parameters Setting in Wire Electrical Discharge Machining”, Journal of Materials Processing Technology,87, 69–81.
20. Y. S. Liao and Y. P. Yu (2004), “Study of Specific Discharge Energy in WEDM and its Application”, International Journal of Machine Tools & Manufacture, 44, 1373–1380.
21. H. Singh and R. Garg (2009), “Effects of Process Parameters on Material Removal Rate in WEDM”, Journal of Achievements in Materials and Manufacturing Engineering, 32 (1), 70-74.
22. N. G. Patil and P. K. Brahmankar (2010), “Some Studies Into Wire Electro-Discharge Machining of Alumina Particulate-Reinforced Aluminum Matrix Composites”, International Journal of Advanced Manufacturing Technology, 48, 537–555.
23. S. Mahapatra and A. Patnaik (2006), “Optimization of Wire Electrical Discharge Machining (WEDM) Process Parameters Using Taguchi Methods”, International Journal of Advance Manufacturing Technology, 34, 911-925.
24. C.-H. Kim, “Influence of the Electrical Conductivity of Dielectric Fluid on WEDM Machinability”
25. S. Datta and S. S. Mahapatra (2010), “Modeling, Simulation and Parametric Optimization of Wire EDM Process Using Response Surface Methodology Coupled with Grey-Taguchi Technique”, International Journal of Engineering, Science and Technology, 2, 162-183.

26. K. Kanlyasiri and S. Boonmung (2007), “An Investigation on Effects of Wire-EDM Machining Parameters on Surface Roughness of Newly Developed DC53 Diesteel”, J. Mater. Proc. Technol., 187, 26-29.
27. M. P. Groover (2007). “Fundamentals of Modern Manufacturing – Materials, Process and Systems, Chapter 26” John Wiley & Sons.
28. F. Othman (2008). “EDM Wirecut of Titanium Alloy (Ti-6A14V) Using Brass Coated Wire Electrode” Universiti Teknologi Malaysia: Master Thesis.
29. N. Tosun, C. Cogun and G. Tosun (2004), “A Study on Kerf and Material Removal Rate in Wire Electrical Discharge Machining Based on Taguchi Method”, Journal of Material Processing Technology, 152, 316-322.
30. A. Mohammadi, A. F. Tehrani, E. Emanian and D. Karimi (2008), “A New Approach to Surface Roughness and Roundness Improvement in Wire Electrical Discharge Turning Based on Statistical Analyses”, International Journal of Advance Manufacturing Technology, 39, 64–73.
31. C. Kim and K. Hur (2002), “Discharge Frequency of WEDM Machinability of Polycrystalline Diamond tool blank (PCD Blank)”, The 35th CIRP International Seminar on Manufacturing Systems, 35, 547-550.
32. H. Juhr, H.-P. Schulze, G. Wollenberg and K. Künanza (2004), “Improved cemented Carbide Properties after Wire-EDM by Pulse Shaping”, Journal of Materials Processing Technology, 149, 178–183.
33. W. Y. Peng and Y. S. Liao (2003), “Study of Electrical Discharge Machining Technology for Slicing Silicon Ingots”, Journal of Materials Processing Technology, 140, 274–279.
34. M. N. Islam, N. H. Rafai and S. S. Subramanian (2010), “An Investigation into Dimensional Accuracy Achievable in Wire-cut Electrical Discharge Machining”, Proceedings of the World Congress on Engineering, 3.
35. D. Rakwal and E. Bamberg (2009), “Slicing, Cleaning and Kerf Analysis of Germanium Wafers Machined by Wire Electrical Discharge Machining”, Journal Of Materials Processing Technology, 209, 3740–3751.
36. W. J. Hsue, Y. S. Liao and S. S. Lu (1999), “Fundamental Geometry Analysis of Wire Electrical Discharge Machining in Corner Cutting”, International Journal of Machine Tools & Manufacture, 39, 651–667.

37. S. Plaza, N. Ortega, J. A. Sanchez, I. Pombo and A. Mendikute (2009), "Original Models for the Prediction of Angular Error in Wire-EDM Taper-Cutting", International Journal of Advanced Manufacturing Technology, 44, 529–538.
38. D. Rakwal, S. Heamawatanachai, P. Tathireddy, F. Solzbacher and E. Bamberg (2009), "Fabrication of Compliant High Aspect Ratio Silicon Microelectrode Arrays Using Micro-Wire Electrical Discharge Machining", Microsystem Technology, 15, 789–797.
39. K. D. Murphy and Z. Lin (2000), "The Influence of Spatially no Uniform Temperature Fields on the Vibration and Stability Characteristics of EDM Wires", International Journal of Mechanical Sciences, 42, 1369-1390.
40. O. Dodun, A. M. Gonçalves-Coelho, L. Slatineanu and G. Nagit (2009), "Using Wire Electrical Discharge Machining for Improved Corner Cutting Accuracy of Thin Parts", International Journal of Advanced Manufacturing Technology, 41, 858–864.
41. F. Han, G. Cheng, Z. Feng and I. Soichiro (2009), "Measurement of Wire Electrode Temperature in WEDM", International Journal of Advanced Manufacturing Technology, 41, 871–879.
42. T. A. Spedding and Z. Q. Wang (1997), "Study on Modeling of Wire EDM Process", Journal of Materials Processing Technology, 69, 8- 28.
43. S. F. Miller, A. J. Shih and J. Qu (2004), "Investigation of the Spark Cycle on Material Removal Rate in Wire Electrical Discharge Machining of Advanced Materials", International Journal of Machine Tools & Manufacture, 44, 391–400.
44. P. Saha, A. Singha, S. K. Pal and P. Saha (2008), "Soft Computing Models Based Prediction of Cutting Speed and Surface Roughness in Wire Electro-Discharge Machining of Tungsten Carbide Cobalt Composite", International Journal of Advanced Manufacturing Technology, 39, 74-84.
45. R. Ramakrishnan and L. Karunamoorthy (2006), "Multi Response Optimization of Wire EDM Operations Using Robust Design of Experiments", International Journal of Advance Manufacturing Technology, 29, 105–112.
46. S. Kuriakose and M. S. Shunmugam (2004), "Characteristics of Wire-Electro Discharge Machined Ti_6Al_4V Surface", Materials Letters, 58, 2231– 2237.
47. Y.-F. Tzeng and N.-H. Chiu (2003), "Two-Phase Parameter Design for the Optimisation of the Electrical-Discharge Machining Process using a Taguchi

Dynamic Experiment", International Journal of Advanced Manufacturing Technology, 21, 1005-1014.

48. O. Guven, U. Esme, I. E. Kaya, Y. Kazancoglu, M. K. Kulekci and C. Boga (2010), "Comparative Modelling of Wire Electrical Discharge Machining (WEDM) Process using Back Propagation (BPN) and General Regression Neural Networks (GRNN)", Materials and Technology, 44 (3), 147–152.
49. J. L. Lin and C. L. Lin (2005), "The Use of Grey-Fuzzy Logic for the Optimization of the Manufacturing Process", Journal of Materials Processing Technology, 160, 9–14.
50. V. M. Kumar, A. S. Babu, R. Venkatasamy and M. Raajenthiren (2010), "Optimization of the WEDM Parameters on Machining Incoloy800 Super alloy with Multiple Quality Characteristics" International Journal of Engineering Science and Technology, 2 (6), 1538-1547.
51. V. Parashar, A. Rehman, J. L. Bhagoria and Y. M. Puri (2009), "Investigation and Optimization of Surface Roughness for Wire Cut Electro Discharge Machining of SS 304L using Taguchi Dynamic Experiments", International Journal of Engineering Studies, 1 (4), 257–267.
52. F. Mahmood, B. Bidanda and J. Rajgopal, "WEDM Process Modeling using the Regression Approach".
53. V. K. Pasam, S. B. Battula, P. M. Valli and M. Swapna (2010), "Optimizing Surface Finish in WEDM Using the Taguchi Parameter Design Method", Journal of the Brazilian Society of Mechanical Science & Engineering, 32 (2), 107-113.
54. S. K. Gauri and S. Chakraborty (2010), "A Study on the Performance of Some Multi-Response Optimisation Methods for WEDM Processes", International Journal of Advanced Manufacturing Technology, 49, 155–166.
55. P. Saha, D. Tarafdar, S. K. Pal, P. Saha, A. K. Srivastava and K. Das (2009), "Modeling of Wire Electro-Discharge Machining of TiC/Fe In Situ Metal Matrix Composite using Normalized RBFN with Enhanced *k*-means Clustering Technique", International Journal of Advanced Manufacturing Technology, 43, 107–116.
56. A. Bhattacharya, A. Batish and G. Singh (2010), "Optimization of Powder Mixed Electric Discharge Machining using Dummy Treated Experimental Design with Analytic Hierarchy Process", Proceedings of the Institution of Mechanical Engineers, Part B: Journal of Engineering Manufacture, 225.